

THE REPRESENTATION OF THE NON-IDEAL MIXING
IN A FLOW REACTOR
BY A NETWORK OF IDEALIZED COMPONENTS

THE REPRESENTATION OF THE NON-IDEAL MIXING
IN A FLOW REACTOR
BY A NETWORK OF IDEALIZED COMPONENTS

BY

P. B. MELNYK, B. Eng.

A THESIS
SUBMITTED TO THE FACULTY OF GRADUATE STUDIES
IN PARTIAL FULFILLMENT OF THE REQUIREMENTS
FOR THE DEGREE
MASTER OF ENGINEERING

McMASTER UNIVERSITY

MAY, 1970

MASTER OF ENGINEERING
(Chemical Engineering)

McMASTER UNIVERSITY
Hamilton, Ontario

TITLE: The Representation of the Non-Ideal
 Mixing in a Flow Reactor by a Network
 of Idealized Components

AUTHOR: P. B. Melnyk, B.Eng. (McMaster University)

SUPERVISOR: Dr. J. D. Norman

NUMBER OF PAGES: 139, xi

SCOPE AND CONTENTS:

The frequency response resulting from the non-ideal mixing occurring in a steady state flow-through vessel was obtained. The vessel was tested under two different sets of mixing conditions.

The response data was interpreted such that it could have resulted from an equivalent network of ideally mixed components. The components represent the ideal states of either a completely mixed reactor volume, or no mixing occurring in the direction of flow. Particular emphasis was placed on the detection of parallel flow paths occurring in the test vessels.

In the first study the mixing conditions were represented by a cascade of four components. The second

set of data was interpreted by a similar cascade network and a dual branched parallel network of six components. Evaluation of the model parameters in the frequency domain was computerized.

In the second case, it was concluded that the cascade and parallel networks were best discriminated on the basis of their prediction of reactant conversion rather than their predicted frequency response. Experimental conversion data from both studies was compared to the model predictions.

ACKNOWLEDGEMENTS

The author wishes to express his sincere gratitude to:

1. My wife, Rosslyn, for her patience and understanding throughout the year.
2. Dr. J. D. Norman for his role as the initial catalyst of this project and for the interest he has shown throughout.
3. Miss I. Ellis for typing of the manuscript.
4. Mr. A. W. Wilson, a fellow graduate, for his suggestions and collaboration on this project.

Financial assistance provided by the Ontario Teaching Fellowship and the Department of Chemical Engineering, McMaster University, is appreciated.

TABLE OF CONTENTS

	<u>PAGE NUMBER</u>
ACKNOWLEDGEMENTS	
LIST OF FIGURES	
LIST OF TABLES	
CHAPTER 1 <u>INTRODUCTION</u>	1
1.1 PROBLEM STATEMENT	1
1.2 GENERAL APPROACH	1
CHAPTER 2 <u>REVIEW OF PREVIOUS WORK</u>	3
2.1 INTRODUCTION	3
2.2 RESIDENCE TIME DISTRIBUTION (R.T.D.)	4
2.3 STATISTICAL ANALYSIS	7
2.4 DISPERSION COEFFICIENT	10
2.5 S-PLANE	13
2.6 FREQUENCY RESPONSE	14
2.7 EVALUATION OF PREVIOUS WORK	20
CHAPTER 3 <u>EXPERIMENTATION</u>	22
3.1 TEST EQUIPMENT	22
3.1.1 Flow Vessel	22
3.2 SIGNAL AND MONITORING EQUIPMENT	26
3.2.1 Monitoring Equipment	27
3.2.2 Signal Equipment	28
3.3 EXPERIMENTAL PROCEDURE	30
3.3.1 Tracer	30

	<u>PAGE NUMBER</u>
3.3.2 Calibration and Preliminary Testing	32
CHAPTER 4 <u>CONCEPTS OF FREQUENCY RESPONSE</u>	39
4.1 DATA ANALYSIS	39
CHAPTER 5 <u>MECHANICS OF ANALYSIS</u>	48
5.1 GENERAL METHOD	48
5.2 PROGRAM FORMAT	50
5.2.1 Executive Program	52
5.3 EXPERIMENTAL RESULTS AND INTERPRETATION	57
CHAPTER 6 <u>EVALUATION OF THE RESULTS AND TECHNIQUES</u>	77
6.1 LINEARITY OF THE TEST SYSTEM	77
6.2 DISCUSSION OF THE ADVANTAGES OF THE MODELLING TECHNIQUE	78
6.3 DISCUSSION OF THE USE OF EXPERIMENTAL DATA FOR MODEL DISCRIMINATION	79
6.3.1 Amplitude Ratio Data	79
6.3.2 Phase Lag Data	83
6.3.3 Reaction Data	85
6.4 DISCUSSION OF EXPERIMENTAL STRATEGY FOR IMPROVED DISCRIMINATION AMONG MODELS	90
6.5 DATA REQUIREMENTS FOR FREQUENCY RESPONSE TESTING	91

	<u>PAGE NUMBER</u>
CHAPTER 7 <u>CONCLUSIONS</u>	94
REFERENCES	95
APPENDICES	101
APPENDIX I LINEARITY EXPERIMENT	101
APPENDIX II ANALYSIS OF EXPERIMENTAL ERROR	107
APPENDIX III COMPUTER PROGRAMMING	112
APPENDIX IV EXPERIMENTAL DATA	131
APPENDIX V CONDUCTIVITY PAPER	139

LIST OF FIGURES

<u>FIGURE NUMBER</u>		<u>PAGE NUMBER</u>
1	EXPERIMENTAL APPARATUS	24
2	TEST CONFIGURATIONS	25
3	SINE WAVE FUNCTION GENERATOR	31
4	CALIBRATION CHARACTERISTIC OF THE CONDUCTIVITY MONITOR	33
5	ROTAMETER CHARACTERISTIC	34
6	BODE DIAGRAM OF AN IDEAL CSTR	42
7	BODE DIAGRAM OF AN IDEAL PFTR	42
8	PLOT OF EXPERIMENTAL DATA FROM CONFIGURATION A	59
9	PLOT OF SERIES MODEL FOR CONFIGURATION A DATA	63
10	PLOT OF EXPERIMENTAL DATA FROM CONFIGURATION B	64
11	PROPOSED NETWORK CONFIGURATIONS	67
12	PLOT OF THE AMPLITUDE RATIO FOR TWO CSTR'S IN PARALLEL	93
13	COMPARISON OF INPUT SIGNAL TO SINE FUNCTION	105
14	COMPARISON OF OUTPUT SIGNAL TO SINE FUNCTION	106

FIGURE
NUMBER

PAGE
NUMBER

15	PREDICTED RESPONSE FROM MODEL 5A TO EXPERIMENTAL DATA FROM CONFIGURATION B	75
16	PREDICTED RESPONSE OF MODEL #13 TO EXPERIMENTAL DATA FROM CONFIGURATION B	76

LIST OF TABLES

<u>TABLE NUMBER</u>		<u>PAGE NUMBER</u>
3-1	COEFFICIENTS OF THE CALIBRATION EQUATION	35
5-1	INITIAL ESTIMATES OF RESIDENCE TIMES	62
5-2	INITIAL ESTIMATES OF RESIDENCE TIMES	71
5-3	FINAL PARAMETER ESTIMATES OF MODELS PROPOSED FOR CONFIGURATION B	73
6-1	COMPARISON OF MEASURED AND PREDICTED REACTOR CONVERSION	88
7-1	COMPARISON OF WAVEFORMS TO SINE FUNCTION	103
II-1	ANALYSIS OF REPLICATES	111
III-1	TRANSFER FUNCTIONS FOR PROPOSED NETWORKS	113
III-2	LISTING OF INPUT DATA & OUTPUT RESULTS	119
IV-1	EXPERIMENTAL DATA	132

CHAPTER 1

INTRODUCTION

1.1 Problem Statement

Waste treatment, in many cases, is simply the reduction or degradation of pollutants by means of a chemical or bio-chemical reaction. The flow regime in which the kinetics occur, varies as from a well-defined mixed state, as one finds in an aeration vessel, to a partially mixed state as in an aerated lagoon, or to an arbitrary state as the flow encountered in a river system.

The purpose of this work is to define and demonstrate a method by which the mixing phenomenon occurring in any hydraulic flow regime may be characterized. This mixing information should be presented in such a manner that the application of previously known kinetic information is straightforward and flexible.

1.2 General Approach

Prediction of reactant conversion for a given kinetic mechanism is conveniently handled, when one considers a reactor to exist as one of two extreme states of mixing.

O. Levenspiel (30) has defined these two ideal steady-state flow reactors as:

(i) The stirred tank reactor or CSTR (completely stirred tank reactor) is a reactor in which the contents are well stirred and uniform in composition throughout. Thus the exit stream from this reactor has the same composition as the fluid within the reactor.

(ii) For a plug flow reactor we may have lateral mixing of the fluid; however, there must be no mixing of fluid longitudinally along the flow path. A necessary and sufficient condition for plug flow is to state that the residence time in the reactor is the same for all elements of the fluid. This reactor will be denoted as a PFTR.

Adopting a modular approach to a network composed of these ideal reactors, the prediction of conversion is still straightforward. It is proposed that the conversion for each reactor be estimated individually, and this information be applied to a succeeding reactor as one moves through the network. If recycle exists, then an iterative approach must be taken in order to calculate the overall conversion. Thus it is proposed to express the mixing phenomenon occurring in any flow regime by a lump parameter model; a model whose variables consist of the location, type, and residence times of the ideal components. An alternative approach would be the characterization of mixing by a distributed parameter model. One could derive such a model by solving the Navier Stokes equations with appropriate boundary conditions particular to a flow regime. From this approach the extent of mixing is defined continuously at every location in the fluid, (as opposed to a lump parameter model where a flow system is treated as a "black box" with the ideal components having no dimensional significance). The distributed parameter approach; however, in comparison it does not offer the flexibility for reaction computations to that of the modular approach.

CHAPTER 2

2 REVIEW OF PREVIOUS WORK

2.1 Introduction

Experimentally, the approach to characterize mixing has been to stimulate a system by imposing an inert tracer concentration into the input stream and measuring the system response (via output tracer concentration). If the system is dynamically tested (e.g., input signal varies as to time) the output response is measured on a time base. The output response as a function of both the mixing state and time can be characterized by the following techniques:

- (i) Residence Time Distribution
- (ii) Statistical Analysis
- (iii) Dispersion Coefficient
- (iv) S-plane
- (v) Frequency Response

In this review,

- (i) The manipulation of experimental data,
- (ii) the form of the lump parameter model proposed to represent the mixing state,
- (iii) and the calculation procedure to determine model parameters will be considered in each area.

The greatest amount of interest in the representation of mixing by networks of ideal reactors has been in Chemical Engineering, and specifically to the problem of reactor

mixing. The review is centred in this area. Attention is drawn however to those techniques that have been applied to waste treatment processes, particularly aeration and gravity settling.

2.2 Residence Time Distribution (R.T.D.)

The stimulus-response technique is used to define the distribution of ages of fluid molecules within a system or its exit stream. Usually the input stimulus is a step change or impulse (Dirac - delta function) of tracer concentration. The curves obtained from monitoring concentration as function of time are called F or C curves respectively.

P. V. Danckwerts (14) derived the F and C function for ideal CSTR and PFTR reactors. Imperfect mixing resulted in continuous full scale reactors having a conversion different than that measured on a laboratory scale. T. K. Sherwood (52) proposed that R.T.D. curves could be used to evaluate imperfect mixing.

Chollette et al (9), (10), (11), initiated the concept of representing mixing patterns by simple combinations of CSTR's and PFTR's. The conversions of elemental first and second order reactions as effected by these combinations were considered. Both isothermal and adiabatic reactors were studied.

Wolf and Resnick (67) and O. Levenspeil (31) have postulated that the R.T.D. of a real system could be dup-

licated by mixed models containing perfectly mixed reactors with plug flow, dead volume and short circuiting. These authors presented the mathematical functions and F and C curves to demonstrate their mixed models.

J. G. Van Vusse (64) developed a model for a real stirred tank reactor consisting of all these four mixing phenomena operating in parallel by varying magnitude. Comparison of a real reactor to his model was based on the R.T.D.

Gilliland and Mason (18) had obtained experimental curves similar to the theoretical distribution of a CSTR: whereas separate measurements taken inside the vessel showed very little backmixing had occurred. Noar and Shinnar (38) defined a new function called the intensity function - " $I(t)$ ". Physically this function is a measure of the probability of escape for a particle which has stayed in the system for a period " t ". Noar and Shinnar stated that this intensity function:

- (i) displayed more clearly the difference in the flow mechanism of two systems, and
- (ii) rendered a physical insight into the mixing process of the system, particularly stagnancy ("which the authors associated in a system in which the total flow is unevenly divided among parallel branches").

In a more sophisticated approach to simulation of mixing phenomena, consideration has been given to internal recycling in a flowthrough vessel. Haddad, Wolf and Resnick (19) had developed (the time-based) F-function for a model consisting of a CFTR and PFTR in series arrangement with and without a PFTR (or lag) situated in the cycle loop. P. W. T. Rippen (46) had developed an expression to describe the R.T.D. in a PFTR reactor with recycle under both extremes of molecular mixing (i.e., maximum mixedness and segregation).

Shinnar and Noar (39) postulated a model of N CSTR's in series. Provision is provided for recycle (or reflux) between two adjacent reactors; thus allowing arbitrary flow-rates to each reactor. Their method allows the derivation of the Laplace transform for the model as well as its R.T.D.

An innovation in measurement technique is to use a reactant whose conversion is first order as a tracer to measure the R.T.D. The advantage of this tracer over the conventional inert one is:

- (a) experimental R.T.D. will include diffusion effects caused by the reaction occurring in a poorly mixed system, and
- (b) more adaptable to field conditions.

In summary, it has been seen that the simulation of mixing phenomena has been developed from the simple

PFTR and CSTR ideal reactors to the more sophisticated development of networks of ideal reactor components. The disadvantage of the R.T.D. technique is, however: first, the complexity of the equations describing the mixed models in the time domain, and secondly, the difficulty in interpretation of experimental R.T.D. The establishment of a mixed model is usually achieved in the iterative approach of proposing a configuration and then confirming the hypothesis by experiment.

2.3 Statistical Analysis

The statistical approach is essentially an extension of network modelling reviewed in the last section. Predicted results from a statistical (or stochastic) model are compared to experimental residence time distributions. As before, impulse and step changes in tracer concentration are the most commonly considered input stimuli.

To characterize a system by one tracer experiment, one assumes a steady flow or at least the R.T.D. of any small volume of fluid entering the system is constant and independent of the time this volume entered the system. Adopting this assumption one characterizes a system as being deterministic. In a flow situation where dispersion of a reactant is occurring in a slowly moving fluid, or the unsteady nature of flow in fluidized bed, the random nature or component of the system may warrant simulation. Another

important feature of this technique is the identification of the system by random input disturbances. Applying this approach, a flow system is reduced to network of ideal CSTR's in which interconnecting flows may be recycled.

Gibilara, Kropholler, and Spikins (17) have derived expressions and have made comparisons of their predictions for a stirred tank. Their network configuration was based on the Van de Vusse stirred tank model. The system randomness was defined by a stationary Markov process. The system or a fluid particle is considered to move from one state to another at discrete time intervals. The probability of a new state is derived by the multiplication of a transition matrix (the probability of a fluid particle moving from one location of the network to another) by the probability of the previous state (also a matrix). The time interval, assumed by the authors, is sufficiently small that a particle has only a twofold option, (i.e., remain at a location in a network, or transfer to only one new location). Buffham, Gibilara and Kropholler (8) have also extended this work to include any network.

Rettlack (44) has proposed to approximate a flow system by a series arrangement of CSTR's in which a particle may reflux or backtrack through the cascade. Given the number of components in the network, a series of distribution

curves are prepared based on the probability density of networks with a varying number of backtracks or entrainment ratios. By comparing the predicted curves to experimental data, the entrainment ratio is estimated. Extending Rettlick's concept, Klenhenberg (22) proposed a better technique by which the entrainment ratio is derived directly from the variance of the experimental curve. The total probability density of the network is calculated as the sum of individual terms, each of which represent the probability for a specific number of backtracks through the network and each of which is weighted by a factor as to the probability of occurrence of that number of backtracks. Rettlick has prepared a grid of these weighting factors.

Krambeck, Shinnar and Katz (26) propose a mixing model consisting of a network of CSTR's with interconnecting flows that are random functions of time. The probability functions are derived by means of a stationary Markov process. Expressions of R.T.D. to a step stimulus for two CSTR's in series and two CSTR's in parallel models are developed, and analysed as to sensitivity as a function of transition probability and magnitude of flow fluctuations. The average yield from the models under first order kinetics is also considered.

In a theoretical discussion by King (21) the output of a continuous CSTR is derived when its transfer function is based on parameters which are random variables. The

affect on both white noise and a deterministic input stimulus by the stochastic transfer function is analysed.

Sinclair and McNaughton (54) propose a formal procedure to combine the probability density functions of individual components by multiple convolution integrals in order to obtain the overall R.T.D. of a complex network.

Silveston et al (53) have characterized the operation of a primary clarifier as a stochastic process. The rate of hindered settling is proposed to be linear function. The size distribution of the influent particles is represented as both a normal and x-chi squared type. The effluent distribution thus results from the transformation of the influent distribution by the hindered settling rate.

Similar treatment to a natural stream has been given by Thayer and Krutchkoff (60). The random variables in this study are the Biological Oxygen Demand and Dissolved Oxygen Content.

Though this approach adds a new dimension in the characterization of mixing, one must decide if the system behaved in a random manner to the extent that the additional complexity introduced is warranted.

2.4 Dispersion Coefficient

In some cases, it is possible to represent the information contained in a R.T.D. by a single parameter, the dispersion coefficient. With this technique, the flow system

is assumed to approximately resemble a PFTR with correction terms present for axial and radial diffusion. The existence of by-passing and dead volumes are not considered, because the model is one reactor. The model function is a second order differential equation. To predict conversion a kinetic expression (as a function of concentration) is added. Though this technique is lacking in the modular approach in the handling of kinetics, conversion can be expressed as a function of distance along the flow system.

A short review of the work done in this field is as follows. The following authors have considered only axial dispersion:

- (i) Levenspeil and Smith (32) have showed the variance at the R.T.D. curve can be used to evaluate the dispersion coefficient for an impulse stimulus.
- (ii) Van der Laan (62) extended the treatment to finite vessels and solved the differential equation under appropriate boundary conditions.
- (iii) Aris (3), Bischoff and Levenspeil (5) demonstrated that the restriction of obtaining a perfect impulse (Dirac - delta function) may be removed by sampling at two locations.

Bischoff and Levenspeil (5) developed a general solution to simulate axial and radial diffusion in a plug flow model.

Comparison of dispersion models have been carried out by Taylor (56), (57), Aris (4), Bischoff and Levenspeil (6).

Deans and Lapidus (15) have investigated the suitability of a number of tanks in series model to simulate small deviations from plug flow. The deviation between R.T.D. curves predicted by the two models increased with increased deviation from plug flow.

Initially the aeration tanks (used in the activated sludge process) had been idealized as a PFTR. The first mathematical description of non-ideal flow was given by Thomas and McKee (61). More recently, Murphy and Timpany (34) have considered the non-ideality or short circuiting as caused by longitudinal diffusion in this system. Equal and unequal, mixed tanks in series, complete mixing, complete PFTR and Axial Dispersion models have been applied to the R.T.D. data obtained by a pilot plant spiral-flow aerator. The dispersion model was found to be the best fit. A similar conclusion was reached when Murphy and Boyko (35) extended this work to a full sized system.

The use of dispersion coefficients has also been applied to natural streams. The work of Thackston and

Krenkel (59) utilizes this approach with the inclusion of stagnat flow areas in their model.

2.5 S-Plane

The identification of model parameters is simplified when response data is represented in the s-plane. The output response of ideal reactor components is described by differential equations in the time domain. A transfer function in the s-domain simplified the differential equation to an algebraic form. The transfer function of a linear system is defined as the ratio of the Laplace transform of the output variable to the Laplace transform of the input variable, with all initial conditions assumed to be zero.

The s-plane was defined in the following studies as a plot of the ratio of the model's or the experimental system's input and output response integrated over the time axis versus the variable "s" (which is an inverse function of the integral of time). Only real and positive values of "s" were considered on this plot in a numerical range from 0.5 to 10.

Rooze (47) and Alder (1) have developed a numerical technique to perform s-plane transformations. Response data is recorded as a R.T.D. This data is normalized, and the concentration axis displaced horizontally to eliminate dead volume and lag contributions. The experimental curve is then assumed to be composed of straight line segments

over small time intervals. Each segment is transformed and then summed to yield the output response "y(s)" at one "s" value. The procedure is repeated at different "s" values to obtain a plot of "y(s)" versus "s".

Impulse (Dirac - delta), step pulses and random input signals were considered by the authors. R.T.D. predictions based on the Hovorka (20) model were compared to experimental data. The Hovorka model is a cascade of stages; each stage consisting of two CSTR's in parallel and subject to backmixing. The numerical s-plane transformation, estimation of model parameters, and model predictions have been computerized.

Clements (12) has also attempted parameter estimation in the s-plane for both a diffusion model and the Hovorka model with success. Experimental data was obtained from an extraction column.

2.6 Frequency Response

The characterization of a system by identification of its steady state response to a periodic stimulus is a powerful and widely used method of analysis. Pioneer development and application of this technique has been centered in electrical and control engineering fields. A control text such as "Modern Control Systems" by R. C. Dorf (16) provides an excellent background to frequency response analysis.

Traditionally a sinusoidal signal has been used as an input stimulus. The resulting output signal for a linear system is sinusoidal differing only in phase angle and amplitude from the input waveform. The unique advantage of this method is that the amplitude and phase lag characteristics are sufficient conditions for identification.

The characterization of frequency response data graphically, and mathematical representation (labelled transfer functions) of the response of electro-mechanical machines is well explained by Dorf.

Again this technique is useful as the system response is represented by a complex algebraic polynomial, whose coefficients are functions of the system residence time. This polynomial is obtained from the expression describing the system response in the time domain by means of the Fourier transform. Because the Fourier and Laplace transforms are closely related, the transfer function $T(j\omega)$ (frequency domain) can be obtained from the transfer function $T(s)$ (s-domain) when the time domain function considers time to vary along a positive axis. In section 4.1 it will be shown that the unknown frequency response of a system can be deduced from the experimentally determined frequency response of the system.

The transfer functions of ideal CSTR and PFTR vessels are presented by Murrill, Pike and Smith (37),

alternative approximations of the PFTR transfer which are more compatible with the CSTR expression are developed by Coughanower and Koppel (13).

Wen and Chung (66) have compiled a directory of transfer functions for mixed cell and circulation models under periodic and non-periodic inputs. These models had been developed by various authors earlier in the literature.

Pang and Johnson (41) have shown that the frequency response of a multi-stage process can be developed by consideration of the transfer function for one stage. A liquid-liquid extraction process is used as an example. The interaction amongst stages is represented by a signal flow-graph. The frequency response results from application of Mason's gain formula to this graph.

Leder and Butt (27), performed frequency response tests on a fixed-bed catalytic reactor, using a tracer undergoing a depletion by second order kinetics. Their technique was to calculate the reaction contributions to the output data, remove this effect, and then proceed to analyse the converted response data as to mixing. The reaction order and the reactor mixing had to be pre-judged, however, in the analysis of the data.

Though emphasis has been placed in this work on using frequency response analysis to estimate lump-parameter

models, the method has been used to estimate distributed parameters (55), (23), (24).

Of interest is Kramers and Alberda (25) paper in which frequency response data is axial dispersion model versus a cascade of n stirred tanks.

Wever and Harriot (65), have compared first to fourth order lump-parameter models to a distributed model (based on heat removed from a shared tank). The fourth order lump-parameter model compared best to the distributed model predictions.

The measurement of systems by a periodic stimulus requires numerous experiments (as each frequency of the system is tested individually) and unique dosing equipment (i.e., sine wave generator). To overcome this disadvantage and still retain the advantages of frequency response analysis, much work has been done in the derivation of appropriate data from non-periodic signals.

A definitive work describing the use of a finite pulse to obtain frequency response data has been carried out by Clements (12). His article presents an investigation of:

- (a) the suitability of various pulse forms,
- (b) the development of the theory and a computerized numerical technique to transfer data to a frequency response plot,

- (c) subsequent investigation of the accuracy of this numerical technique,
- (d) experimental data based on mixing and extraction processes, and
- (e) development of lump and distributed parameter models.

A refinement of the numerical techniques for data conversion is offered by Lees and Dougherty (29).

Sawyer (50), obtained frequency response data on a pilot and plant size chlorine contact chamber from both sinusoidal and pulse input signals. Deviation between the response curves was found. The author derived a lump-parameter model consisting of our small CSTR's in series followed by a large PFTR.

The concepts developed for finite pulses have also been extended to step-change and impulse signals. Schechter and Wessler (51), and Hyguist, Schindler and Gilbert (40), present expressions suitable for the conversion of step data. Teasdale (58), offers a graphical technique while Reynolds (45), discussed the use of analog computers for data conversion.

Angus and Lapidus (2), have experimentally verified the response of a stirred tank using non-stationary noise as an input signal. The computational technique has also been investigated for hypothetical systems as large as

fifth order. The methodology necessary to obtain the frequency response and transfer function of a system from random noise and which is based on statistical correlation techniques has been reviewed by Murrill, Pike and Smith (36).

Leeds and Bybee (28), have applied the analogy of an equivalent electrical circuit to solution of the distribution of pollutants in an estuary. The estuary is modelled by a one-dimensional diffusion process. The ensuing differential equations are represented by an equivalent electrical circuit. The frequency and transient response of this circuit is then studied.

2.7 Evaluation of Previous Work

From the literature review, it was felt that improvements concerning the modelling of mixing could be made in specific areas.

It was desired not to restrict the interpretation of response data to one type of reactor form as is inherent in the dispersion coefficient approach, to a particular model as was done by Rooze (41) and Adler (1), or to a series arrangement of ideal components. Sawyer (50) had modelled a chlorine chamber by a cascade of CSTR's and a PFTR as was indicated by the system's frequency response data. His evaluation of the model parameters was performed graphically. It was thought the evaluation procedure could be improved if it were performed numerically on a computer. The scope of the problem could also be increased by first, considering if frequency response data could be used to indicate the presence of parallel flow paths existing in the non-ideal flow, and second if the magnitude and direction of these flow paths could be determined directly from the data. Noar and Shinnar (39) had considered this problem based on the analysis of the R.T.D., but their interpretation of the existence of parallel flow paths was dependent upon the transforming of the initial data by a differential process. Clement's (12) studies on the extraction process occurring in a packed column provided frequency response

data that indicated that parallel flow patterns may have existed in the organic phase. Clements chose, however, to model his system by a diffusion process and the Adler - Hovorka Finite-Stage model.

In summary, the evaluation of frequency response data by a computerized method with particular attention paid to the detection of parallel flow paths becomes the objective of this project.

CHAPTER 3

3 EXPERIMENTATION

Response studies utilizing sinusoidal, impulse and step-change signals were performed on a continuous flow-through vessel. Mixing in this vessel was induced by baffling and impellers. It was deliberately sought to form mixing patterns which were non-ideal (e.g., neither completely mixed nor plug flow). Input stimuli were initiated by concentration gradients of an inert electrolyte, while output response was measured by monitoring conductivity.

3.1 Test Equipment

3.1.1 Flow Vessel

A hydraulic test tank was constructed based on the following criteria:

- (i) system volume and flow rate were to be sufficiently large to make entrance and wall effects negligible,
- (ii) flexibility as to the establishment of mixing patterns,
- (iii) mixing patterns created are arbitrary and non-ideal (internal re-cycling, dead volume, etc., were induced).

An additional design standard was that the tank and fittings must be inert to tracers or reactants, thus: teflon and stainless steel were chosen as materials of construction.

The test vessel was simply a stainless steel tank

with dimensions of 4' by 2' by 1' deep. The entrance into the vessel consisted of a header (3 1/2" O.D. SS. tubes) and impingement baffles. Outlet ports were arranged at 6 inch intervals along one side to allow redistribution of fluid to other areas of the tank. A 60° V-notch weir located opposite the entrance was the exit point. A grid of 1/4" aluminum rod was constructed above the tank to support mixers and baffles. The baffles were 12" by 6" rectangles of 1/32" 316 ss. They were not tight fitting to either each other, or to the tank walls and floor.

During any experiment, the variables to be controlled are tank volume, flowrate and fluid temperature.

Because the weir is a constant head device, at constant flow, tank volume is maintained. This volume can be changed by adjustment of weir elevation.

The flowrate to the tank was controlled by a needle valve (Whitey 18KS12). A centrifugal pump was placed upstream from the valve to provide an adequate head (60 ft. of water) for linear flowrate control. A rotometer of range 0.2 to 2.8 gal./min. was used to monitor the flow continuously.

The fluid was kept at a constant temperature of 25°C by a two-stage process. In the first stage a pneumatic operated valve with feedback control was used to blend hot and cold water to approximately 24°C. In a water holding

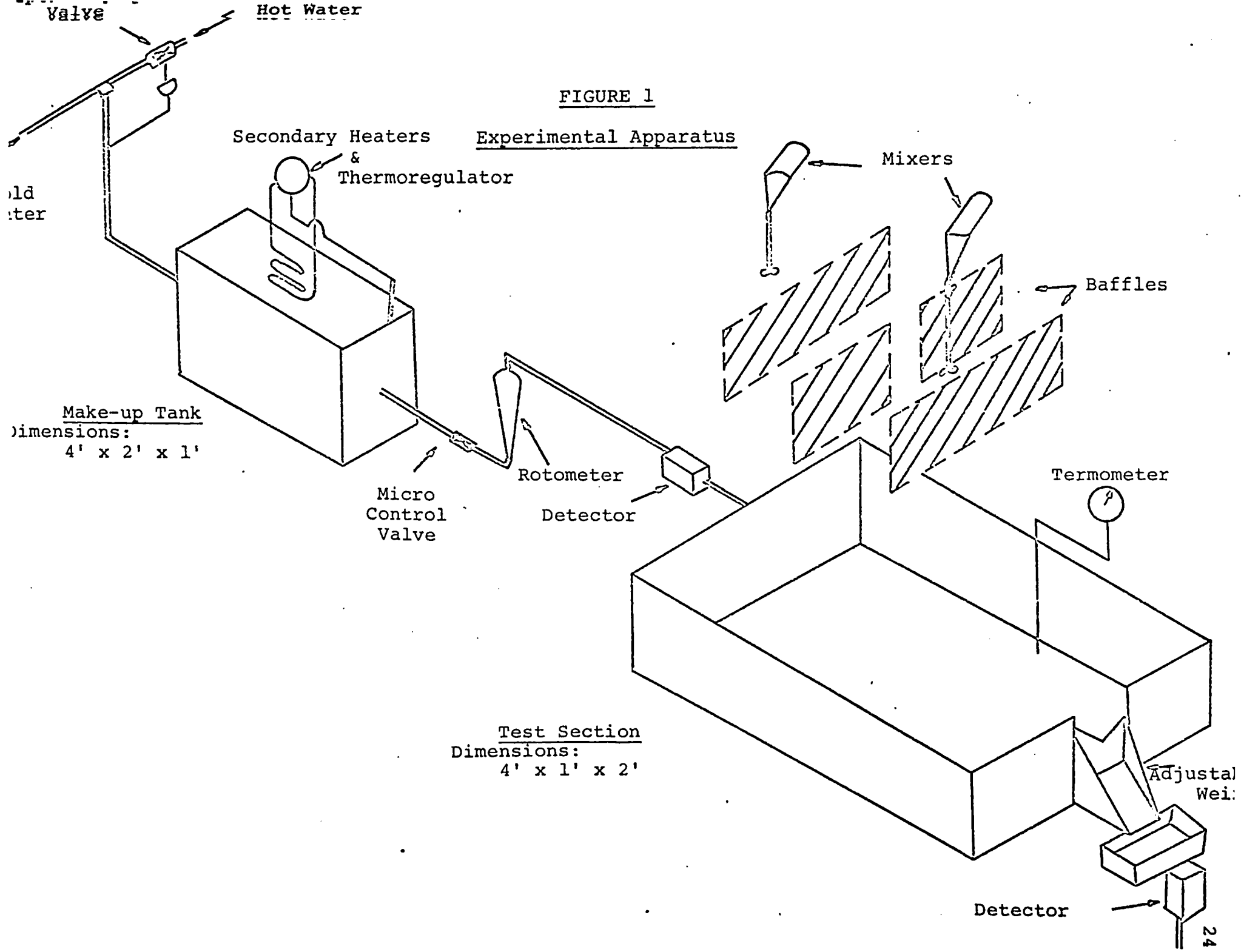


FIGURE 1

Experimental Apparatus

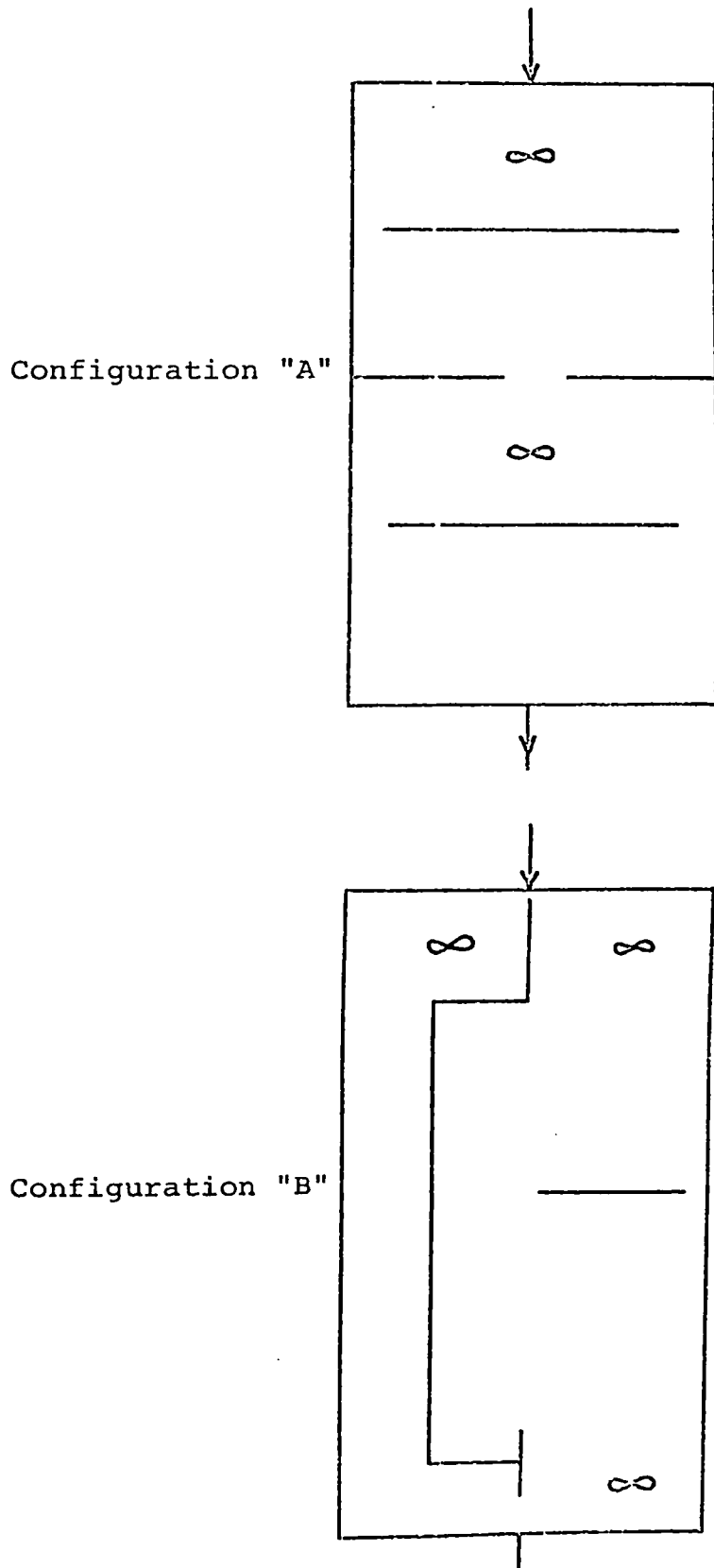
old
ster

Make-up Tank
Dimensions:
 $4' \times 2' \times 1'$

Test Section
Dimensions:
 $4' \times 1' \times 2'$

FIGURE 2

Test Configurations



tank of dimensions 1' by 4' by 2' a 800 watt heating element was controlled by a mercury column regulator and supplied by a transistorized relay (as maximum current loading of the mercury regulator is in the order of .3 milliamperes). The fluid temperature at the exit of the test section was monitored by a resistance thermometer and found not to vary more than $\pm .2$ C°.

Mixing was provided by three portable mixers with a power rating of 1/6 H.P. The impeller speed and depth could be varied continuously and were set arbitrarily.

A schematic view of the flow equipment is presented in Figure 1. The two configurations of baffles and mixers tested are shown in Figure 2.

3.2 Signal and Monitoring Equipment

It was decided to follow the concentration of a tracer by measuring the conductivity of the fluid. An inert electrolyte, NaCl, was used as a tracer. This salt was chosen because:

- (i) it is highly conductive,
- (ii) it is economical and readily available, and
- (iii) the high solubility is desirable for the preparation of concentrations of tracer solutions.

The decision to choose conductivity as the measurement method was made because:

- (i) equipment may be designed that will yield continuous and rapid response to changes in fluid conductivity,
- (ii) the response is approximately linear over the range of interest (allowing the differentiation of small concentration to be measured),
- (iii) measurements are accurate in the dilute solution range studies (0.0 to 0.05 moles/litre), and
- (iv) measurements may be made "in situ" (to eliminate instrument lag) and are independent of flowrate (12).

3.2.1 Monitoring Equipment

A two channel continuous conductivity instrument was constructed by the writer in conjunction with Mr. A. W. Wilson. The measurement principle is simply to record the current passing from one parallel plate through the fluid to an opposite plate. The design principles and details of construction are outlined in the article "Continuous Conductivity Monitoring System" found in Appendix V.

For the mixing studies, sensing units were located in the piping directly before the test section and in the crest of the exit weir.

Temperature control is important to obtain accurate

measurements of conductivity. A one degree change in fluid temperature results in a 2% change in conductivity measurements.

3.2.2 Signal Equipment

Three signal forms were used. An impulse signal was introduced by means of a 50 cc syringe. A step change in tracer concentration was effected by immediately increasing the tracer input, while the sinusoidal input was induced by varying the feed pump to the appropriate periodic function.

The tracer was introduced in line before the centrifugal pump to effect a uniform distribution in the feed line.

A positive displacement peristaltic pump was used to introduce the tracer. The pump capacity or volume output was directly proportional to the speed of the drive motor. The speed characteristic of the DC motor to voltage was also linear. Thus it was required to supply a voltage varying sinusoidally to the pump motor to obtain the corresponding signal based on tracer concentration.

Frequency response data obtained over a two decade range is usually sufficient to identify a system. For the present test system a frequency range from .01 cycles/min. to 1 cycle/min. was required. This sinusoidal signal may be produced either electronically or mechanically.

To produce by electronic circuitry a sine function is difficult. The time constants of electrical components being small do not easily lend themselves to the production of low frequency waves (less than $.02 \text{ Hz}$). A low frequency can be attained by continuously changing the slope of a ramp signal or by treating a higher frequency signal by successive decade frequency dividers and mixers. Such function generators are commercially available, but expensive (e.g., Hewlett Packard model 203A). A more economical approach is to generate the necessary signal by mechanical means. A periodic displacement or change of area can be obtained from a rotating device (e.g., mechanically driven wheel) by projection of one dimension of this rotating device onto a normal plane.

A sinusoidal displacement is defined by the projection of a vector of constant radius " r " rotating at a speed " w ". Amplitude and frequency of the function are directly related to the radius " r " and angular speed " w ". The apparatus simulated this definition.

A wheel rotating at a fixed speed displaces a rack a distance equal to the projection of the wheel radius on to a normal plane. The rack and wheel edge are connected by a rigid rod that pivots and slides at the wheel and is fixed to the rack. If the rod remains always perpendicular to the rack, the sine wave function is perfect.

The horizontal displacement of the rack is converted to an angular oscillation by an idler gear. This oscillation

was used to drive a wiper or tap of a circular wound transformer. Thus the sinusoidal displacement is converted directly to an A.C. voltage, varying sinusoidally in magnitude at a frequency equal to the drive wheel's angular speed. The drive wheel was rotated by a variable speed reducer (Graham model no. N27MW45) with appropriate gearing (10.1) after the reducer drive.

The accuracy of the sine wave produced was found to be perfect within an experimental error of 2%. The procedure used to test this output signal is give in Appendix I. A shcematic of the signal apparatus is shown in Figure 3.

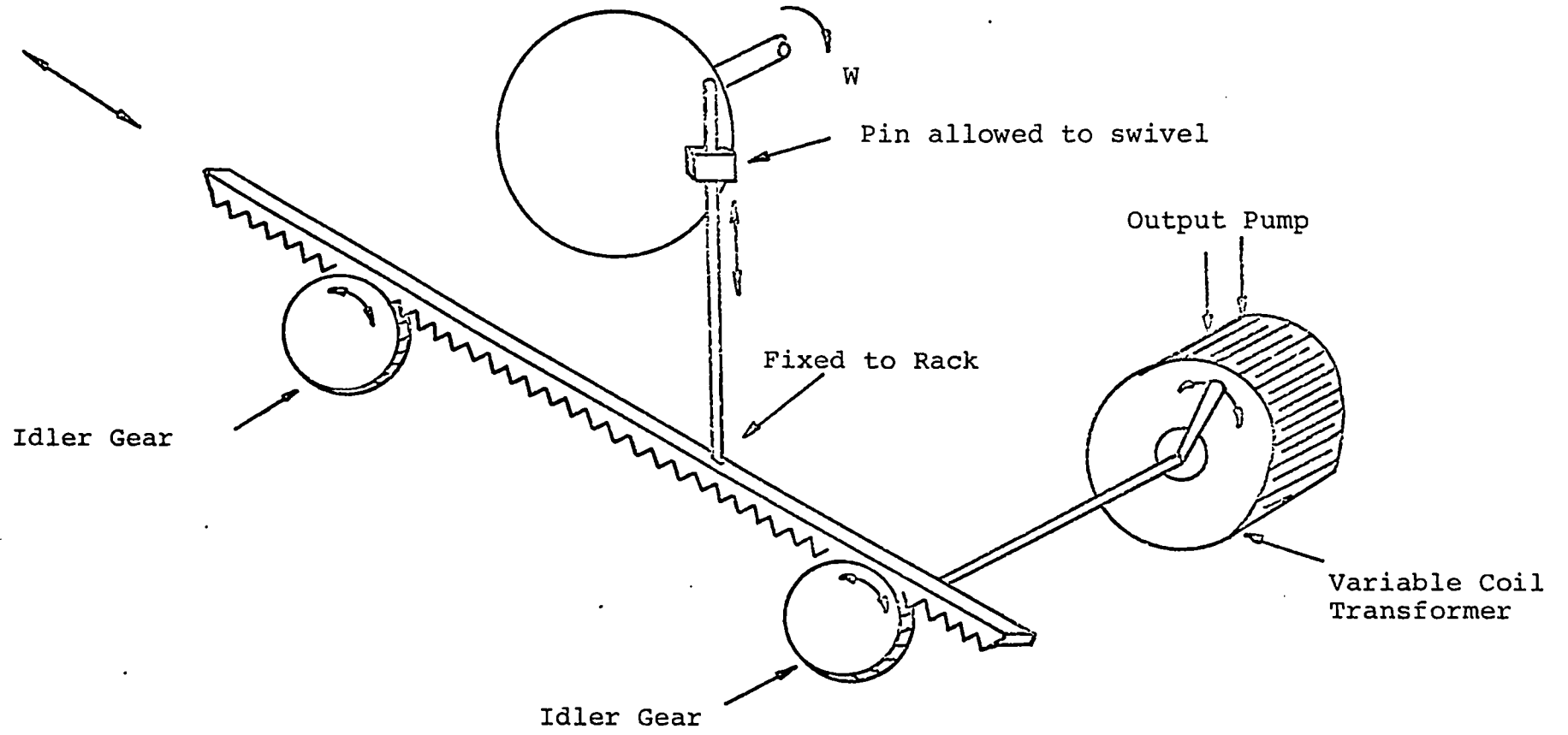
3.3 Experimental Procedure

3.3.1 Tracer

The tracer used was a saturated solution of common salt (solubility 360 gm/100 gm. of water). This saturated solution was injected into the tapwater pipe leading to the test vessel input. The tracer pump flowrate was variable between 0.0 and 45.0 ml./min. corresponding to vessel input concentrations of 0.0 and 1.5 gm/l NaCl respectively.

Van der Reit (63), has demonstrated that for tracer concentrations above 100,000 parts per million, density currents began to distort the output results. Because, firstly, the peak input tracer concentration was below this limit, and secondly, the entrance region in the test section was turbulent, irregularities in the results resulting from density currents were believed to be negligible.

FIGURE 3
Sine Wave Function Generator



From preliminary testing it was found that tracer recovery is 100%.

Because tap water was used as the fluid, a base line conductivity equivalent to .1 gm/l of NaCl was recorded even when no tracer was present. This base line was found to be constant and was accounted for in the subsequent calibration of the instrument.

3.3.2 Calibration and Preliminary Testing

A calibration curve was prepared plotting the concentration of NaCl (gm/l) versus the current passing between the conductivity probes. The calibration tests were performed with the sensor probes located in stream and using tap water as the solvent. Settling the bulk temperature at 25°C, the tracer was introduced at constant rate and the instrument response was recorded when the concentration levels at the input and output were at steady state. The concentration of tracer in the main stream was determined by means of a mass balance. The concentration levels in the saturated solution, main stream flowrate, and the tracer injection flowrate were all known. This procedure was repeated to obtain nine readings for the calibration plot. This plot is shown in Figure 4. The slight displacement of the two curves for the input and output sensing unit are believed to be the result of differences in plate area and the characteristics of circuit components (i.e., matched circuit components were not used in the construction of the instrument).

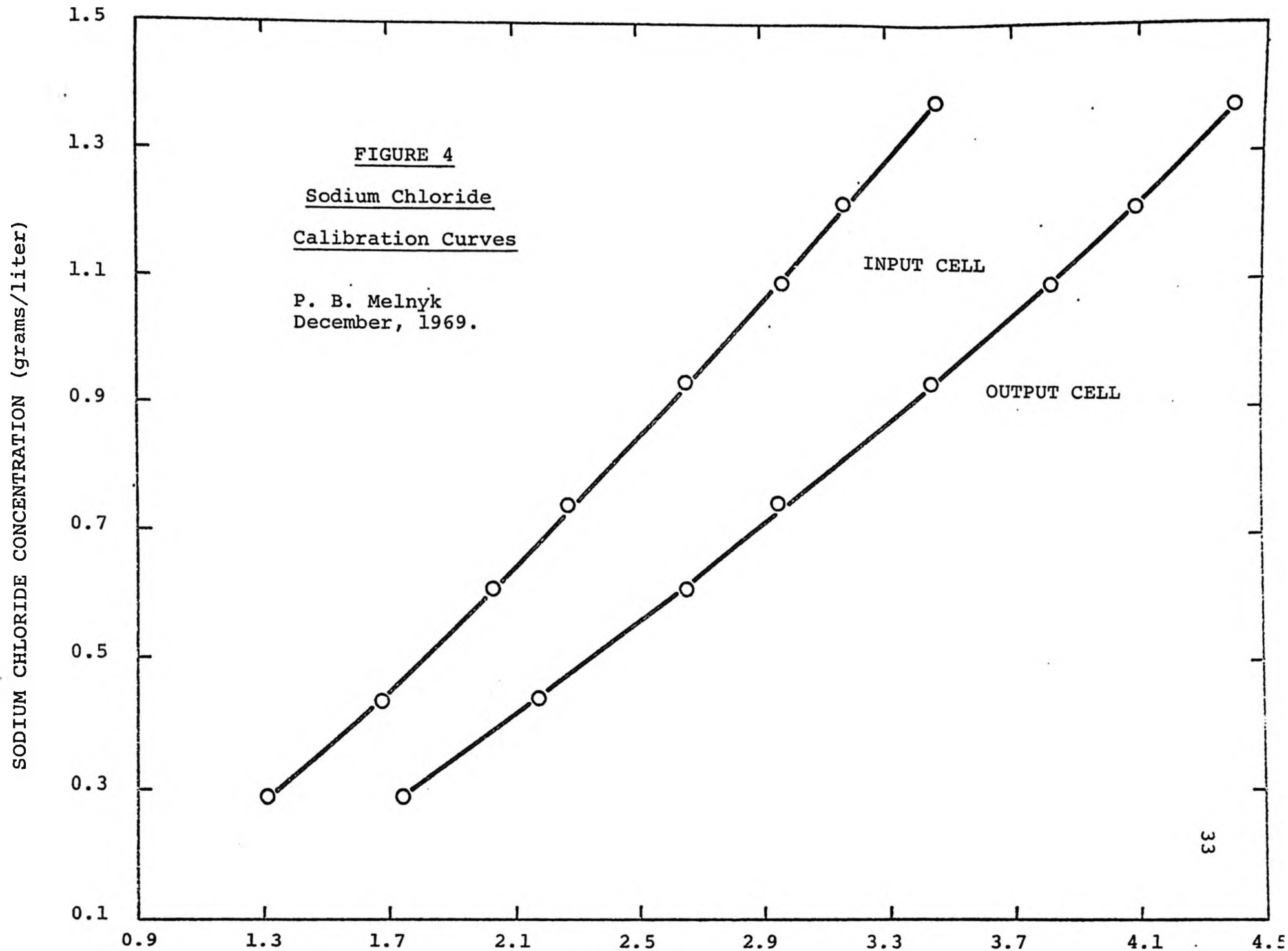
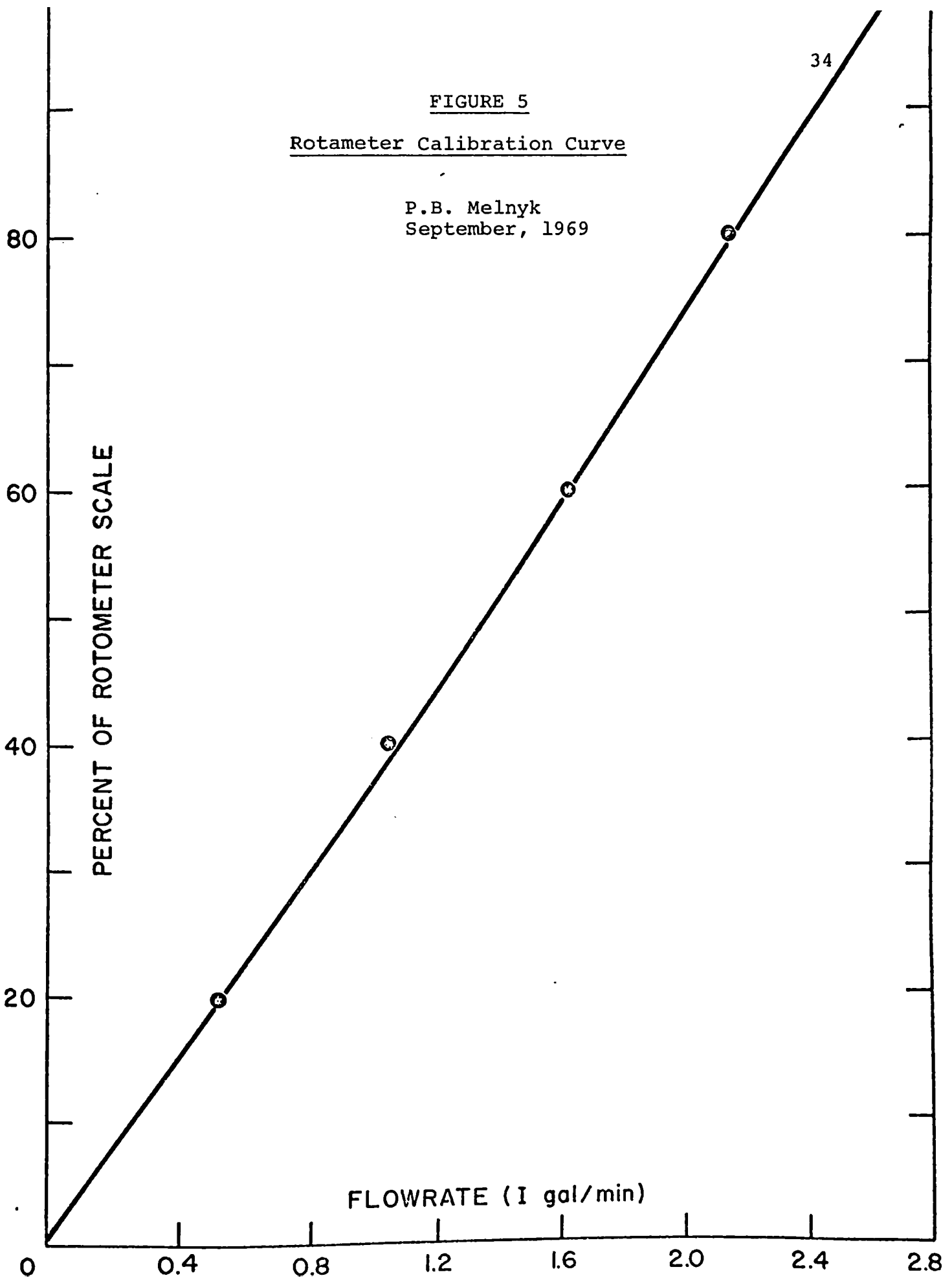


FIGURE 5

Rotameter Calibration Curve

P.B. Melnyk
September, 1969



A stepwise linear regression computer program was used to obtain second order equations to describe the calibration characteristics. The equation coefficients are:

TABLE 3.1 Coefficients of The Calibration Equation		
	<u>Input Probe</u>	<u>Output Probe</u>
Pure Constant	-0.2310	-0.1895
First Order Term	0.3534	0.2278
Second Order Term	0.03076	0.02835
Standard Error of Estimate	0.01842	0.0089
Dependent Variable - Tracer concentration (gm NaCl/l)		
Independent Variable - Conductivity meter response (milliamperes)		

with standard error of estimates.

Note that modifications were made to the sensing equipment between the tests on configurations A and B. This resulted in the necessity of recalibrating the instrument.

Statistically, the use of a second order equation is not justified (first order is adequate based on the error removed by the second order term). It was used to improve the standard error of estimate.

This regression equation formed the basis of a computer program which, given the peak values of the sine wave as an input, calculated:

- (i) peak values in terms of concentration,
- (ii) magnitude ratio in decibels, and
- (iii) average concentration at the input and output and compared the difference.

The rotameter was calibrated in the usual manner of noting the volume displacement over a measured time interval. Its characteristic is shown in Figure 5.

Because the walls and floor of the test section were slightly irregular, the test volume was calibrated. A curve was plotted relating the depth as read from a ruler attached to a wall of the tank, and a known volume of fluid in the test section.

A preliminary investigation was carried out to determine the accuracy of the input and output waveforms. The waveforms were generated at amplitude equal to that used in the mixing studies and also an amplitude at one half of this value. The results of this experiment are shown in Appendix I.

The displacements at fourteen locations along the median of a waveform were measured and compared to the displacement prediction at that point by the sine function. Residuals formed from this comparison were found in all

cases to be less than the standard error of estimate of the calibration equations. These results indicate two important characteristics of the system:

- (i) because input and output waves are both sinusoidal and because reducing the input amplitude results in the same direct reduction in output amplitude, the system response is linear in the range studied, and
- (ii) again because reduction in input amplitude results in a direct linear response in the output amplitude the effect of density currents appears to be negligible. If these density currents were active, one would expect a non-linear response when reducing the signal amplitude.

3.3.3 System Testing

Two configurations were studied as indicated in Figure 2. Both studies were performed under the following experimental conditions:

<u>Flow Rate</u>	<u>System Volume</u>	<u>Residence Time</u>	<u>Fluid Temp.</u>
2.13 gal/min.	17 gals.	8.27 min.	25°C

After an initial period in which flowrate, tank volume, and temperature were constant at the intended levels, the system was stimulated by an appropriate signal.

When a sinusoidal signal was used, it was found that the time required to reach steady state was reduced if the tracer concentration had already been introduced at a rate equal to the mean concentration of the sine wave. The number of waveforms which were needed depended upon the frequency. The tail of the first and last output waveforms began and decayed exponentially. The central portion of the waveform (or waveforms) were sine functions. From the experience it was found that the testing period (i.e., number of waveforms \times $1/\text{frequency}$) must exceed the total residence time of the system.

The input and output signals were recorded on a Honeywell Electronik 194 dual channel recorder. The extremum values, frequency, and phase lag could then be directly read from the recorder chart. The magnitude ratio is calculated after conversion of the extremum values of current to concentration units by a computer program. The frequency is calculated by measuring the distance between peaks of adjacent input or output waveforms and converting this distance to time by the chart speed factor. The phase lag is determined by measuring the distance between peaks of an input wave and the closest output wave following. This distance is converted to units of time, divided by the period of the waveform (reciprocal of frequency) and multiplied by 360 degrees.

CHAPTER 4

4 CONCEPTS OF FREQUENCY RESPONSE

4.1 Data Analysis

The development of a system analysis from frequency response data originated in the Electrical Engineering field. It has been found that the transfer function of a complex electro-mechanical system (such as an automatically controlled servo-mechanism) can be represented by an equivalent network of resistors, capacitors, and inductors. This concept is also useful in achieving the objectives of this work. The transfer function of a complex mixing situation which has been experimentally determined is represented as a network of ideal reactors. Thus the concepts presented here stem directly from automatic control theory (16).

As previously noted in the literature review, the frequency response of a system can be characterized by the change in amplitude and displacement between input and output waveforms. This information may be presented graphically in three ways: (16)

- (i) A curve on a polar plot on which each point is represented by a vector whose magnitude is equal to the amplitude ratio (output amplitude/input amplitude) and whose direction is equal to the system phase lag.

- (ii) A log amplitude and phase curve, on which the amplitude ratio in decibels (20 times the logarithm to base 10 of the amplitude ratio) is plotted against the phase lag in degrees.
- (iii) Bode Plot, a dual curve diagram on which the amplitude ratio in decibels is plotted against the logarithm of frequency and the phase lag in degrees versus the same abscissa.

The last graphical technique is the best with respect to parameter interpretation. This dual curve can be represented by one rational polynomial of the form:

(16)

$$\frac{a_n (j\omega)^n + a_{n-1} (j\omega)^{n-1} + \dots + a_0}{b_m (j\omega)^m + b_{m-1} (j\omega)^{m-1} + \dots + b_0} \quad (4-1)$$

where a and b are coefficients of the polynomial
 ω frequency

j complex operator equal to

This polynomial is labelled $G(j\omega)$ the transfer function of the system. Substitution of "s" for " $j\omega$ " transforms the polynomial to a transfer function in the s-domain (an added advantage). This system transfer function must now be interpreted in terms of ideal components forming a network.

The Bode diagram of an ideal CSTR is shown in Figure 6. The amplitude curve can be represented by two straight line segments, one of zero slope, and the second of slope -20 decibels/decade. The point of intersection of the two asymptotes (labelled the "break frequency") on the frequency axis is equal to the reciprocal of the residence time. The phase lag curve is typified by an "s" characteristic approaching a 90° phase shift at high frequencies. The transfer function of the component is represented by:

$$\frac{1}{\tau s + 1} \quad \text{in the } s\text{-domain} \quad (4-2)$$

$$\frac{1}{\tau j\omega + 1} \quad \begin{array}{l} \text{in the } \omega\text{-domain where } \tau \\ \text{is the residence time} \end{array} \quad (4-2)$$

and derived from mass balance as shown in (13) . Similarly for a PFTR component (13) and its Bode diagram is shown in Figure 7. The amplitude curve is simply a straight line of zero slope, while the phase lag curve is exponential. The expression $e^{-j\omega\tau}$ is an exact representation of this component. The expression, however, is non-rational when combined with the CSTR function. Thus to combine these components into a tractable expression, one requires an approximate representation of the PFTR function. Coughanowr and Koppel (13),

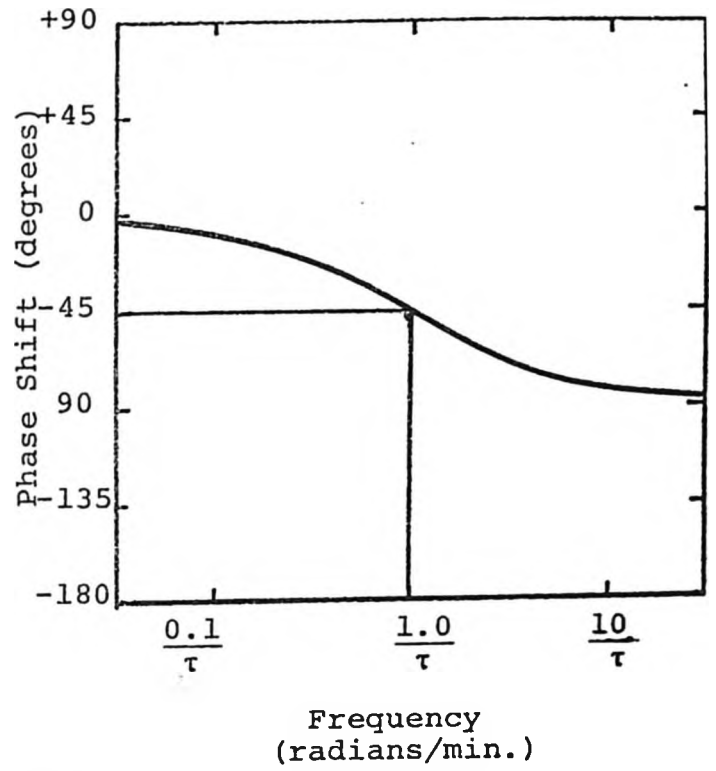
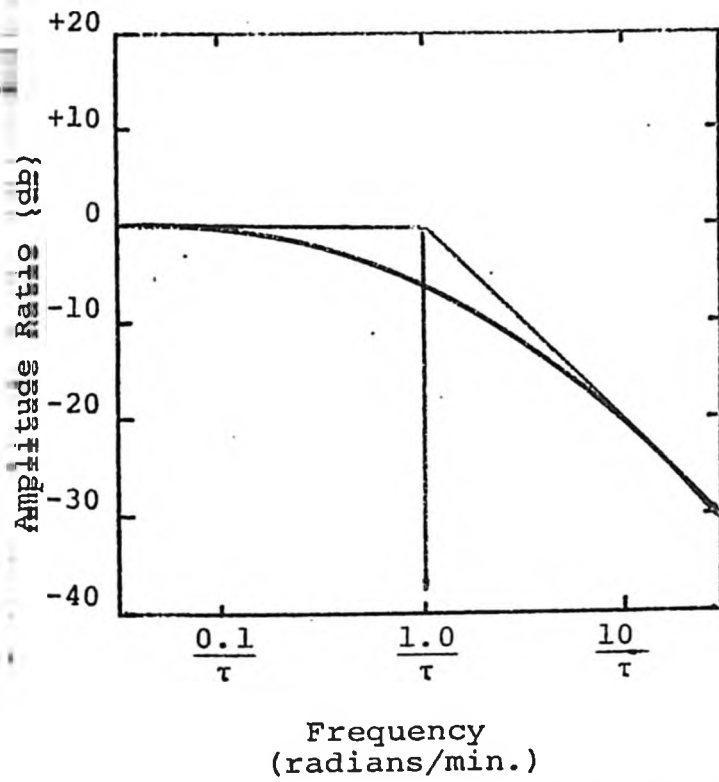


FIGURE 6

Bode Diagram of an Ideal CSTR

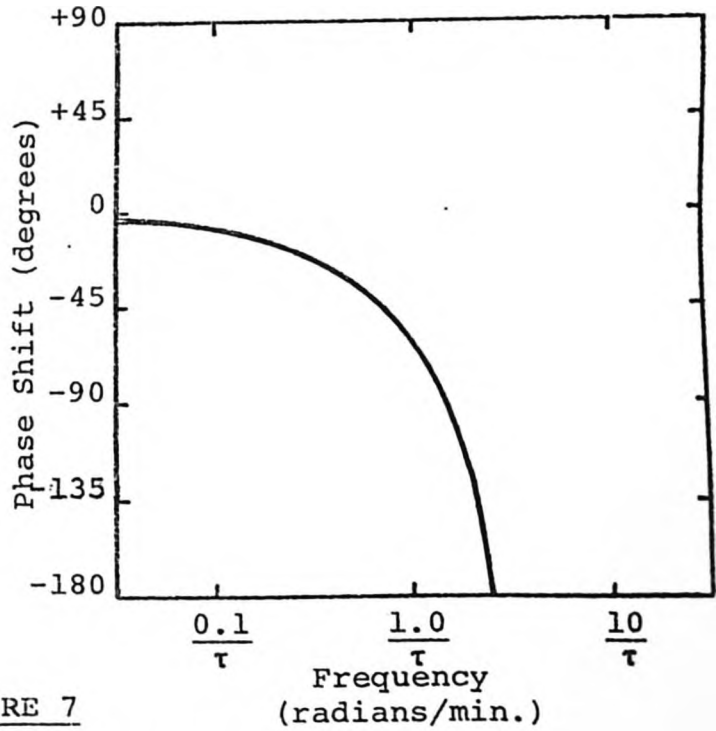
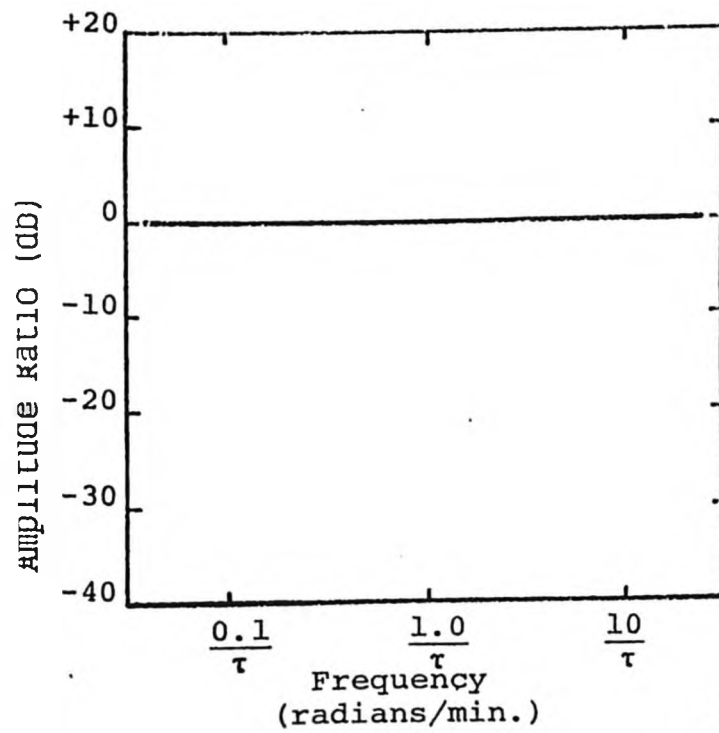


FIGURE 7

Bode Diagram of an Ideal PFTR

discuss the development of approximate forms. In these studies a transfer function was obtained by a Taylor Series expansion:

$$e^{-j\omega\tau} = \frac{e^{-j\omega\tau/2}}{e^{j\omega\tau/2}} = \frac{1 - \tau/2j\omega + \tau^2/2 + \dots}{1 + \tau/2j\omega - \tau^2/2 + \dots} \quad (4-4)$$

A first order approximation is obtained by truncation after the second term in the numerator and denominator.

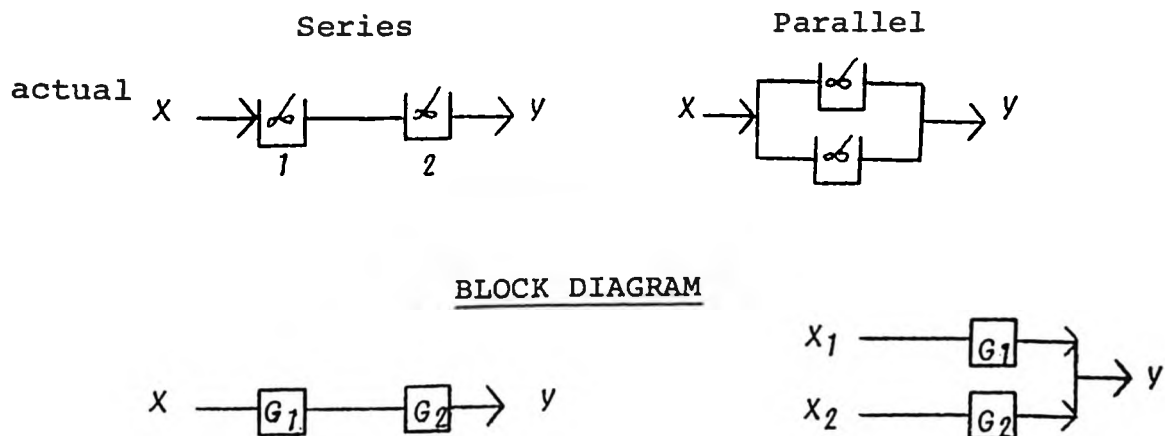
$$e^{-j\omega\tau} = \frac{1 - \tau/2j\omega}{1 + \tau/2j\omega} \quad (4-5)$$

This approximation is valid for amplitude over all frequencies but deviates from the exponential decay after the frequency is equivalent to the reciprocal of one residence time.

The amplitude curve of a system can be presented by line segments of slope $n \times 20$ decibels/decade, where $n = 0, 1, 2, 3, \dots$. As each segment is representative of a component, the number, size and type of components can be realized by this piecewise linearization of the amplitude curve. The system transfer function can also be deduced from these line segments. Both the numerator and denominator of this polynomial may be factored. The factors are called

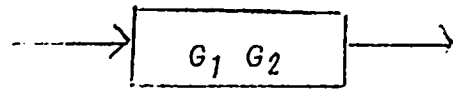
zeros and poles for the numerator and denominator respectively. A zero is illustrated by a straight line of slope +20 decibels/decade and a pole by a line with a slope of -20 decibels/decade. The zero and pole slopes originate on the Bode plot at the root values of the appropriate factor.

The system transfer function is derived from a proposed network of components in the following manner. Each component has its own transfer function as described earlier and is unique in the value of its own residence time. These transfer functions and their interdependence can be represented graphically by a block diagram as illustrated below for two CSTR's.



A formal procedure for the combination of individual transfer functions as represented on a block diagram has been developed in Control Theory (16). For a series network

the system transfer function is simply the product of the individual functions as illustrated:



For a parallel configuration the transfer function is derived as follows:

$$y = G_1 x X_1 + G_2 x X_2 \quad (4-6)$$

The flow split between the branches is not known but is dependent upon the total residence time of each branch after the total flow and volume of the system have been specified.

$$V_1 + V_2 = V_T \quad (4-7)$$

$$X_1 + X_2 = X \quad (4-8)$$

$$\tau_1 X_1 + \tau_2 X_2 = V_T \quad (4-9)$$

where V = volume of components and system. Subscripts 1, 2 and T refer to components 1, 2 and the total system respectively.

Solving equation (4-8) and (4-9) and substituting we have:

$$V_T = \tau_T X \quad (4-10)$$

$$X_2 = X \frac{(\tau_T - \tau_1)}{(\tau_2 - \tau_1)} \quad (4-11)$$

$$X_1 = X \frac{(\tau_T - \tau_2)}{(\tau_1 - \tau_2)} \quad (4-12)$$

Substituting into equation (4-6)

$$\frac{Y}{X} = \frac{\tau_T - \tau_2}{\tau_1 - \tau_2} G_1 + \frac{\tau_T - \tau_1}{\tau_2 - \tau_1} G_2 \quad (4-13)$$

or simplifying and substituting the CSTR transfer function (4-2)

$$\frac{Y}{X} = \frac{(\tau_1 + \tau_2 - \tau_T) S + 1}{(\tau_1 S + 1)(\tau_2 S + 1)} \quad (4-14)$$

It is necessary to express the split of flowrate in the network in order to properly weigh the effect of each branch to the total signal. This weighting of signals is particular to mass flow systems when concentration is monitored and is not usually encountered when one considers a control system in which a signal voltage becomes the dynamic variable.

To interpret the amplitude curve in order to propose a network model, the following observations are significant:

- (i) If the slope of the amplitude curve is continuously increasing and is negative, the ideal network consists of only one branch of components in series.*
- (ii) PFTR components linked in series with a single branch will not be shown on the amplitude curve. Evidence of their existence can be derived from either the phase shift curve or separate experiments utilizing pulse inputs.
- (iii) Portions of the amplitude curve where the slope is zero, increasing in a positive direction, or decreasing in a negative direction are indicative of parallel branches in the ideal network.
- (iv) The magnitude of the slope of the amplitude curve at high frequencies is indicative of the relative order of the zero and pole polynomials. (i.e., If the slope is -40 decibels/decade, the pole polynomial is two orders greater than the zero polynomial. If the slope is -20 decibels/decade, the difference in order is one.)

*This statement is true for all cases except when the transfer function of a parallel network contains a zero and pole having equal roots. This zero and pole will cancel each other, causing the parallel network to have the same amplitude ratio characteristic as a series network.

CHAPTER 5

5 MECHANICS OF ANALYSIS

5.1 General Method

The analytical scheme has three steps. First the experimental amplitude curve is linearized by line segments with slopes = $n \times 20$ decibels/decade (where $n = \pm 0, 1, 2, 3, \dots$). The number of line segments thus indicate the zero and pole content of the system transfer function. The intersections of these segments are noted on the frequency axis. These "break frequencies" are the root values of the pole and zero factors. The system transfer function has been derived graphically.

Second, the system transfer function is examined, and a network of ideal components which would yield that polynomial form are considered. If no zero was noted on the experimental curve, only one network can be proposed, a cascade of CSTR's with individual residence times equal to the reciprocal of the break frequencies. A parallel configuration is indicated when zeros are found. The presence of PFTR components must now be considered as the zero and pole of this component does not cancel when the transfer functions of the branches are added to form a complete network transfer function. It is quite possible that a number of parallel arrangements of ideal reactors can be postulated which will result in the same polynomial expression when simplified. A certain uniqueness, however,

remains for each arrangement. The coefficients of the transfer function are functions of the component residence time, and this functional form is dictated by the arrangement of the network proposed.

The third step is to determine the best estimate of the component residence time for each network. This is performed by the numerical search technique where the best estimates are taken as those leading to the minimum residual sum of squares when compared to the experimental amplitude curve.

Techniques of discrimination among several proposed networks that fit the experimental response equally well are discussed in the section dealing with the author's treatment of experimental data.

The prediction of the phase lag from the proposed network must be considered. Also the magnitude of a PFTR component in series with the remainder of the network must be evaluated. This component does not effect the amplitude curve as its gain is unity. A one dimensional search is used to determine this magnitude. If a series network is proposed, the calculation order is straightforward. For a parallel-type network, an iterative approach is required. To solve for flow split between parallel branches it is required that the total residence time of the system less the residence time of the in-series PFTR component is known.

Initially this value is estimated. A reasonable estimate of this value can be obtained if one considers the delay or dead time found between the input and output signal. The estimate of the residence time of the in-series component is found which minimizes the deviation between experimental and predicted results, based on the least sum of squares criteria. This value is then used to calculate the total residence time of the remainder of the network. If the new estimate differs from the initial by less than a preset convergence limit (1% in this case) the calculation order is terminated. If not, the new total residence time value is used to calculate the flow split between branches. The calculation order is repeated to obtain up-dated residence time estimates for all components of the network. The third step has been adapted to computer programming.

5.2 Program Format

A computer program has been written to estimate the residence times of a single proposed network from the experimental frequency response data. An algorithm, printout, and input and output case data used in these studies is presented in Appendix III. The background of the computation techniques utilized in the program is discussed here. The input frequency response data is presented (as in the Bode diagrams) in two sets, the amplitude ratio, and the system phase lag. Each data set is handled separately resulting

in a two stage calculation order.

First, a numerical search patterned after the Rosenbrock Method (48) is performed on the amplitude data. The best estimates of the component residence times are obtained. The best parameter estimates are taken as those values which lead to predicted amplitude ratios that exhibit a minimum residual sum of squares when compared to the experimental data.

In stage two, these estimates are used in the network model to predict the system phase lag. The phase lag is first calculated without consideration of the in-series component. An attempt is then made to improve the predictions by fitting an in-series PFTR component. As noted in the previous section, the change in magnitude of this component from an initial estimate can effect the parameter estimates of the other components in the network. A convergence test is therefore used to determine if the change in magnitude is sufficient to warrant recalculation of all of the network parameters. In these studies a convergence limit of approximately 1% was chosen.

A summary of the input information required for this programming is:

- (i) experimental frequency, amplitude and phase lag data, as well as the total residence time of the system,

- (ii) initial estimates of the component residence times obtained from the linearization of the experimental amplitude curves and a dead time estimate,
- (iii) operational limits on the search (e.g., number of trials, etc.) and constraints on the values which the parameter estimate may assume,
- (iv) function statements based on a particular network which relate the component residence times to the coefficients of the system polynomial.

5.2.1 Executive Program

The search program consists of two subroutines; "Rosen" an executive program to direct the search pattern, and an object program which provides the sum of squares at each new parameter estimate.

The numerical search is basically a trial and error method to obtain the minimum value on a response surface. All parameter estimates are varied simultaneously. The response surface is a function based on the difference between experimental data and the model predictions and the model parameters.

As the search proceeds across the response surface

the model parameters are varied in an unique manner based on the past history of successes and failures.

The path that is taken across the response surface is directly related to relative incremental change in each parameter. If the preceeding step results in a failure, the magnitude of the stepsize is reduced by multiplication with a factor whose value is less than unity, and the search proceeds in the opposite direction. Similarly if the last step was a success then the succeeding stepsize is increased by a factor whose value is above one. The search moves in the direction of the parameter resulting in the best success. Each of these steps is called a trial.

The overall direction for a set of trials is influenced by a term called the unit vector, with components equal to the number of search variables. The stepsize of a variable is the product of the component term of the vector and the stepsize calculated in the preceeding paragraph. Initially the indices of the unit vector are set approximately at one and zero in order that variables change in directions perpendicular to each other. A set of trials performed under a constant unit vector is called a stage.

The unit vector is modified after the search has met a success with each variable. This must happen. Even when the change of a variable meets in failure the stepsize will decrease to the point where no change has been made

from its initial value and this is taken as a success. The new unit vector is calculated from the normalized vector joining the initial and final point of the search path through one stage. Thus the search path is always proceeding in the direction of that variable resulting in success.

Normally, it is necessary to constrain the search area to those values of the variable that have physical meaning. For example, the residence times must be positive and non zero. Specific constraints used in each case study are discussed in the section titled "Experimental Results and Interpretation".

The constraints are located in the object subroutine. If the executive program calls for a parameter value beyond the constraint, this value is rejected by the object program and replaced by a parameter value at the constraint. The object program then proceeds to calculate the residual sum of squares at this value.

5.2.2 Objective Program

The system transfer function is presented as a polynomial. Receiving the parameter values from the executive subroutine, and after testing to determine if these values lie beyond the constraints, the coefficients of the system polynomial are calculated. The polynomial is then factored numerically to determine the pole and zero content. The polynomial is factored in the s-domain to eliminate the

imaginary coefficients. The conversion to the frequency domain is performed on the poles and zeros by substitution of the frequency term " $j\omega$ " for the Laplace term " s ".

The numerical factoring technique is the La Grange interation method, which is a third order method, starting with a complex guess for each root used. Each time a root is found the polynomial is divided by the linear factor and the process continued. This technique is available as a library subroutine called ROOT3Ø on the CDC 6400 computer. Note the system polynomial was arranged in order that the coefficient of the highest order term is one.

Once the zeros and poles of the transfer function are known, the amplitude ratio at each frequency can be calculated from the following expression:

$$AR_i = 20 \log \frac{\prod_{j=1}^{n} \left((IR_j + \omega_i)^2 + R_j^2 \right)^{1/2}}{\prod_{\ell=1}^{m} \left((IR_\ell + \omega_i)^2 + (R_\ell)^2 \right)^{1/2}} \quad (5-1)$$

at frequency " ω_i " for n zeros and m poles where IR represents the imaginary component of the root, R the real component.

5.2.3 Main Program

The main program performs three functions:

- (i) to receive and transfer input and output information,

- (ii) to calculate the system phase lag, and
- (iii) to decide if calculation order must be repeated to obtain model parameters that satisfy both amplitude ratios and phase lag predictions.

The coefficients of the transfer function are now calculated using the best estimates of the component residence times. The polynomial is again factored numerically to determine the zeros and poles. The phase lag of the network is then given by the expression:

$$\begin{aligned}
 PL_i &= \sum_j^n \tan^{-1} \left(\frac{\omega i + j IR_j}{R_\ell} \right) \\
 &- \sum_\ell^m \tan^{-1} \left(\frac{\omega i + IR_\ell}{R_\ell} \right) \quad (5-2)
 \end{aligned}$$

at the frequency " ωi " for n zeros and m poles.

It is now required to add the phase lag contribution of the in-series PFTR component. The phase lag of this component is given by

$$PL_i = - \omega i \tau_{PFTR} \quad (5-3)$$

as derived from its exact transfer function.

The residence time " τ_{PFTR} " is found by a grid search. First a large step value is used to find approximately the best estimate. The search is then conducted again in the neighborhood of this estimate with a stepsize one-tenth of the original.

Equations (5-2) and (5-3) are then added to obtain the total predicted phase lag. If a series network is being tested the calculation order is complete.

As seen in Section (5-1) the residence time of the in-series PFTR component effects the calculation of the flow split between branches of a parallel network. Consequently, all parameter estimates are affected. The computation is complete when the estimate of τ_{PFTR} is not significantly different from its previous estimate. Initially this estimate is usually zero (i.e., it is assumed no in-series component exists). A significant change in " τ_{PFTR} " is taken as a value that causes a 1% change in the residence time of the remainder of the network. The computation order is repeated until this convergence limit has been met. After iteration, the parameter estimates will provide model predictions that satisfy both experimental curves.

5.3 Experimental Results and Interpretation

As stated earlier, two flow patterns were tested. The configurations of baffles and mixers are shown in Figure 2.

For configuration "A" the rectangular test section was divided into four compartments. The fluid in the first and third compartments was well agitated by portable mixers. The second and fourth sections were allowed to remain quiescent. The baffle arrangement was such that the fluid must flow consecutively from the first to the last compartment and short circuiting through each section was minimized. This system was tested at eighteen separate frequencies over a two decade range as illustrated in the plot of the experimental data (Figure 8).

Examining the experimental data, the following was deducted. First, the experimental amplitude ratio points defined a curve whose slope was monotonically decreasing. This characteristic indicates a lack of zeros in the system polynomial; suggesting that the mixing components are arranged in a series or cascade network. Second, the final slope at high frequencies (3 to 6 rad/min) approached a line segment whose slope is -60 decibels/decade. This occurrence is an indication that at least three poles occur in the system polynomial, or an equivalent network may be constructed from three components in series.

In the second step, the experimental amplitude curve was linearized in a piecewise manner by three line segments having slopes of -20, -40, and -60 decibels/decade respectively. The intersection of these line segments with each other, and

FIGURE 8

Experimental Data

From Configuration A

P.B. Melnyk
November, 1969.

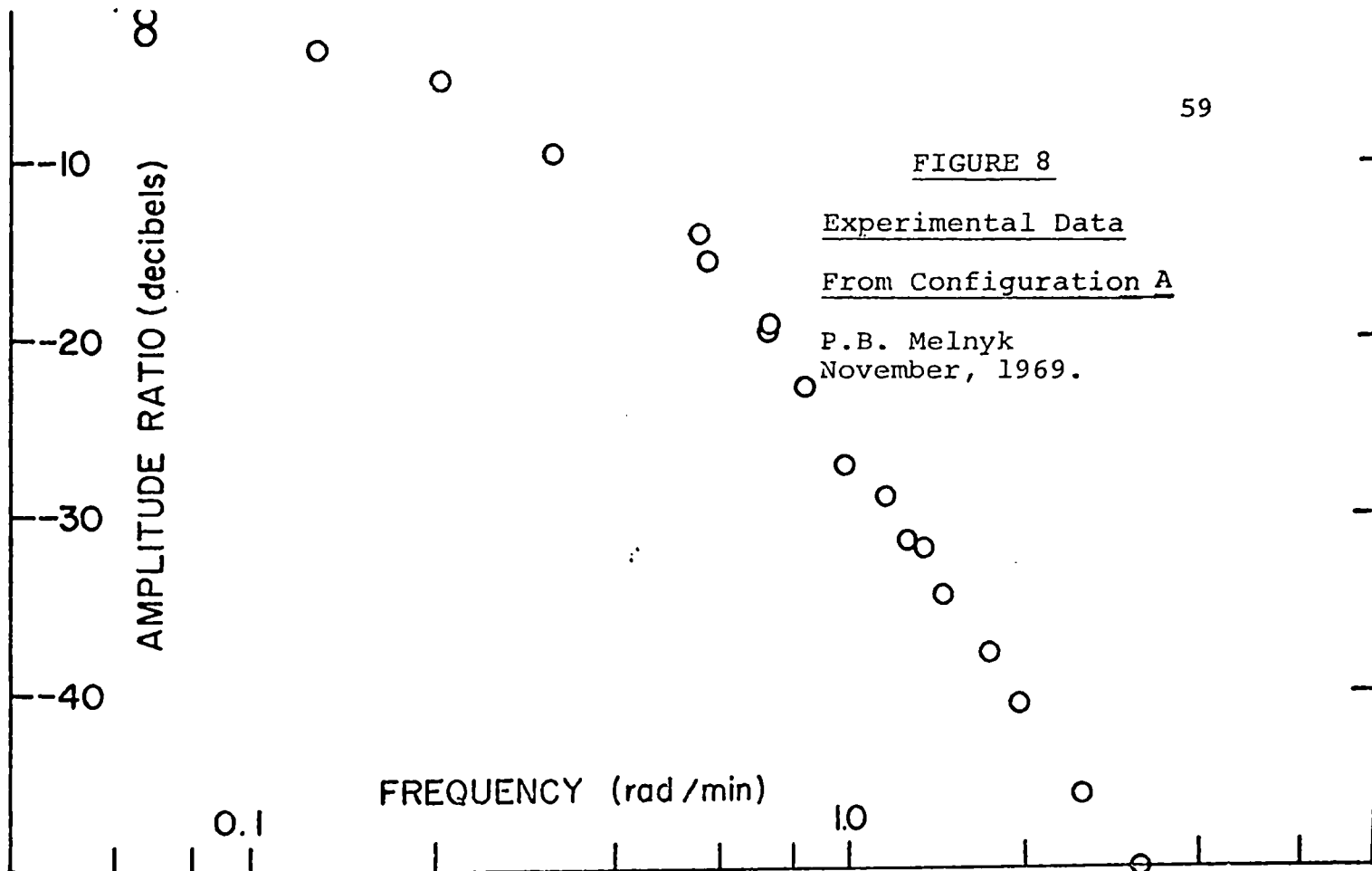
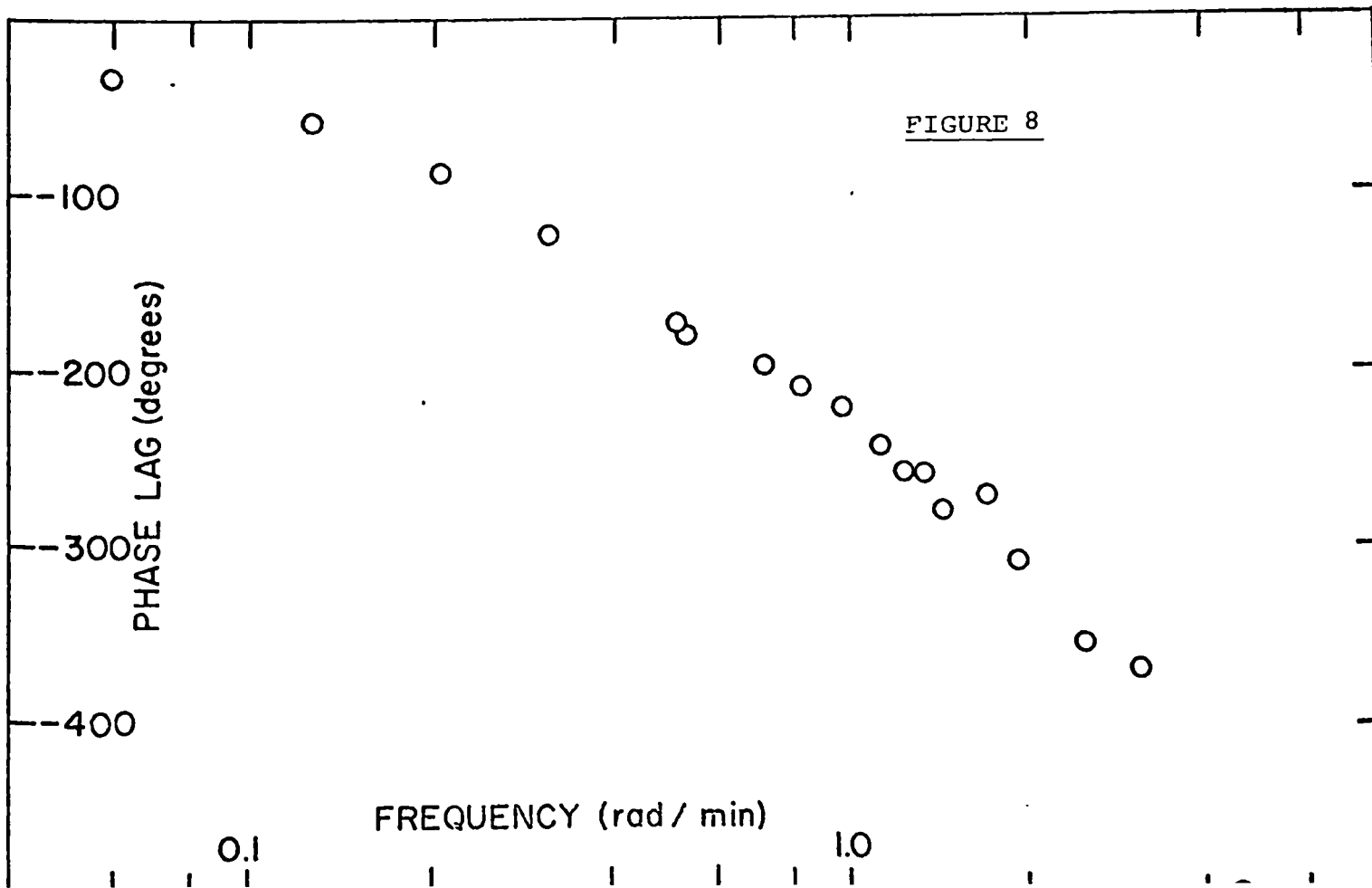


FIGURE 8



The residence time of a PFTR component in-series to the cascade network was also found. This component minimized the deviation between the phase lag predicted by the "3 CSTR's" model and that experimentally measured. Two constraints were placed on the numerical search for model parameters:

- (1) The residence time of each component was positive and non-zero.
- (2) The sum of all of the component residence times was less than or equal to the residence time experimentally measured for the test system.

The final estimates of residence times are:

- (i) for the three CSTR components: 1.96, 2.54, and 2.44 min.
- (ii) for the in-series PFTR: 0.862 min.

The standard errors of estimate (defined as the square root of the residual sum of squares over the degrees of freedom) for the amplitude and phase lag curves respectively are 2.675 decibels and 11.24 degrees. An inherent disadvantage in numerical search techniques is that the search path may be prematurely terminated at a local minimum rather than the global minimum. This may be overcome in two ways. First the search may be initiated at a number of different locations on the response surface. Secondly, a general indication of

the topography of the surface can be obtained from a coarse grid search. Both methods were utilized in this case to confirm the location of the global minimum on the response surface.

A naive analysis may be performed on the standard errors of estimate to determine if this error is the result of experimental errors. As shown in Appendix II, the experimental error was found to be correlated to the frequency (i.e., as the frequency increases, the experimental error on the amplitude curve increases). Noting Figure 9. it is seen, however, that large deviation between experimental and predicted values on the amplitude curve occur at frequencies of less than 0.8 rad/min. Thus an experimental deviation of .15 will be chosen to compare the standard error of estimate. Conversely, the estimate of the standard deviation for the phase lag curve was found independent of frequencies. A pooled estimate is 5.74 degrees. The following F-ratio values were obtained:

Amplitude curve: $F = 16.7$

Phase lag curve: $F = 1.9$

while $F_{.05, 15, 4} = 5.87$

These results would indicate that the deviation between predicted and experimental values on the amplitude curve are greater than that which may be accounted for by experimental error. The opposite conclusion is reached in regard

the uppermost segment with the zero axis determined the "break frequencies". The reciprocal values of these "break frequencies" were taken as the initial estimates of the component residence times. These values are listed in the following table:

TABLE 5.1 Initial Estimates of Residence Times		
<u>Component #1</u>	<u>Component #2</u>	<u>Component #3</u>
1.59 min.	5.24 min.	0.4 min.

As the experimental amplitude curve gave no indication of the presence of zeros in the transfer function, the three components were taken to be CSTR's. The combination of the transfer functions of three CSTR's results in a system transfer function composed solely of three poles.

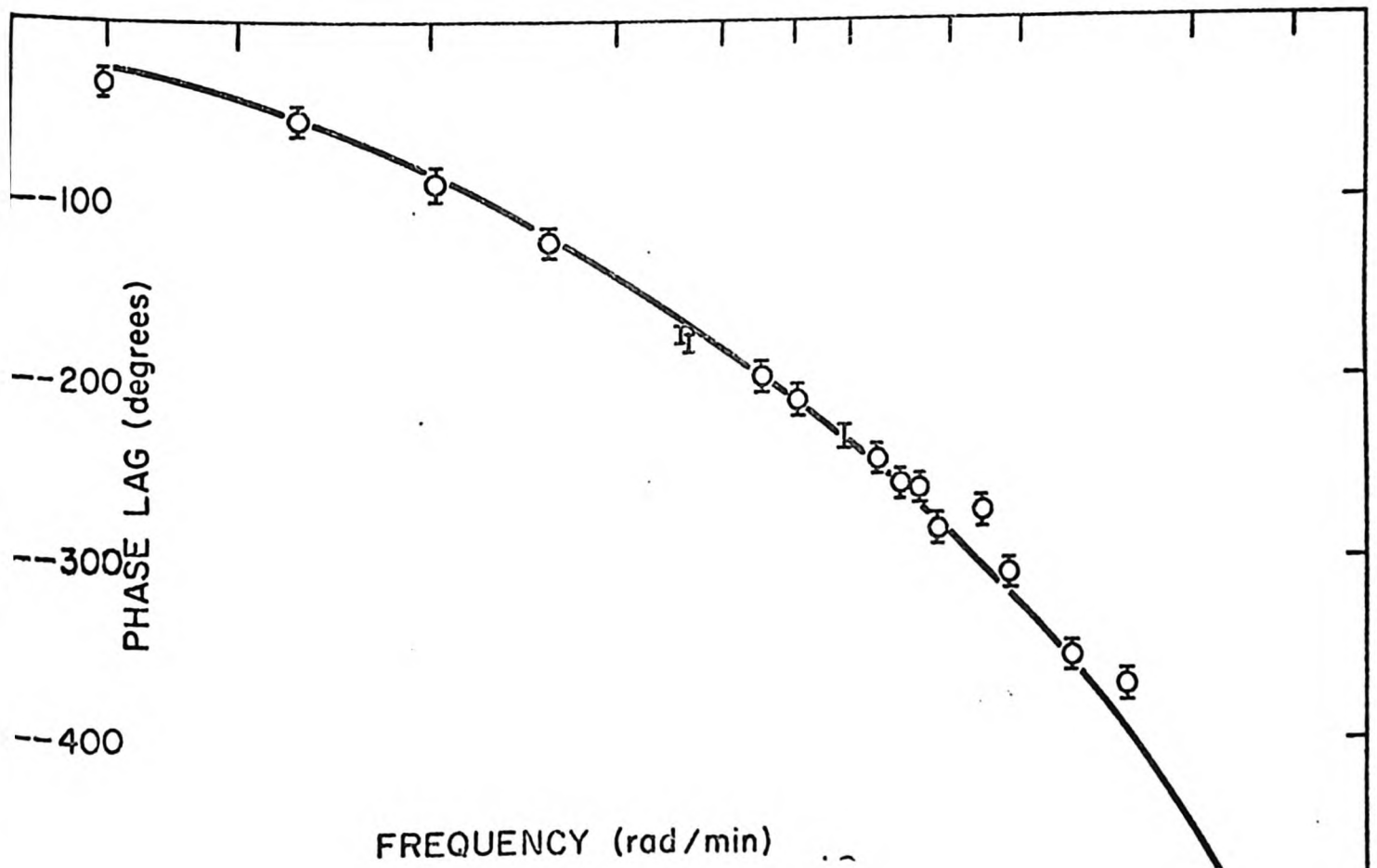
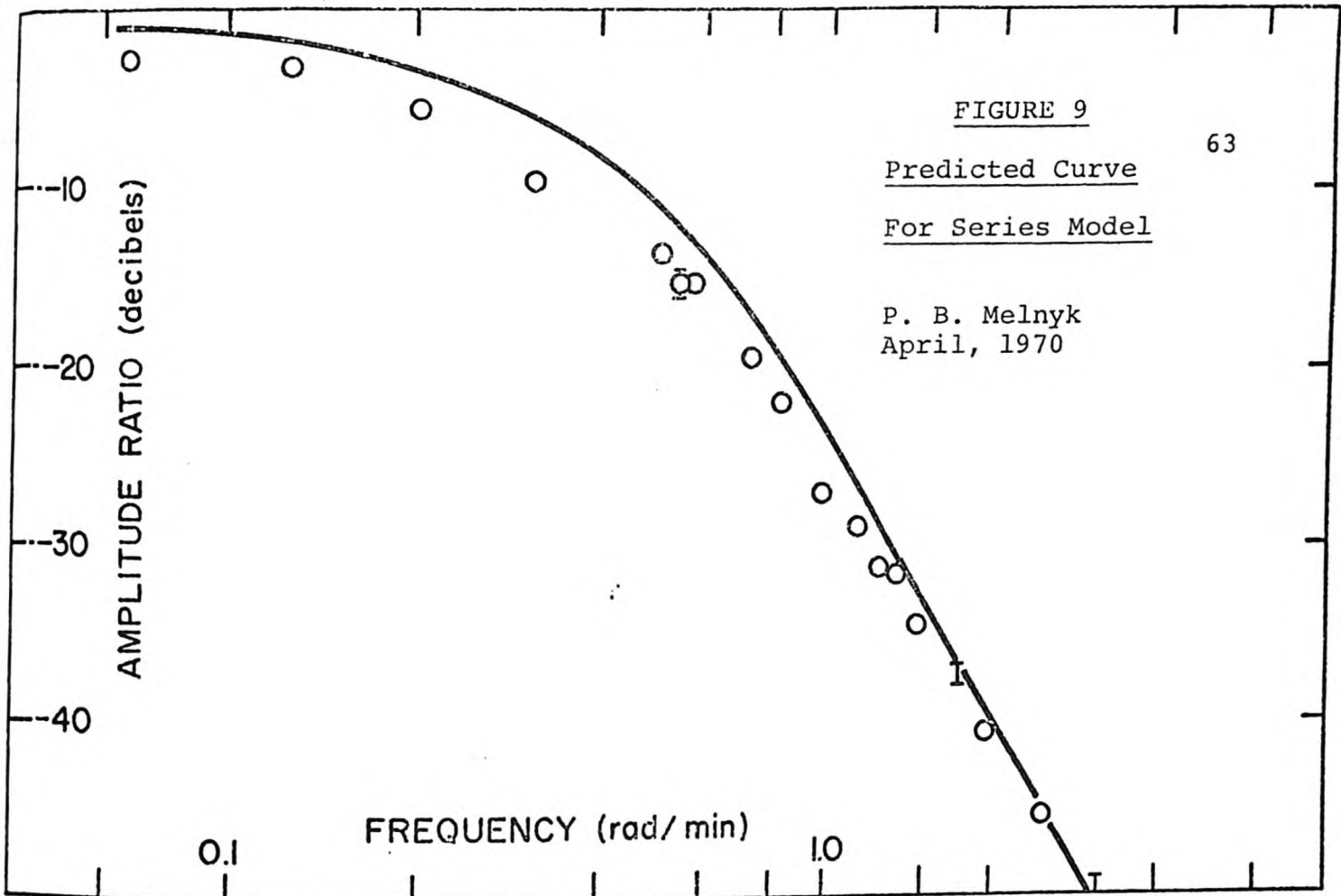
$$T = \frac{1}{(\tau_1 j\omega + 1) (\tau_2 j\omega + 1) (\tau_3 j\omega + 1)} \quad (5-4)$$

These initial residence time estimates were used to calculate the final parameters for a "3 CSTR's" in-series model. The calculations were carried out by the computer search program discussed at length in the previous section.

FIGURE 9

Predicted Curve
For Series Model

P. B. Melnyk
April, 1970



AMPLITUDE RATIO (decibels)

FIGURE 10

Experimental Data

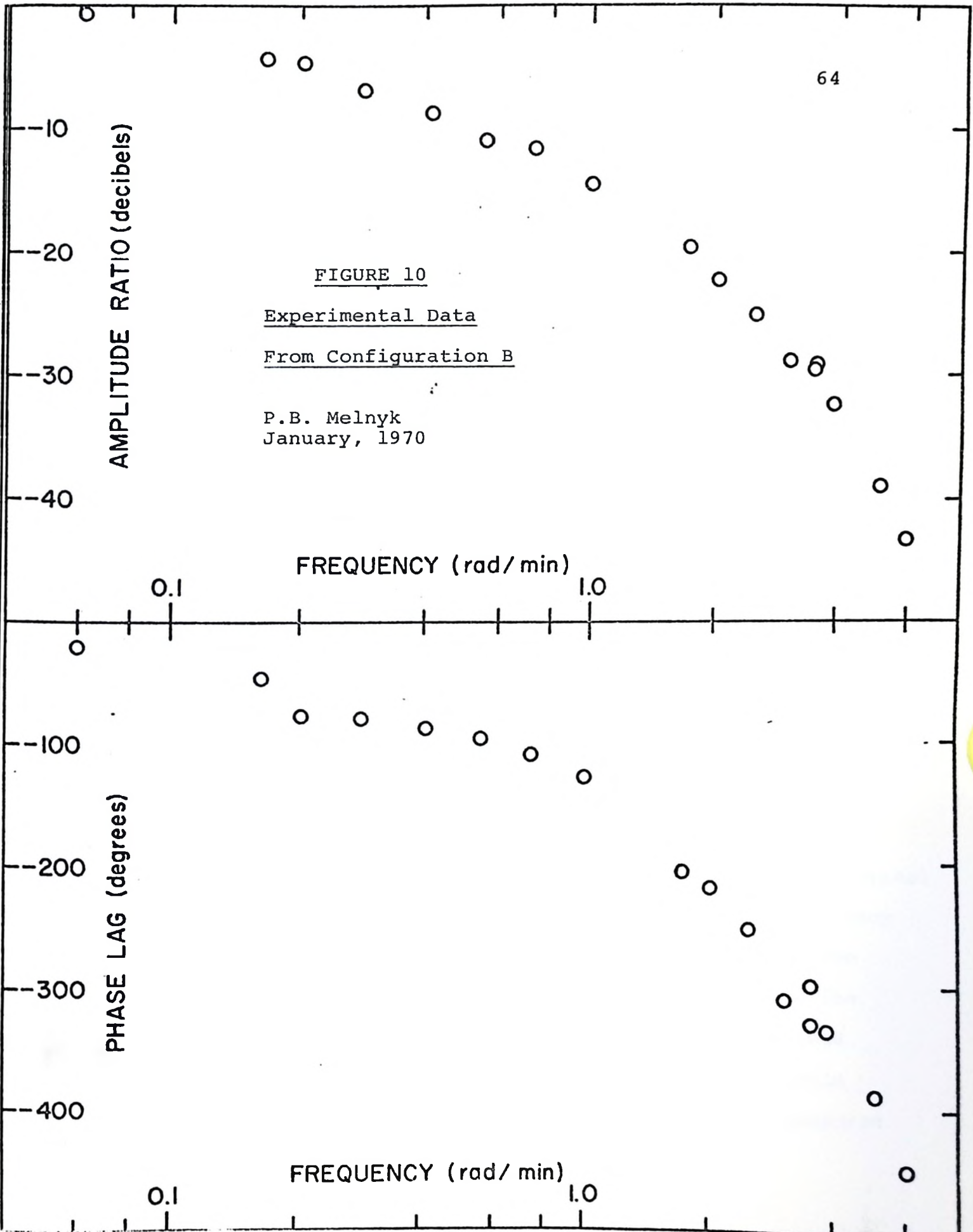
From Configuration B

P.B. Melnyk
January, 1970

FREQUENCY (rad/min)

PHASE LAG (degrees)

FREQUENCY (rad/min)



to the phase lag curve. The model may also be tested against another type of response, the prediction of conversion. The information gained from testing conversion predictions will be discussed in the succeeding chapter.

The baffle configuration (labelled "B" in Figure 2) was arranged to obtain non-ideal parallel flow. The flow split between the sections was approximately 2:1. One branch of the system was also divided into two compartments. Portable mixers were located at junction points of the parallel branches to provide well mixed regions. The intermixing of fluid between parallel streams was quite possible as the baffles dividing these streams were not tight fitting. This system was tested at sixteen different frequencies as shown in the plotted experimental data in Figure 10.

Examining the amplitude ratio curve the trend of the experimental points indicated a definite discontinuity occurring at frequencies between 3 and 4 rad/min. The significance of this discontinuity was confirmed by statistical analysis and duplication of the experiment at this frequency range. If the amplitude curve was continuous between the frequencies 3 rad/min. and 4 rad/min., an estimate of the amplitude ratio at a frequency of 3.55 rad/min. obtained by interpolation on a slope of -40 decibels/decade would yield a value of 31.4 decibels. The average value measured

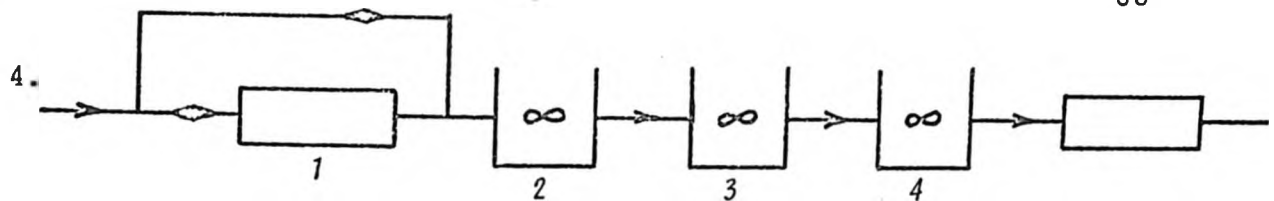
at this location from five replicate trials is 29.12 decibels with an estimated standard deviation of .717 decibels. The two amplitude ratios were compared by a one-sided test under the null hypothesis that the amplitude value is equal to and not less than the true mean (interpolated value). This hypothesis was rejected at the 95% confidence level. The experimental t-value was 3.18. Thus it is concluded this discontinuity is greater than that which would result from experimental error. The importance of this discontinuity is that it indicates the presence of a zero in the system polynomial.

The final slope of the amplitude curve approaches a line segment whose slope is -60 decibels/decade. From this information, one may conclude the system polynomial is composed of at least four poles and one zero.

A zero is obtained in the system polynomial if the proposed network includes at least two CSTR components with unequal residence times in parallel with each other or short circuiting about one component. These proposed networks are illustrated by configurations #1 and #4 in Figure 11.

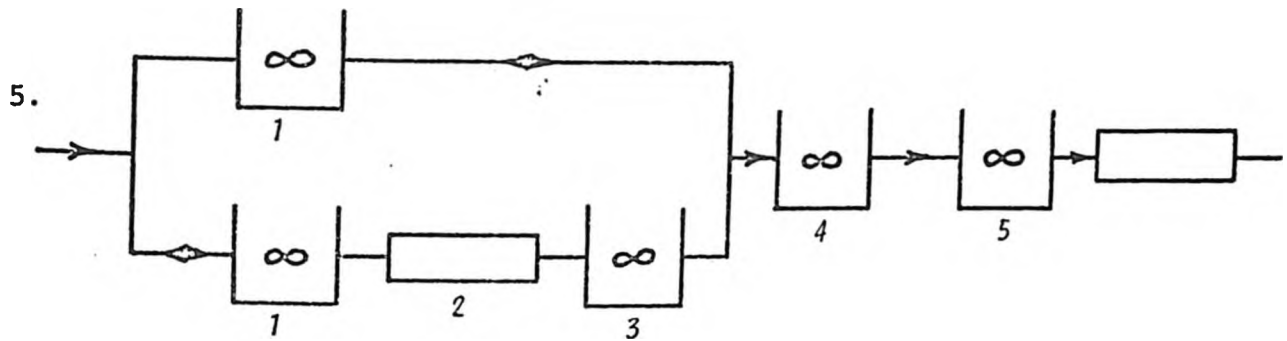
A slight discontinuity was also noted between frequencies 0.55 rad/min. and 0.7 rad/min. Therefore, the possibility of two zeros occurring in the system polynomial was tested. The addition of a zero to the system transfer

FIGURE 11, Con't.



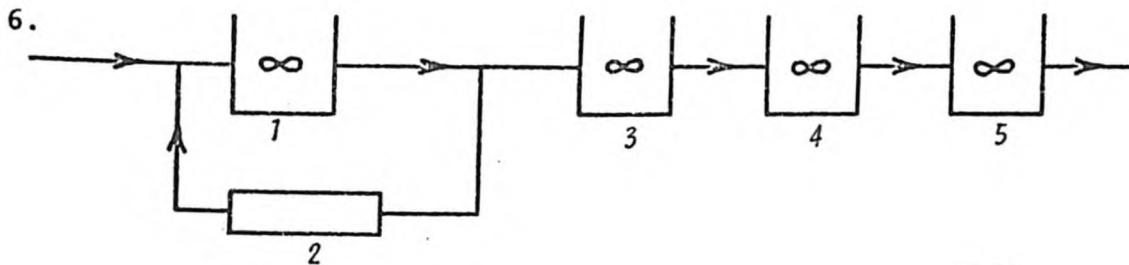
FLOW SPLIT

- A. TOP 84% BOTTOM 16%
- B. TOP 143% BOTTOM -43%



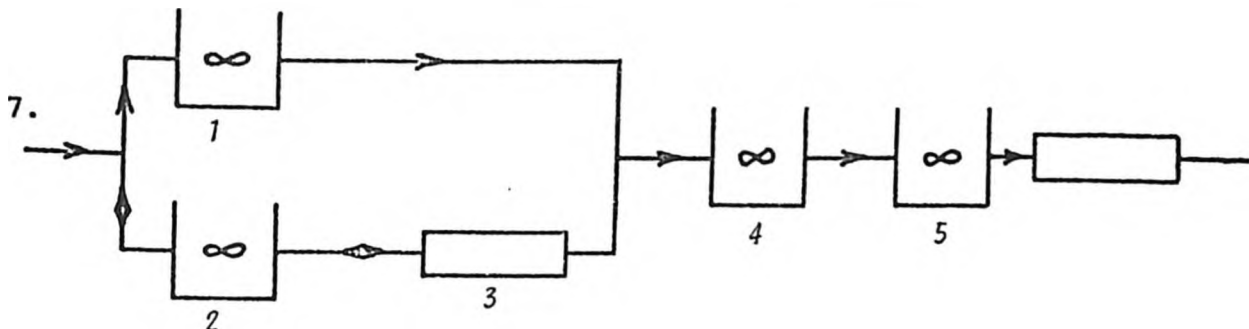
FLOW SPLIT

- A. TOP 24% BOTTOM 76%
- B. TOP 144.5% BOTTOM -44.5%



FLOW SPLIT

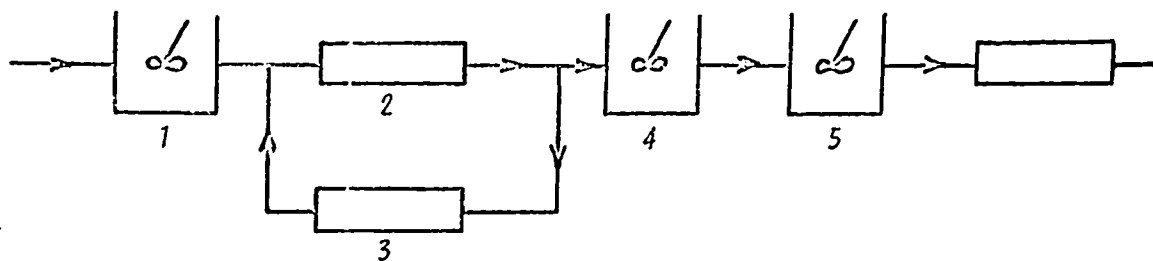
- A. TOP 115% BOTTOM -15%
- B. TOP 175% BOTTOM -75%



FLOW SPLIT

- A. TOP 129.5% BOTTOM -29.5%
- B. TOP 0% BOTTOM 100%

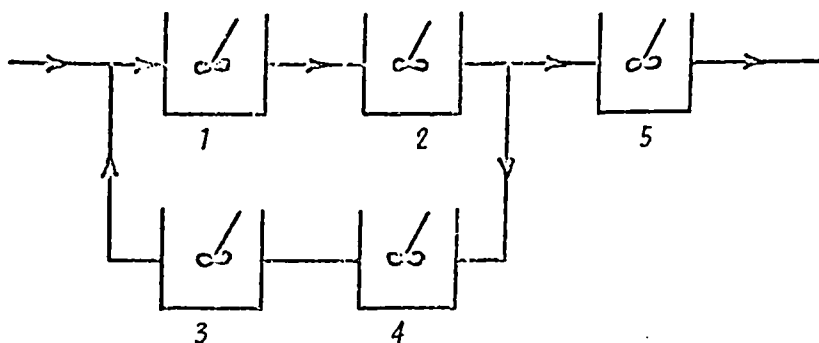
8.



FLOW SPLIT

A. TOP 151.5% BOTTOM -51.5%
 B. TOP 139.3% BOTTOM -39.3%

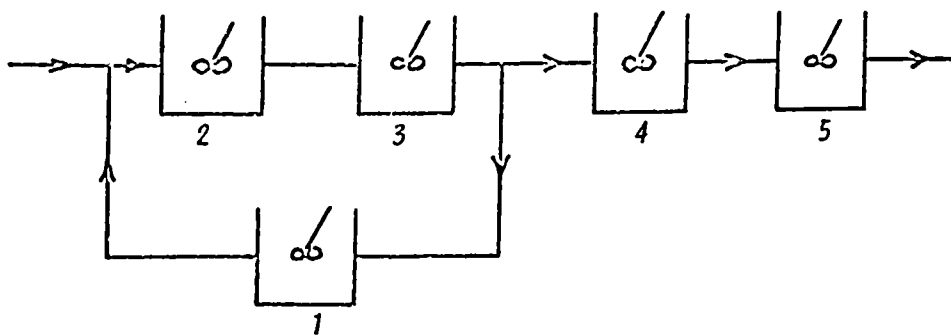
9.



FLOW SPLIT

A. TOP 125.6% BOTTOM -25.6%
 B. TOP 100% BOTTOM 0%

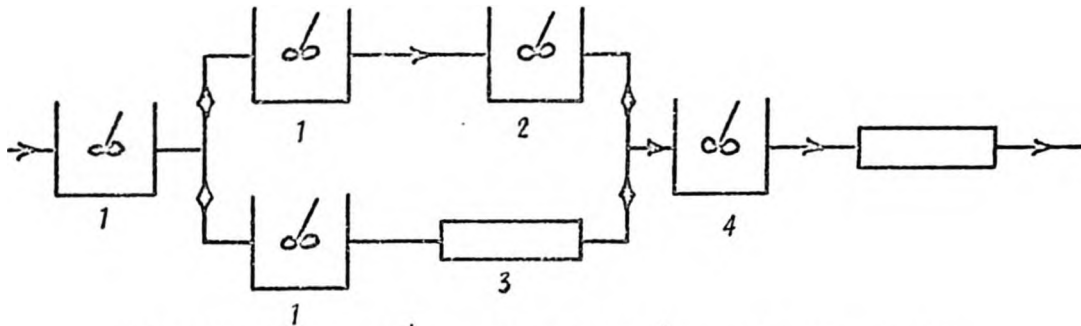
10.



FLOW SPLIT

A. TOP 183.3% BOTTOM -83.3%
 B. TOP 183.3% BOTTOM -83.3%

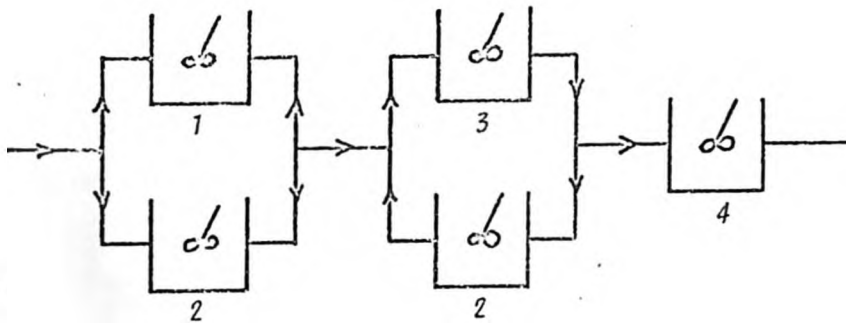
11.



FLOW SPLIT

A. TOP 104.8% BOTTOM -4.8%
 B. TOP -30% BOTTOM 130%

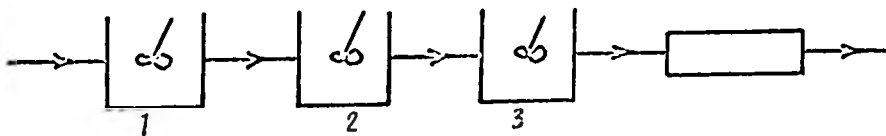
12.



FLOW SPLIT

First Section TOP 38% BOTTOM 62%
Second Section TOP 183.5% BOTTOM -83.5%

13.



function necessitated the inclusion of a pole. Because the final slope of the amplitude curve approached -60 decibels/decade, the orders of the zero and pole polynomials must differ by three.

Eight parallel networks which yield a second-fifth order transfer function are illustrated in Figure 11. Also a cascade of three CSTR's which yield a third-order transfer function was tested as a mixing model. In all cases, the residence time of an in-series PFTR was included.

The initial estimates of the residence times of the components were determined by the piecewise linearization technique discussed earlier. These original values are:

	<u>Component #1</u>	<u>#2</u>	<u>#3</u>	<u>#4</u>	<u>#5</u>
Third-order model	6.0 min	0.7	0.4		
First-Fourth order model	6.0 min.	1.4	0.7	0.4	
Second-Fifth order model	6.0 min.	1.4	0.7	0.4	0.4

Each of the parallel networks were tested twice; first with the largest component residence time placed in one of the branches and secondly with this estimate placed in the series portion of the network. The analytical transfer

function of all of the networks are listed in Appendix III.

The final parameter estimates are listed in Table 5.3, along with the standard error of estimate for each curve. It is quickly realized that parameter values can be chosen for most of the networks, such that they provide equally good predictions of the amplitude ratio. The decision as to which of the proposed networks is the best representation of the mixing state of a system must be made by testing the models by another type of response. Thus model discrimination becomes the main topic of the next chapter.

Table 5-3

Configuration Number	<u>Residence Time Estimates</u> (min.)					<u>Standard Error of Estimate</u>		
	Component #1	Component #2	Component #3	Component #4	Component #5	In-Series PFTR	Amplitude (decibels)	Phase Lag (degrees)
1	0.43	0.43	0.43	0.43	5.96	0.0	1.0	48.0
2-4A	15.21	.85	2.20	.11		0.35	2.39	19.3
B	0.37	0.37	7.40	0.36		.68	1.36	15.7
5 A	1.98	.44	6.45	.33	.14	.556	1.13	12.8
B	.34	1.54	.6	8.73	.3	.631	.93	11.6
6 A	6.25	2.32	0.46	0.42	0.44	0	.98	44.7
B	1.42	1.43	6.15	0.32	0.41	0	1.00	44.0
7 A	.29	1.35	3.76	9.26	.183	0.645	1.37	19.9
B	1668	1.4	.23	14.36	1.05	0	1.66	115.0
8 A	8.40	.34	1.78	0.30	0.45	.382	0.86	15.3
B	8.14	3.56	1.14	0.34	0.32	.068	0.97	32.2
9 A	6.01	.15	.47	.41	.3	0	.89	47.4
B	.41	.24	.41	.24	6.09	0	.93	47.3
10 A	1.01	0.37	0.57	7.41	0.37	0.56	.89	36.9
B	1.28	.86	.86	6.7	.299	0	1.01	44.0

Con't.

Con't.

Table 5-3

		<u>Residence Time Estimates</u> (min.)					<u>Standard Error of Estimate</u>		
Configuration Number		Component Number					In-Series PFTR	Amplitude (decibels)	Phase Lag (degrees)
		#1	#2	#3	#4	#5			
11	A	.40	6.4	2.9	.13	0.226	2.68	24.0	
	B	.09	.65	2.79	6.07		2.89	17.1	
12		7.38	.42	.73	2.90	0	.88	71.1	
13		.28	.26	5.08		.652	1.44	16.15	

AMPLITUDE RATIO (decibels)

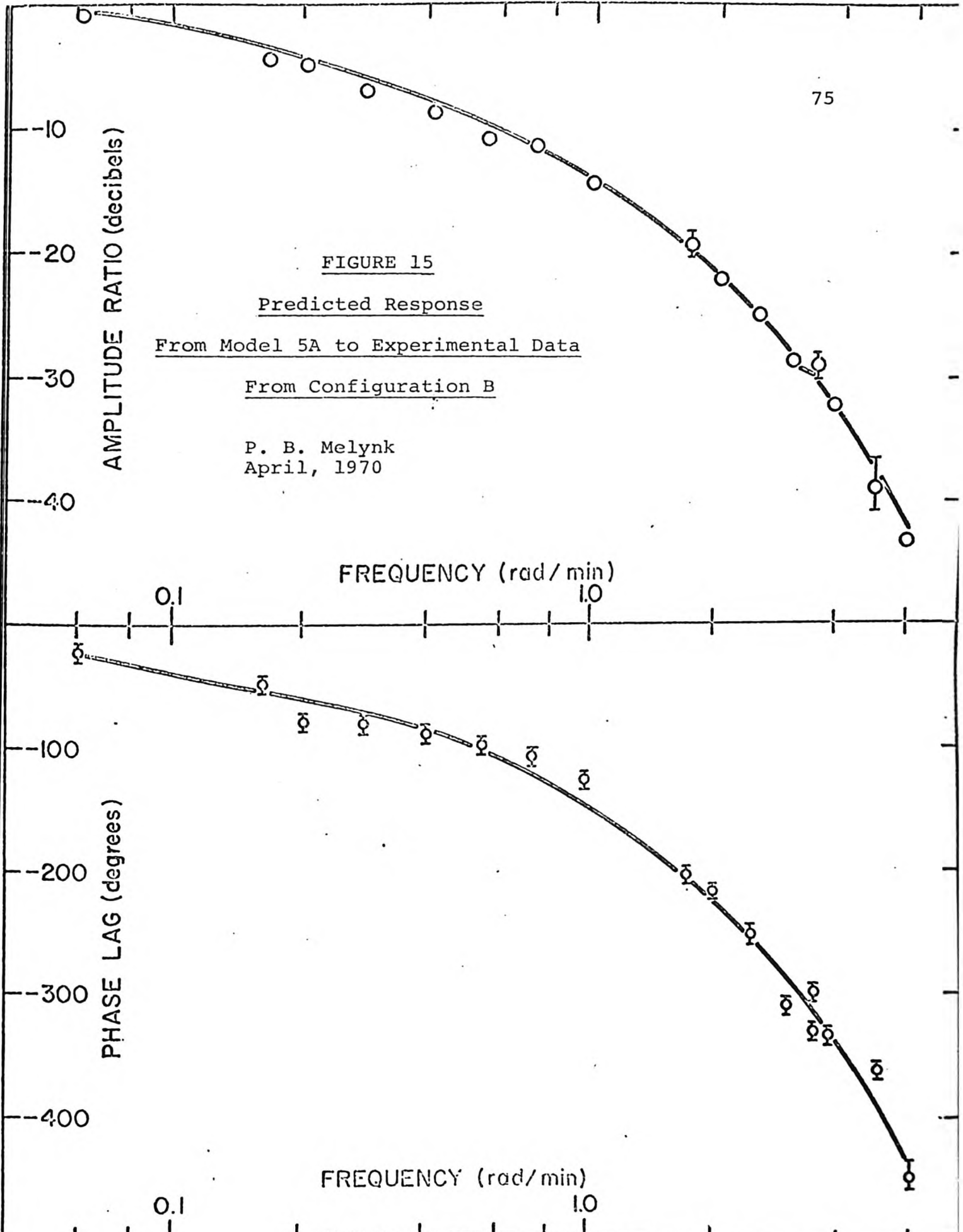
FIGURE 15

Predicted ResponseFrom Model 5A to Experimental DataFrom Configuration BP. B. Melynk
April, 1970

FREQUENCY (rad/min)

PHASE LAG (degrees)

FREQUENCY (rad/min)



AMPLITUDE RATIO (decibels)

0.1

FREQUENCY (rad/min)

1.0

PHASE LAG (degrees)

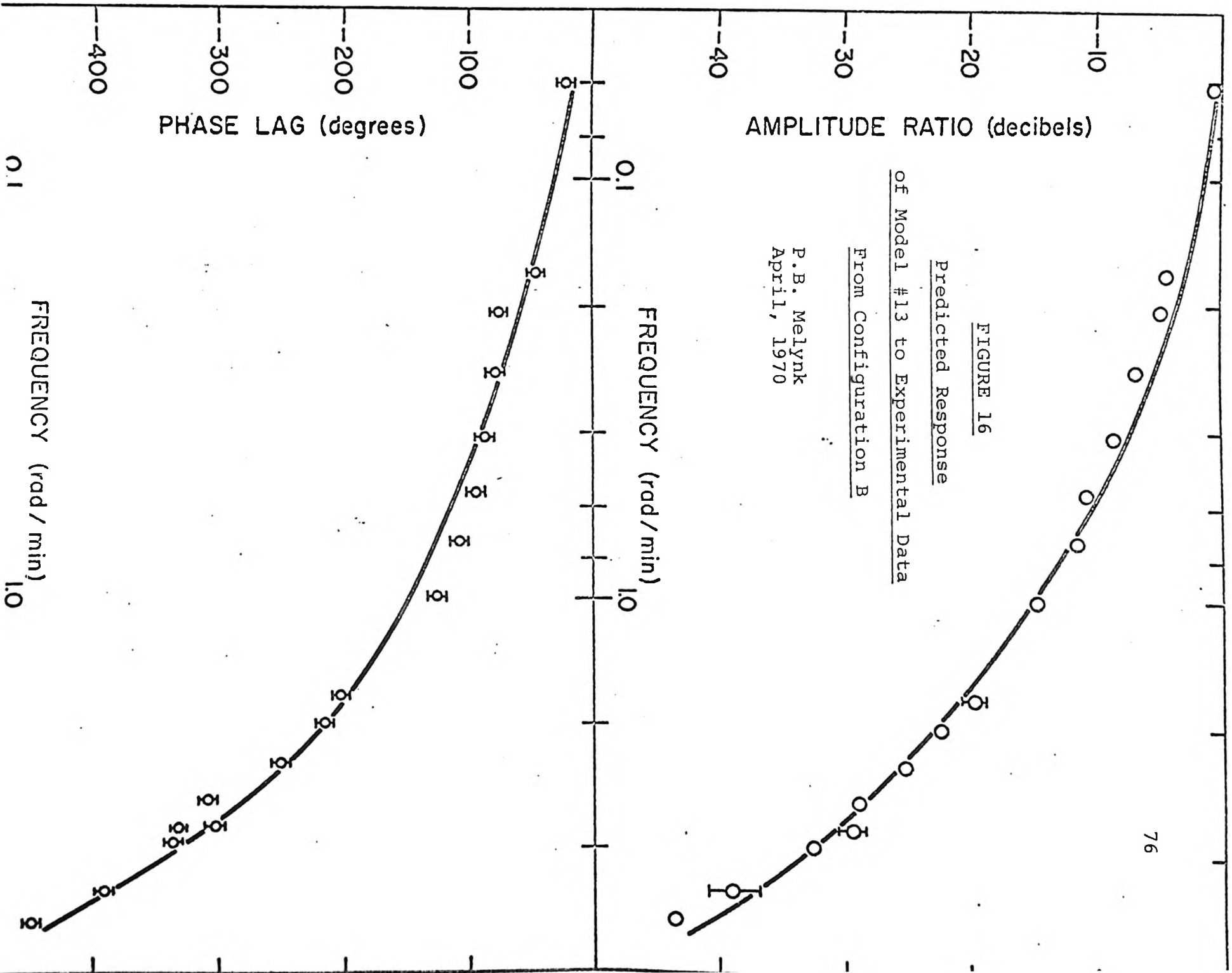
0.1

FREQUENCY (rad/min)

1.0

FIGURE 16
Predicted Response
of Model #13 to Experimental Data
From Configuration B

P.B. Melynk
April, 1970



CHAPTER 6

6 EVALUATION OF THE RESULTS AND TECHNIQUES

6.1 Linearity of the Test System

In order to describe the transfer function of a system by frequency response testing, it is necessary that the system be linear and stationary. A system is stationary if its parameters are constant with respect to time. Linearity is defined in terms of the system excitation and response.

Necessary properties for a linear system are:

- (i) superposition, defined when the system response from two superimposed signals is the sum of responses if the system were excited by each signal separately,
- (ii) homogeneity, defined when a reduction in the input signal results in a directly corresponding reduction in the output signal.

As the response from an ideal reactor to the stimulus of an inert tracer is linear, the response of a non-ideal flow system will be linear if this system can be represented by a network of ideal components. This is a result of the additivity property of linear processes. An experiment, as described in Appendix I, was performed to determine if the output was sinusoidal and homogeneous. The linearity of the test system was confirmed, in the concentration range studied.

6.2 Discussion of the Advantages of the Modelling Technique

The interpretation of a non-ideal mixing regime by a network of ideal components is straightforward and flexible when this interpretation has been based on frequency response data.

First, the number and residence time of the components can be determined directly from the Bode diagram by piecewise linearization.

Second, the presence of parallel flow paths in a system is determined if the slope of the amplitude ratio curve of the Bode plot is not monotonically decreasing. No further transformation of the experimental data is required. To obtain this same information from a R.T.D. Noar and Shinnar (39) have shown that R.T.D. data must be differentiated. In their approach the differentiation of the R.T.D. curve yields a plot of the intensity function. The characteristic curve of this function determines if parallel flow paths or "stagnancy" exists. The experimental error associated with the intensity function plot is increased by the differentiation process.

Third, the arrangement of components in a network, flow split between parallel paths, and the location of recycle streams, within this network is resolved by the experimental data and is therefore unique to the flow system tested. This advantage is lacking in the approach taken by Rooze (47) and Adler (1) where one particular model is first proposed and

fitted to the experimental data from all flow systems. In their studies it was felt that any flow regime could be represented by a cascade of stages, with each stage consisting of two CSTR's connected in parallel. The size of these CSTR's and the interchange of flow between them was constant and equal for all stages.

A last advantage is that the estimation of model parameters, flow splits, and flow direction within a network has been adapted to computer programming.

6.3 Discussion of the use of Experimental Data for Model Discrimination

Referring to the original objective of this work, it was desired to define the mixing phenomena occurring in a non-ideal flow regime by one unique network of ideal flow components. This has not been fully realized, particularly in the case in which the non-ideal flow involves the movement of fluid by multi-paths or parallel branches. The problem as shown by the tests performed on configuration B is, first, which of the twelve parallel networks proposed is the best representation of actual mixing phenomena, and second, should these parallel networks be abandoned if the simpler cascade network provides an adequate prediction of the system's frequency response. Note, only transfer function can, in theory, simultaneously satisfy the amplitude ratio and phase lag curves exactly.

6.3.1 Amplitude Ratio Data

Originally it had been thought that a discrimination

among proposed networks could be made on the basis of the standard error of estimate for the amplitude ratio. Referring to Table 5.3 this does not appear to be true. The transfer functions (Appendix III) for the second-fifth order models are similar functions with the exception of the coefficient of the second order term of the zero polynomial. The search for parameters of these models was constrained only in that the parameter values must be positive and non-zero. Thus it is not unexpected that the search technique should provide parameter estimates that result in each model fitting the response equally well. The parameter estimate for networks 2, 3, 4, 5, and 7 have shown that more than one set of parameter values exist that provide a minimum value on the response surface (defined by the sum of the squared deviations between measured and predicted values). Differentiation between these two sets of parameters must also be made. The change in parameter estimates had the effect of predicting recycling occurring in one case and not the other, as shown in Figure 11. In other cases studies, as seen in networks 8 and 10, changing the initial estimates of the parameters has not changed the direction of flow through the network.

Certain proposed networks may at first be rejected if the residence time parameter estimates for these networks are unrealistic when compared to the actual system tested. Configurations numbered 7A and B, 5B, and 8A and B, can be

rejected because they have components located on the main stream that receives the entire system flow, and have an estimated residence time that is greater than the total residence time measured on the actual system.

Statistically, the model networks may be discriminated by means of a formal Bayesian analysis. This method has been described by P. M. Reilly (43). The Bayesian analysis is subjective, in that one is allowed to use information that is not contained in the experimental data. From Bayes theorem, it may be stated that the posterior probability of the model is defined as being directly proportional to the product of the prior probability (or belief) and the likelihood of the experimental data given the model. In equation from this definition is:

$$P(M) \propto \text{Prior } M \times L(Y/M) \quad (6-1)$$

The likelihood function describes the probability of an event (in this case the experimental data) as a function of some parameter. Normally the likelihood function is based on both the model and its parameters. To simplify the problem, the model parameters are removed from the likelihood function by integrating them out. As a result, the models are tested at an average value of all possible parameter values, where each value has been weighted according to its probability.

These nuisance parameters can also be removed by expressing the model in a linearized form and then taking expectations and covariance (43).

At this point, one has an initial estimate of the model parameters and an estimate of the experimental error. One can assign a subjective prior probability to each model. If no model is thought to be more significant or correct than any other, then equal probabilities are assigned to each model. It is now necessary to perform a new experiment and test the models. The most desirable location (in this case a frequency) to perform this experiment is one in which the deviation between the predicted values of the models is greatest, or that point at which the models are in the greatest jeopardy. Four criteria which have been discussed in the literature can be used to predict the operating conditions of the next experiment. These are the Roth (49), Reilly (42), Box and Hill (7), and Entropy (42) criteria. For all of these methods the model predictions are made from parameter estimates based on all experimental data. Also the discrimination between models is weighted as to the probability of those models being correct. The latter two methods also account for the uncertainty of the measured variable when defining the regions of discrimination. This new data point is used with the Bayesian analysis to test the models. The cycle is repeated, with the prior probabilities

of the models for the next experiment being the posterior probabilities that were calculated for the last. Thus, the posterior probabilities of the model providing the best predictions is continually improved. This series of sequential experiments is continued until the desired discrimination is reached. It is the author's belief that the chance of success in discriminating among parallel network type models is poor. The model parameters are re-estimated after each experiment. It is thought that one will find each of these models fitting equally as well - the same situation that was noted initially. More simply, no separation would exist in the predictions of these models. Discrimination between series and parallel type models would achieve greater success, as the analysis would be conducted at an area where the deviation between series and parallel models is greatest.

6.3.2 Phase Lag Data

Preference has been given to the use of amplitude ratio data compared to phase lag data for the following reasons. First, the graphical experimental error associated with the phase lag measurements is greater than the corresponding error associated with amplitude ratio measurements. This is a result of the greater difficulty in locating the median of the sinusoidal peak in comparison to measuring the displacement between high and low values of the wave form. Second, the

phase lag cannot be considered as an independent response to test the data. As explained previously, this experimental data is used to predict the residence time of the in-series component. It is necessary, however, that an acceptable network model provide a satisfactory representation of the phase lag curve as well as the amplitude ratio curve. And finally, the reliability of phase lag predictions by the parallel flow networks is questionable. As noted by Coughanower and Koppel (13) the first order approximation of the PFTR component is accurate in its phase lag predictions up to a frequency equal to the reciprocal of that component's residence time. In these studies, a PFTR component whose residence time is 0.2 min. or less would be accurate over the frequency range studied. Examining the standard error of estimate as listed in Table 5.3, we find that configurations numbered 11B and 7B offer especially poor predictions, while configurations 6A and B, 9A and B, 1 and 10B also offer large error estimates. No trend could be seen in the data between the size of the PFTR component used in the network and the network's standard error of estimate on the phase lag curve.

Comparing the experimental error estimated for the phase lag curve (5.74 degrees) to the standard error of estimate calculated for each model, it is found that only model number 5A has a F-ratio lower than the tabulated value at 95% confidence level ($F_{17, 14, 0.5} = 2.60$). One

could conclude that only model number 5A has a standard error of estimate which could result from experimental error and not a lack of fit. Note that though the in-series model number 13 does not pass the F-ratio test, it is certainly the closest rival to model number 5A. Though it has been shown that discrimination is possible among models, the results must be taken with caution due to the uncertainty of both the experimental data and the model predictions.

6.3.3 Reaction Data

The final purpose of these network models is to predict the conversion of a reactant given a kinetic mechanism. Thus to discriminate among these models on the basis of their predicted conversions in comparison to experimental data would be the most severe and meaningful test. To obtain experimental data it is required that the test system be utilized as a reactor and the conversion of a specific initial concentration of reactants be measured. The choice of the reaction mechanism used is important. If the experiments are performed with reactant species that behave in a known linear manner, the arrangement of the components in the model network will not affect the final predicted conversion.

Conversely, if the reactants interact in accordance with a non-linear mechanism the series arrangement of components within any branch will affect the final estimate. If the

reaction order is greater than one, the reactor is most efficient if mixing occurs late. This means that to obtain the highest conversion it is necessary to locate the PFTR components before the CSTR components. Note that with the frequency response data, the in-series PFTR component was treated as occurring at the end of the network. The location is valid for the conversion predictions of non-linear kinetic mechanism only if the lowest efficiency is desired. It is valid to consider the residence time estimated for this component to be the sum of the residence times of a number of PFTR components which may assume many different locations on the main branch of the network. The prediction of conversion by a non-linear mechanism poses an uncertainty that is defined between the extremes of molecular mixing. A fluid can be thought to exist between two extremes of microscopic behavior - a micro or macrofluid. In the former case the individual molecules can be thought of as free to move about and intermix. With a macrofluid, the molecules are grouped in aggregates of packets where each packet behaves as an extremely small batch reactor. The definitions of these mixing states and their effect upon conversion predictions are outlined by Levenspiel (30).

A second order saponification reaction was carried out in the test system with both configurations of baffles and mixers (33). This reaction between sodium hydroxide and

2- ethoxyethyl acetate results in the substitution of the hydroxide ion in solution by the acetate ion. Subsequently, the ionic activity, or the conductivity of the solution decreases with reactant depletion. The conversion taking place in the reactor is measured by monitoring conductivity.

In those situations in which the model consisted of more than one component, the components are arranged for minimum efficiency (i.e., early mixing). Note that the experimentally determined conversions were 8 to 10% lower. This was thought to be due to the value of the reaction rate constant used. A value had been obtained from the literature. The series model for configuration A predicted a conversion below that where the test system was considered to behave as one CSTR. This is only possible if inactive or dead volume existed in the actual test system. The model predicts this inactive volume. The total residence time of the components was found to be 7.90 min., 0.37 min. less than the total residence time measured for the system. Thus for a total system flow of 2.13 gal/min., the inactive volume was calculated as 0.78 gal or 4.5% of the system volume. The low conversion value experimentally measured supported the hypothesis that the active volume used in the reactor was less than the system volume measured. A similar trend

Table 6.3

Comparison of Measured and Predicted Reactor Conversion

The reactor as:		<u>Configuration A</u>				
		a CSTR	a PFTR	3 CSTR's & 1 PFTR (in-series)		
micromixing				micromixing	macromixing	
38.6%-40.8%		50.6%		37.6%-38%		
Experimentally Measured Conversion						
30%						
The reactor as:		<u>Configuration B</u>				
		a CSTR	a PFTR	3 CSTR's & 1 PFTR		Parallel Network Model No. 5A
micro-macro mixing			micro- mixing	macro- mixing	micro- mixing	macro- mixing
38.6%-40.8%		50.6%	34.9%	35.9%	38.5%	39.4%
Experimentally Measured Conversion						
24%						

was noted for configuration B. The inactive volume predicted by the series model of 3 CSTR's and 1 PFTR is 24%. This increase in inactive volume corresponds to the decrease in the experimentally measured conversion. The parallel model predicted a conversion value above the series model prediction by 3.5%. The inefficiency of the reactor is shown by the short circuiting of approximately a third of the flow through, the branch having the shorter residence time. The higher predicted conversion for the parallel network may result from the fact that flow split between branches was solved by a function in which the total volume of the system was considered to be active. To do otherwise, would necessitate the inclusion of another search parameter, the total volume.

In summary, the following observations have been made concerning the tests performed on configuration B. For all but four trials, the parameters of the parallel network model provide a better fit to the experimental amplitude ratio curve in comparison to the series network model. The small difference, however, among the standard errors of estimate for all of the models resulted in no model being selected as the "best". Only one parallel model (model #5A) provided predictions of the system phase lag which resulted in a standard error of estimate being equal or less than the experimental error. The series model was however, a close

rival. The difference between the conversion predictions made by model no. 5A and the series model no. 13 was sufficiently small as to render any discrimination between these two models to be inconclusive. Thus further experimental data is required in order to select one model which is the best representation of the test system.

6.4 Discussion of Experimental Strategy for Improved Discrimination Among Models

The first step is to review among the proposed models, those networks which have provided sufficient short circuiting to cause a prediction of low conversion, that is compatible with experimental conversion that had been measured for configuration B. Models numbered 1, 2A, 3A, 4A, and 12 appear as suitable candidates under this category. These models had originally been rejected because of the magnitude of their standard errors of estimate with respect to the phase lag curve. The models which predict a reactant conversion similar or better than those predictions given by models numbered 5A and 13 are included in a general discrimination scheme.

Any of the four experimental design criteria mentioned previously (Section 6.3.1) can be used to establish co-ordinates at which to carry out a reaction study. The experimental co-ordinates for a second order reaction study are the initial concentration of one reactant and its molar

ratio with respect to the other reactant. It is desired that the experimental co-ordinates are located in an area in which one finds the maximum deviation among the reactant conversions predicted by different models. The uncertainty associated with a model's predicted conversion because the reactor fluid is assumed to behave as either a micro or macrofluid can be represented as an error associated with the model's prediction. This sequential procedure determining the site of a suitable reaction study, second, measuring the experimental conversion, and third, using this data to test the model will continue until one model can be selected as "best" or the difference between the conversion predictions of rival models is so small as to be insignificant in comparison to the experimental error associated with these predictions.

6.5 Data Requirements for Frequency Response Testing

The number of frequencies required to define a model for a test system depends whether the test system contains parallel flow paths. If the test system is characterized by an amplitude ratio curve of continuously decreasing slope, then the number of frequency tests needed is minimal. This minimum number of tests is determined by the number of parameters in the proposed model to be fitted, and must provide at least one degree of freedom. Because the parallel flow systems are characterized by a discontinuity in the amplitude

ratio curve, the number of data points must be sufficient to clearly locate this discontinuity. It is seen from the plot of the experimental data from configuration B (Figure 10), the size of these discontinuities are slight and easily missed if insufficient data is taken. The slightness of these areas is further emphasized in Figure 12. The amplitude ratio curves for this diagram were calculated by a hypothetical network of two CSTR's connected in parallel. The flowrate and volume of this network and the actual test apparatus were similar. The flowrate split between the components was varied from 10:1 to 2:1. The discontinuity on the curve occurs at lower frequencies and almost disappears as the flow split ratio decreases. Note, to prevent the curves from lying on top of one another, the curves were plotted at five decibel intervals apart. Both the experimental data and Figure (12) emphasize that a large number of data points in the proper area are required to locate discontinuities on the amplitude curve. Also the accuracy of the monitoring equipment becomes important.

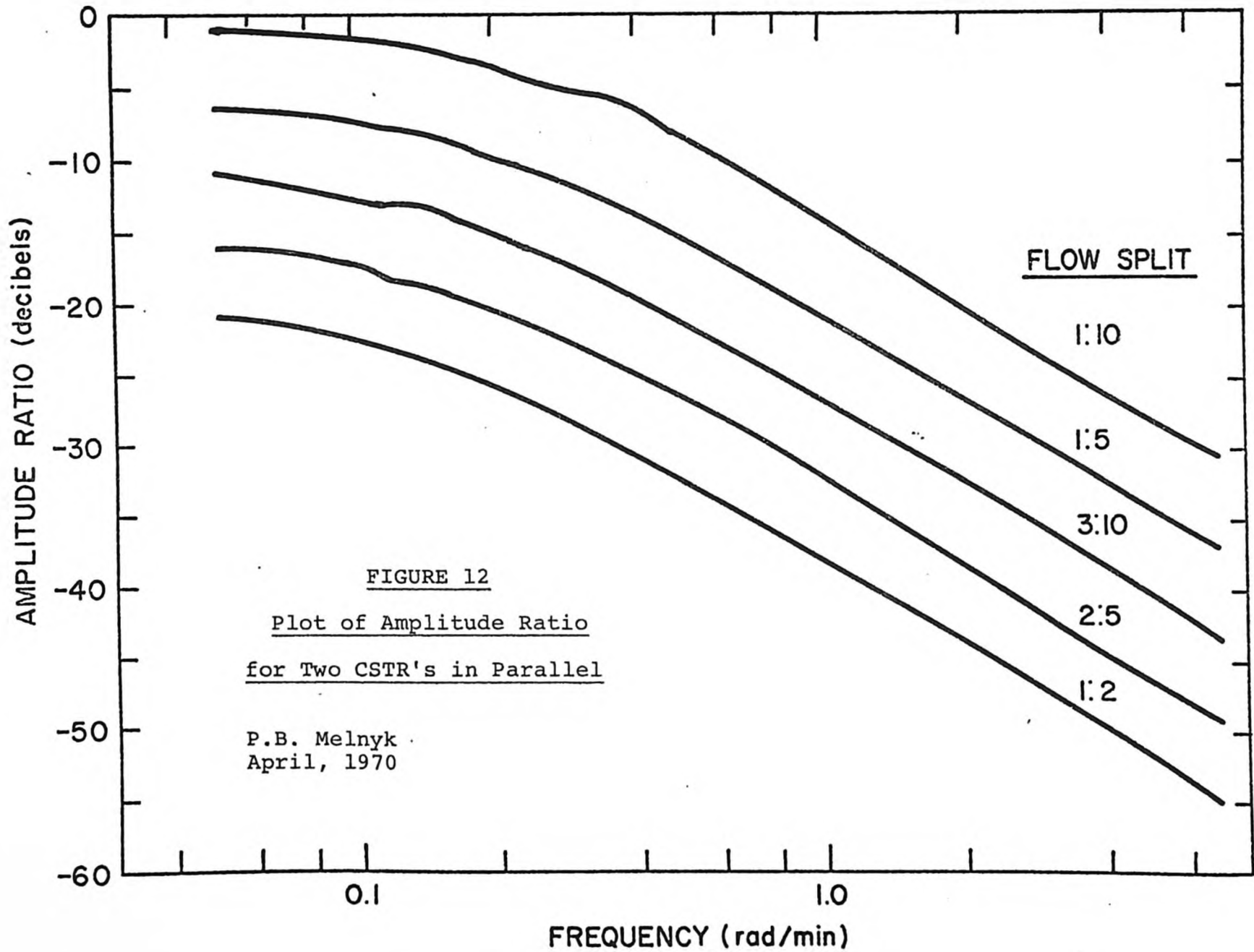


FIGURE 12

Plot of Amplitude Ratio
for Two CSTR's in Parallel

P.B. Melnyk
 April, 1970

CHAPTER 7

7 CONCLUSIONS

The mixing occurring in a non-ideal continuous isothermal reactor can be characterized by frequency response testing. A network model constructed from two types of ideal components can be interpreted, and its parameters estimated from frequency response data. The characteristic shape of the amplitude ratio curve determines whether the ideal components of the network model are to be arranged in series or parallel.

These models derived from the frequency response tests do provide satisfactory predictions of the reactant conversion in the test system in which a second order reaction is taking place.

It was found that a number of parallel networks could be proposed to fit the experimental frequency response data. The selection of one "best" model appears to be best accomplished by comparing the predicted conversions of the models to experimental reaction data.

REFERENCES

- (1) ADLER, R. J., "Finite Stage Modelling", 4th. Nat. Chem. & Petroleum Symposium of the Instrument Society of America, (1962).
- (2) ANGUS, R. M., and LAPIDUS, L., "Characterization of Multiple-Variable Linear Systems from Random Inputs", AIChE, J. Vol.9, No. 6, 810, (1963).
- (3) ARIS, R., and AMUNDSON, N.R., "Statistical Analysis of Reactor", Chem.Eng. Sci., Vol. 9, No. 4, 250 (1959).
- (4) ARIS, R., "On the Dispersion of a Solute in a Fluid Flowing Through a Tube", Proc. Roy. Soc., A235, 67, (1956).
- (5) BISCHOFF, K.B., and LEVENSPIEL, O., "Fluid dispersion-generalization and comparison of mathematical models - I. Generalization of models", Chem.Eng. Sci., Vol. 17, 245, (1962).
- (6) BISCHOFF, K.B., and LEVENSPIEL, O., "Fluid dispersion-generalization and comparison of mathematical models - II. Comparison of Models
- (7) BOX, G., and HILL, W.J., "Discrimination Among Mechanistic Models", Technometrics, Vol. 9, No. 1, 57, (1967).
- (8) BUFFMAN, G.A., GIBILARO, L.C., and KROPHOLLER, H.W., "Network combining of complex flow-mixing models", Chem.Eng. Sci. Vol. 24, 7, (1969).
- (9) CHOLLETTE, A., and CLOUTIER, L., "Mixing Efficiency Determinations for Continuous Flow Systems", Can. J. Chem.Eng., Vol. 37, 105, (1959).
- (10) CHOLLETTE, A., CLOUTIER, L., and BLANCHOT, J., "Performance of Flow Reactors at Various Levels of Mixing", Can. J. Chem.Eng. Vol. 38, 1, (1960).

- (11) CHOLLETTE, A., and BLANCHET, J., "Optimum Performance of Combined Flow under Adiabatic Conditions", *Can. J. Chem.Eng.*, Vol. 39, 192, (1961).
- (12) CLEMENTS, W. C. (Jr.), "Pulse Testing for Dynamic Analysis", Ph.D. Thesis, Chem. Eng. Dept. Vanderbilt University, (1963).
- (13) COUGHANOWER, D.R., and KOPPEL, L.B., "Process Systems Analysis and Control", McGraw-Hill, New York, (1965).
- (14) DANKWERTS, P.V., "Continuous Flow Systems (Residence Time Distribution)", *Chem.Eng. Sci.*, Vol. 12, No. 1, (1953).
- (15) DEANS, H.A., and LAPIDUS, L., "A Computational Model for Predicting and Correlating the Behaviour of Fixed Bed Reactors", *AIChE J.*, Vol. 6, 656, (1960)
- (16) DORF, R.C., "Modern Control Systems", Addison-Wesley, Reading Mass, (1969).
- (17) GIBILARO, L.G., KROPHOLLER, H.W., and SPIKINS, D.J., "Solution of Mixing Model Due to Van de Vusse by Simple Probability Method", *Chem.Eng. Sci.* Vol. 22, No. 4, 517, (1967).
- (18) GILLILAND, E.R., and MASON, E.A., "Gas and Solid Mixing in Fluidized Beds", *Ind. & Eng. Chem.*, Vol. 41, No. 6, 1191, (1949).
- (19) HADDAD, A., WOLF, D., and RESNICK, W., "Residence Time Distributions in Multi-Stage Systems with Recycle", *Can. J. Chem.Eng.*, Vol. 42, No. 5, 216, (1964).
- (20) HOVORKA, R., and ALDER, R.J., "A Finite Stage Model for High Assymetric Residence Time Distributions", Joint Automatic Control Conference, Denver, AIChE preprint No. 3, (1961).
- (21) KING, R.P., "Continuous flow systems with stochastic transfer functions", *Chem.Eng. Sci.*, Vol. 23, 1035, (1968).
- (22) KLENHENBERG, A., "Distribution of Residence Times in a Cascade of mixed vessels with Backmixing", *Ind. & Eng. Fund.*, Vol. 5, No. 2, 283, (1966).
- (23) KOPPEL, L.B., "Dynamics of a Flow-Forced Heat Exchanger", *Ind. & Eng. Chem. Fund.*, Vol. 1, No. 2, 131, (1962).

- (24) KOPPEL, L.B., "Dynamics of a class of non-linear distributed parameter reactors", Ind. & Eng. Fund., Vol. 4, No. 3, 269, (1965).
- (25) KRAMERS, H. and ALBERDA, G., "Frequency response analysis of continuous flow systems", Chem. Eng. Sci., Vol. 12, 173, (1953).
- (26) KRAMLECK, F.J., SHINNAR, R., and KATZ, S., "Stochastic Mixing Models for Chemical Reactors", Ind. & Eng. Chem. Fund., Vol. 6, No. 2, 276, (1967).
- (27) LEDER, F., and BUTT, J.B., "Dynamic Behaviour of Fixed Bed Catalytic Reactor", AIChE J. Vol. 12, No. 6, 1057, (1966).
- (28) LEEDS, J.V., and BYBEE, H.H., "Solution of Estuary Problems and Network", Proc. ASCE J. San. Eng. Div. Vol. 93, SA3, 29, (1967).
- (29) LEES, S., and DOUGHERTY, R.C., "Refinement of the Pulse Testing Procedure - Computer Limitations", Research Report, Thayer School of Engineering, Dartmouth College, Hanover, New Hamp., (1964).
- (30) LEVENSPIEL, O., "Chemical Reaction Engineering", J. Wiley & Sons, Inc., New York, (1967).
- (31) LEVENSPIEL, O., "Mixed Models to Represente Flow of Fluids through Vessels", Can. J. Chem. Eng., Vol. 40, 135, (1962)
- (32) LEVENSPIEL, O., and SMITH, W.K., "Notes on the Diffusion Type of Model for the Longitudinal Mixing of Fluids in Flow", Chem. Eng. Sci., Vol. 6, 227, (1957).
- (33) MELYNK, P.B., NORMAN, J.D., and WILSON, A.W., "Frequency Response Approach to Modelling Continuous Reactors", 5th Annual Symposium on Water Pollution Research, Waterloo University, (1970).
- (34) MURPHY, K.L. and TIMPANY, P., "Design and Analysis of Mixing for an Aeration Tank", ASCE J. San. Eng. Div. Proc., Vol. 93, No. SA5, 1, (1967).
- (35) MURPHY, K.L., and BOYKO, B.I., "Longitudinal Mixing in Spiral Flow Aeration Tanks", ASCE J. San. Eng. Div. Proc., Vol. 96, SA2, 211, (1970).
- (36) MURRILL, P. W. , PIKE, R.W., and SMITH, C.L., "Random Inputs Yield System Transfer Function", Chem. Eng. April 7, 151, (1969).

- (37) MURRILL, P.W., PIKE, R.W., and SMITH, C.L., "The Basis for Bode Plots", Chem.Eng., October 7, 177, (1969).
- (38) NAOR, P., and SHINNAR, R., "Representation and Evaluation of Residence Time Distrutions", Ind. & Eng. Chem. Fund., Vol. 2, No. 4, 278, (1963).
- (39) NAOR, P., and SHINNAR, R., "Residence Time Distributions in Systems with Internal Reflux", Chem. Eng. Sci., Vol. 22, No. 10, 1369, (1967).
- (40) NYQUIST, J.K., SCHINDLER, R.N., and GILBERT, R.E., "Determination of Frequency Response from Step Response", Chem. Eng. Prog. Symposium Ser., Vol. 59, No. 4, 98, (1963).
- (41) PANG, K.H., and JOHNSON, A.I., "The Determination of Theoretical Frequency Response of Some Stagewise Processes", Can. J. Chem. Eng., Vol. 47, No. 5, 477, (1969)
- (42) REILLY, P.M., "Entropy", Unpublished Lecture Notes, McMaster University, (1969).
- (43) REILLY, P.M., "Statistical Methods in Model Discrimination", 3rd. Canadian Symposium on Catalysis, Edmonton, Alberta, (1969).
- (44) RETALLICK, W.B., "Distrubtion of Residence Times in a Cascade of Mixed Vessels with Backmixing", Ind. & Eng. Chem. Fund., Vol. 4, No. 4, 88, (1965).
- (45) REYNOLDS, J.B., (Jr.), "Two Ways to Get Frequency Response from Transient Data - Analog Machine Approach", Contol Eng., October, 60, (1955).
- (46) RIPPEN, D.W.T., "Recycle Reactor as a Model of Incomplete Mixing", Ind. & Eng. Chem. Fund. Vol. 6, No. 4, 488, (1967).
- (47) ROOZE, J.W., "Determination of Residence Time Distribution Using Deterministic and Random Signals", M.Sc. Thesis, Case Institute of Technology, (1963).
- (48) ROSENBROCK, H.H., "An Automatic Method for finding the greatest or least value of a function", Comp. J., Vol. 3, No. 3, 175, (1960).
- (49) ROTH, P.M., "Design of Experiments for Model Discrimination among Rival Models", Ph.D. Thesis, Chem. Eng., Princeton University, (1966).

- (50) SAWYER, C.M., "Tracer Studies on a Model Chlorine Contact Tank", M.Sc. Thesis, Virginia Polytechnic Institute, (1967).
- (51) SCHECHTER, R.S., and WISSLER, E.H., "Frequency Response from Step Input Response", Ind. & Eng. Chem., Vol. 51, No. 8, 945, (1959).
- (52) SHERWOOD, T.K., "Continuous Flow Reactors - Problem of Variable Residence Times", Chem. Eng. Prog. Vol. 51, No. 7, 363, (1955).
- (53) SILVESTON, P.L., SINGH, D.P., and BRYSON, A.W. (Jr.) "A Stochastic Model for Primary Settlers", 5th Annual Symposium on Water Pollution Research, University of Waterloo, (1970).
- (54) SINCLAIR, C.G., and McNAUGHTON, K.J., "Residence Time Probability Density of Complex Flow Systems", Chem. Eng. Sci., Vol. 20, No. 4, 261, (1965).
- (55) STERMOLE, F.J., and LARSON, M.A., "Dynamic Response of Heat Exchangers to Flow Rate Changes", Ind. & Eng. Chem. Fund., Vol. 2, No. 1, 62, (1963).
- (56) TAYLOR, G.I., "The Dispersion of Matter in Turbulent Flow Through a Pipe", Proc. Roy. Soc., A223, 446, (1954).
- (57) TAYLOR, G., "Dispersion of Soluble Matter in Solvent Flowing Slowly Through a Tube", Proc. Roy. Soc., A219, 186, (1953).
- (58) TEASDALE, A.R. (Jr.), "Two Ways to Get Frequency Response From Transient Data - A Graphical Approach", Control Eng., October, 55, (1955).
- (59) THACKSTON, E.L., and KRENKEL, P.A., "Longitudinal Mixing in Natural Streams", ASCE J. San. Eng. Div., Vol. 93, No. SA5, 67, (1967).
- (60) THAYER, R.P., and KRUTCHKOFF, R.G., "Stochastic Model for BOD and DO in Streams", Proc. ASCE J. San. Eng. Div., Vol. 97, SA3, 59, (1967).
- (61) THOMAS, H.A., and McKEE, S.E., "Longitudinal Mixing in Aeration Tank", Sewage Works J. Vol. 16, 42, (1944).
- (62) VAN DER LAAN, E., "Letter to the Editors", Chem. Eng. Sci., Vol. 7, 187, (1958).
- (63) VAN DER REIT, J.L., "Surge Effects on the Residence Time of a Horizontally Baffled Contact Time", M.Sc. Thesis, Virginia Polytechnic Institute, (1965).

- (64) VAN DE VUSSE, J.C., "A New Model for the Stirred Tank Reactor", Chem.Eng., Vol. 17, 507, (1962).
- (65) WEBER, T.W., and HARRIOT, P., "Dynamics of Heat Removal from An Agitated Tank", Ind. & Eng. Chem. Fund., Vol. 4, No. 2, 155, (1965).
- (66) WEN, C.Y., and CHUNG, S.F., "Dynamics Response Equations for Various Reactor Models", Can. J. Chem. Eng., Vol. 45, No. 3, 101, (1965).
- (67) WOLF, D., and RESNICK, W., "Residence Time Distribution in Real Systems", Ind. & Eng. Chem. Fund., Vol. 2, No. 4, 287, (1963).

APPENDIX ILINEARITY EXPERIMENT

A transfer function can only be defined for a linear stationary system. A system is stationary when the parameters of its transfer function are constant with respect to time.

The linearity of a system is defined in terms of its excitation and response. If a system possesses the properties of homogeneity and superposition, it is linear. A system is homogenous if an input signal "x" is decreased by the factor " β ", the output signal is reduced by the same factor and thus equal to " βy ". The principle of superposition applied to a linear system requires that if the response of a system to a signal $x_1(t)$ is $y_1(t)$ and similarly for a signal $x_2(t)$ the response is $y_2(t)$ the double excitation of $x_1(t)$ and $x_2(t)$ results in the response $y_1(t) + y_2(t)$.

It is also a necessary property that if a stable linear system is excited by a constant sinusoidal signal, the output signal is sinusoidal in the steady state.

An experiment was carried out in the test system designated configuration B to test for homogeneity and to compare the input and output waveforms to the sine function.

The system was tested for its frequency response at a frequency of 0.966 rad/min. The test was repeated

at the same frequency, but the amplitude of the input signal was cut approximately in half. The amplitude ratios as calculated after each test were -17.365 decibels, and -17.142 decibels respectively. System homogeneity is thus confirmed as the amplitude ratios did not differ by an amount greater than the experimental error of .687 decibels (Table II-I).

The input and output waveforms from a frequency test made at 0.323 rad/min. were compared to the sine function in the following manner:

- (i) The maximum amplitude for each signal was measured.
- (ii) The current data at fourteen intervals along each waveform was noted and transferred to equivalent concentrations.
- (iii) The concentration at each measured interval was predicted by the sine function and compared to those values measured at the corresponding intervals. The results are listed in Table I-I and illustrated in Figure 13 and 14.

The excellent conformity of the measured data points to the sine function confirming the system linearity.

Table I-1
Comparison of Waveforms to Sine Function

Input Wave

Maximum Amplitude 1.046 gm NaCl/l

Concentration (gm NaCl/l)		Location (degrees)
<u>Measured</u>	<u>Predicted</u>	
1.106	1.105	25.2
1.276	1.278	49.2
1.383	1.383	73.2
1.405	1.403	84
1.354	1.335	120
1.193	1.190	144
1.000	0.991	168
0.695	0.670	204
0.436	.494	228
0.395	0.385	252
0.359	0.359	268.8
0.418	.409	295.2
0.551	0.541	319.2
0.744	0.731	343.2

Con't.

Con't.

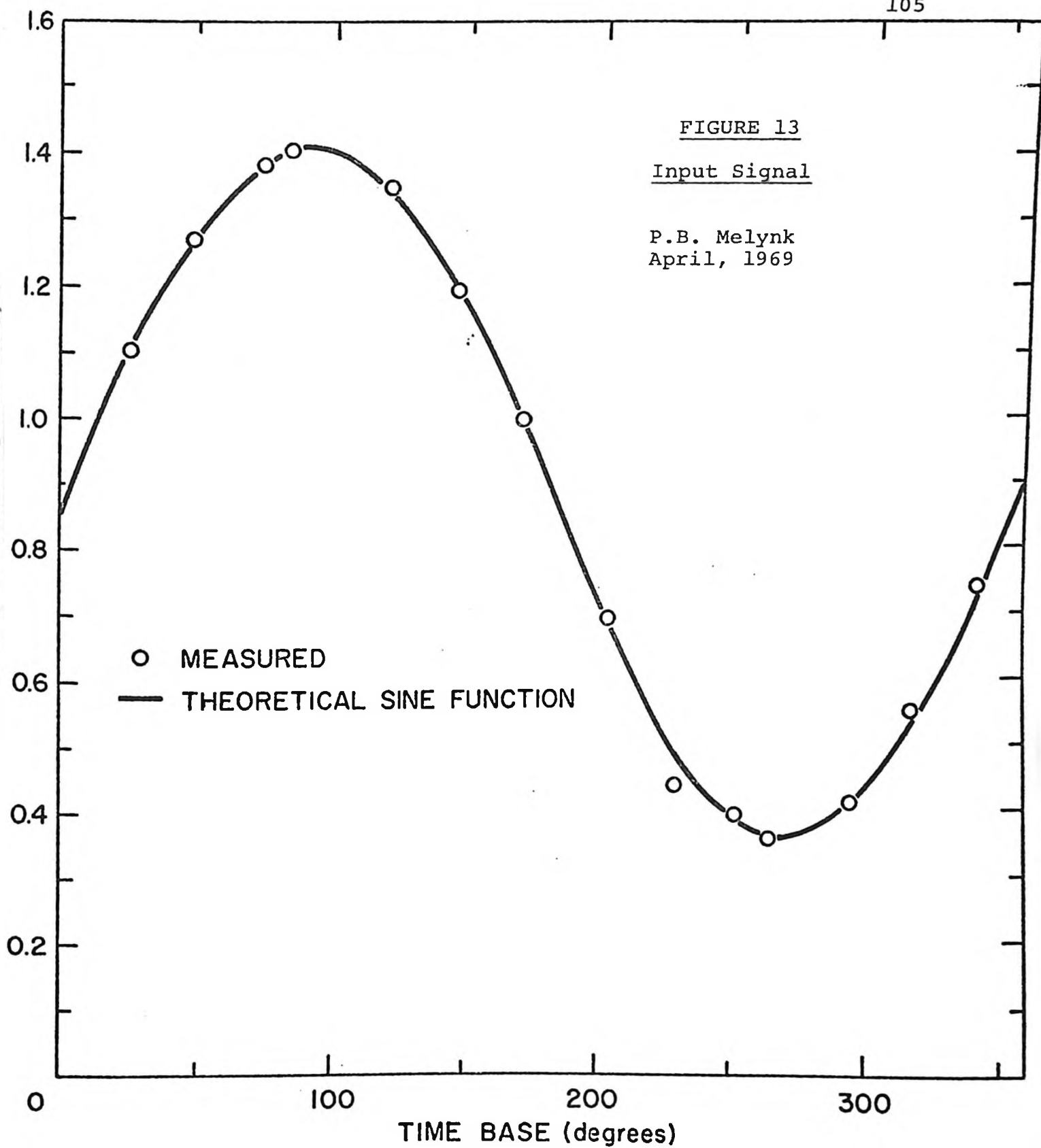
Table I-1

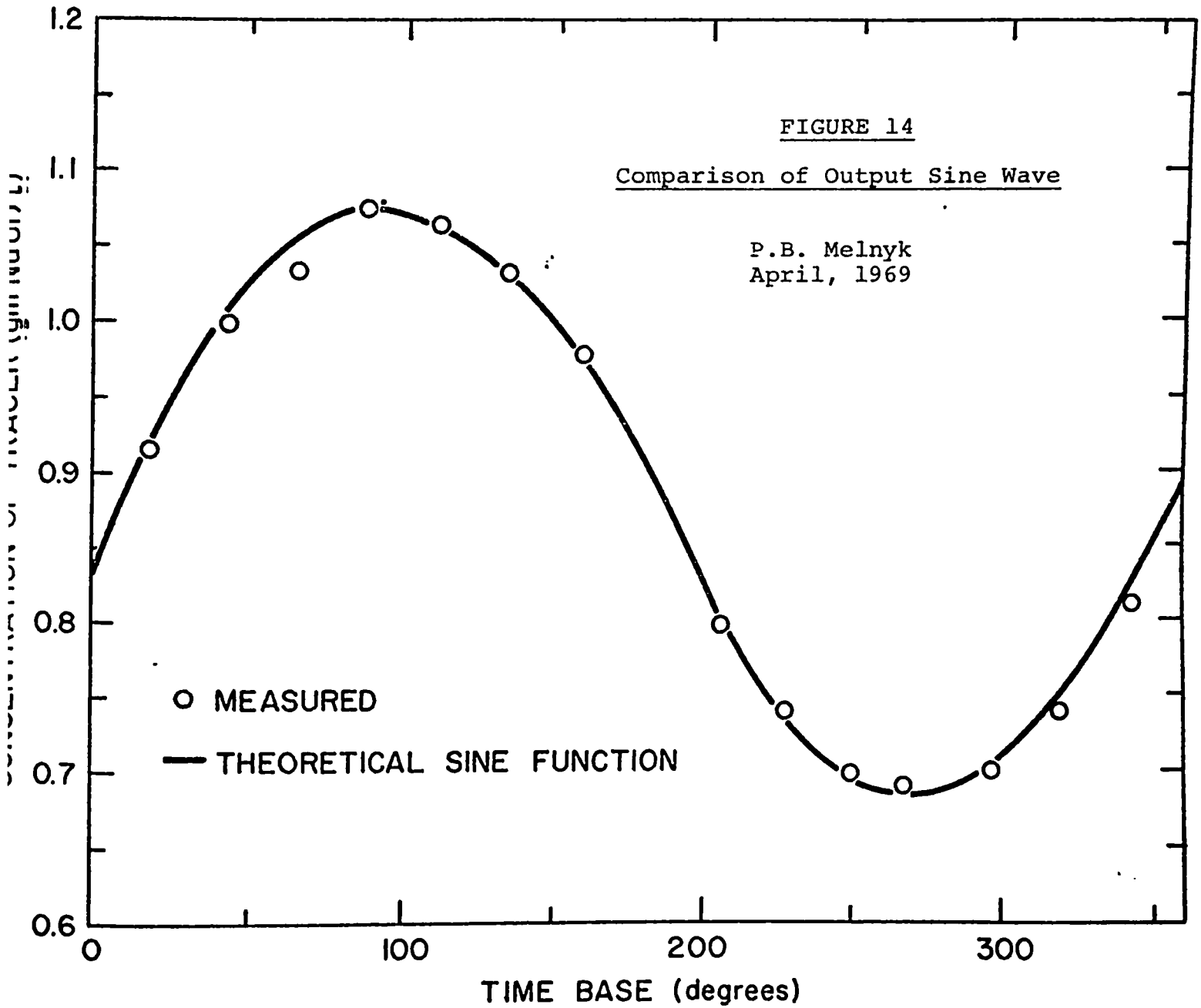
Output Wave

Maximum Amplitude 0.394 gm NaCl/l

Concentration (gm NaCl/l)		Location (degrees)
<u>Measured</u>	<u>Predicted</u>	
0.934	0.942	18.58
1.002	1.011	41.81
1.033	1.058	65.03
1.077	1.076	87.1
1.063	1.064	110.32
1.033	1.022	133.55
0.964	0.957	156.88
0.799	0.802	203.22
0.739	0.736	226.45
0.700	0.694	249.68
0.690	0.682	267.1
0.698	0.702	296.13
0.737	0.751	319.55
0.809	0.820	342.58

FIGURE 13

Input SignalP.B. Melynk
April, 1969



APPENDIX II
ANALYSIS OF EXPERIMENTAL ERROR

An error or deviation in the experimental results was thought to result from three sources:

- (1) limiting precision of the potentiometer,
- (2) the graphical interpretation of signal data, and
- (3) conversion of experimental data from current to an equivalent concentration of tracer (for the amplitude curve only).

An estimate of error was obtained by the analysis of replicate determinations at five frequency locations. The result of this analysis is shown in Table II-1. An F-ratio test was performed on the largest and smallest standard deviation to determine if the experimental error is correlated as to the frequency tested.

The F-ratios obtained were:

14.4 for the amplitude curve

4.02 for the phase lag curve.

At the 95% confidence level, the tabulated F-value is $F_{.05,4,3} = 9.12$.

The conclusion is therefore, that the experimental error in regard to amplitude is dependent upon the frequency tested, while independent in regard to phase lag at any

frequency. This result was expected. In measuring the amplitude of a sine curve the graphical interpretation error is essentially constant. The error associated with the amplitude is, however, not. This can be shown from the following error analysis.

Consider σ graphical and potentiometer errors which are constant for both input and output waveforms.

a_1 input amplitude which is also constant

a_2 output amplitude which is correlated
with frequency (i.e., $a_2 = f(\omega)$)

The amplitude ratio A.R. is equal to $\frac{a_2}{a_1}$ and the experimental error is defined as:

$$\sigma_{AR} = (A.R.) \left(\frac{\sigma}{a_1} + \frac{\sigma}{a_2} \right) \quad (II-1)$$

substituting $A.R. = a_2/a_1$

$$\sigma_{AR} = \frac{a_2}{a_1^2} \sigma + \frac{1}{a_1} \sigma \quad (II-2)$$

σ/a_1 & σ/a_1^2 are constants equal to k_1 & k_2 , respectively.

$$\text{Therefore } \sigma_{AR} = (a_2 k_2 + k_1) \sigma \quad (II-3)$$

Now on the Bode diagram the amplitude ratio is expressed in decibels, and the effect of this transformation on the standard deviation must be considered. The transformation is represented by the equation

$$\begin{aligned} \text{A.R. (decibels)} &= 20 \log (A.R.) \\ &= 46.06 \ln (A.R.) \end{aligned} \quad (II-4)$$

From the general expressions

$$X = f(x_1) \quad (\text{II-5})$$

$$\sigma^2(X) = \frac{\delta X^2}{\delta x_1^2} \sigma^2(x_1) \quad (\text{II-6})$$

Substituting into these expressions

$$\begin{aligned} \frac{\sigma}{AR} &= 46.06 \frac{1}{A.R} \sigma_{AR} & (\text{II-7}) \\ &= 46.06 \frac{1}{\frac{a_2}{a_1}} (a_2 k_2 + k_1) \sigma \\ &= 46.06 (a_1 k_2 + \frac{a_1}{a_2} k_1) \sigma \\ &= 46.06 k_1 (1 + \frac{a_1}{a_2}) \sigma \end{aligned}$$

From this expression it is seen as the output amplitude decreases (as the frequency increases) the standard deviation in decibels increase.

As the standard deviation of the phase lag is independent of frequency, a pooled estimate may be taken. This pooled estimate is given by

$$\sigma(x) = \frac{\sum_i^m n_i (\sigma a_i)}{\sum_i^m n_i - m} \quad (\text{II-8})$$

where n_i number of replicate for each set
 $\sigma^2(x_i)$ variance estimate at each set
 m number of sets

The pooled estimate of the standard deviation associated with phase lag is therefore 5.74 degrees.

A larger graphical error was expected with the phase lag measurements in comparison to the amplitude measurements. It is rather precise to determine the extremum values of a sine wave, however, locating the centre of the sine wave peak is subject to large inaccuracies.

Table II-1

Analysis of Replicates

Frequency Location Analysed	Number of Replicates	Standard Deviation		Percent Standard Deviation	
		Amplitude (decibels)	Phase Lag (degrees)	Amplitude	Phase Lag
(rad/min)					
.241	4	.17	2.49	3.63 %	4.37 %
.557	4	.15	4.21	1.4 %	4.57 %
1.73	5	.687	8.12	3.57 %	4.05 %
3.55	5	.717	8.32	2.46 %	2.71 %
5.11	5	2.16	10	5.61 %	2.78 %

APPENDIX III
COMPUTER PROGRAMMING

In this appendix the mechanics of the computational techniques are outlined. The following are included:

- (i) A list of the system transfer functions for the networks tested, Table III-1,
- (ii) Algorithms of the program and its subroutines used to estimate the model parameters, and
- (iii) Listing of the computational program.

TRANSFER FUNCTIONS FOR PROPOSED NETWORKS

Configuration
Number

(in the s-domain)

$$1 \quad \frac{(\tau_1 + 2\tau_2 + \tau_3 - \tau) s + 1}{(\tau_1 s+1)(\tau_2 s+1)(\tau_2 s+1)(\tau_3 s+1)}$$

$$2,3,4 \quad \frac{\sum_{i=1}^4 \tau_i - \tau) s + 1}{\prod_{i=1}^4 (\tau_i s + 1)}$$

$$5 \quad \frac{A s^2 + (\sum_{i=1}^4 \tau_i - \tau + B) s + 1}{\prod_{i=1}^4 (\tau_i s + 1)}$$

$$\text{Where } A = \frac{(\sum_{i=1}^5 \tau_i - \tau) \tau_2 \tau_3 - \tau_1 \tau_2 (\tau - \tau_4 - \tau_5 - \tau_1)}{2\tau_2 + \tau_3}$$

$$\text{And } B = \frac{\tau_1 (\tau - \tau_4 - \tau_5 - \tau_1)}{2\tau_2 + \tau_3}$$

$$6 \quad \frac{[(\sum_{i=1}^5 \tau_i - \tau) (\tau_1 \tau_2) (1/(\tau_1 - 2\tau_2))] s^2 + (\sum_{i=1}^5 \tau_i - \tau) s + 1}{\prod_{i=1}^5 (\tau_i s + 1)}$$

$$7 \quad \frac{A s^2 + (\sum_{i=1}^5 \tau_i - \tau) s + 1}{\prod_{i=1}^5 (\tau_i s + 1)}$$

Continued

Configuration
Number

(in the s-domain)

7
Cont'd

$$\text{Where } A = \frac{\tau_2\tau_3(\tau-\tau_4-\tau_5-\tau_2-2) + \tau_1\tau_3(\tau-\tau_4-\tau_5) + \tau_1\tau_1\tau}{\tau_1 - \tau_2 - \tau_3}$$

8

$$\frac{-2\tau_2\tau_3s^2 + (\sum_{i=1}^5 \tau_i - \tau) s + 1}{\prod_i^5 (\tau_i s + 1)}$$

9

$$\frac{A s^2 + (\sum_{i=1}^5 \tau_i - \tau) s + 1}{\prod_i^5 (\tau_i s + 1)}$$

$$\text{Where } A = \frac{\tau_1\tau_2(\tau_1+\tau_2+\tau_5-\tau) + \tau_3\tau_4(\tau-\tau_5-\tau_3-\tau_4)}{\tau_1 + \tau_3 - \tau_4}$$

10

$$\frac{[(\tau_3\tau_2)(\tau - \sum_{i=2}^5 \tau_i)(1/\tau_1-\tau_2\tau_3)] s^2 + [\sum_{i=1}^5 \tau_i - \tau] s + 1}{\prod_{i=1}^5 (\tau_i s + 1)}$$

11

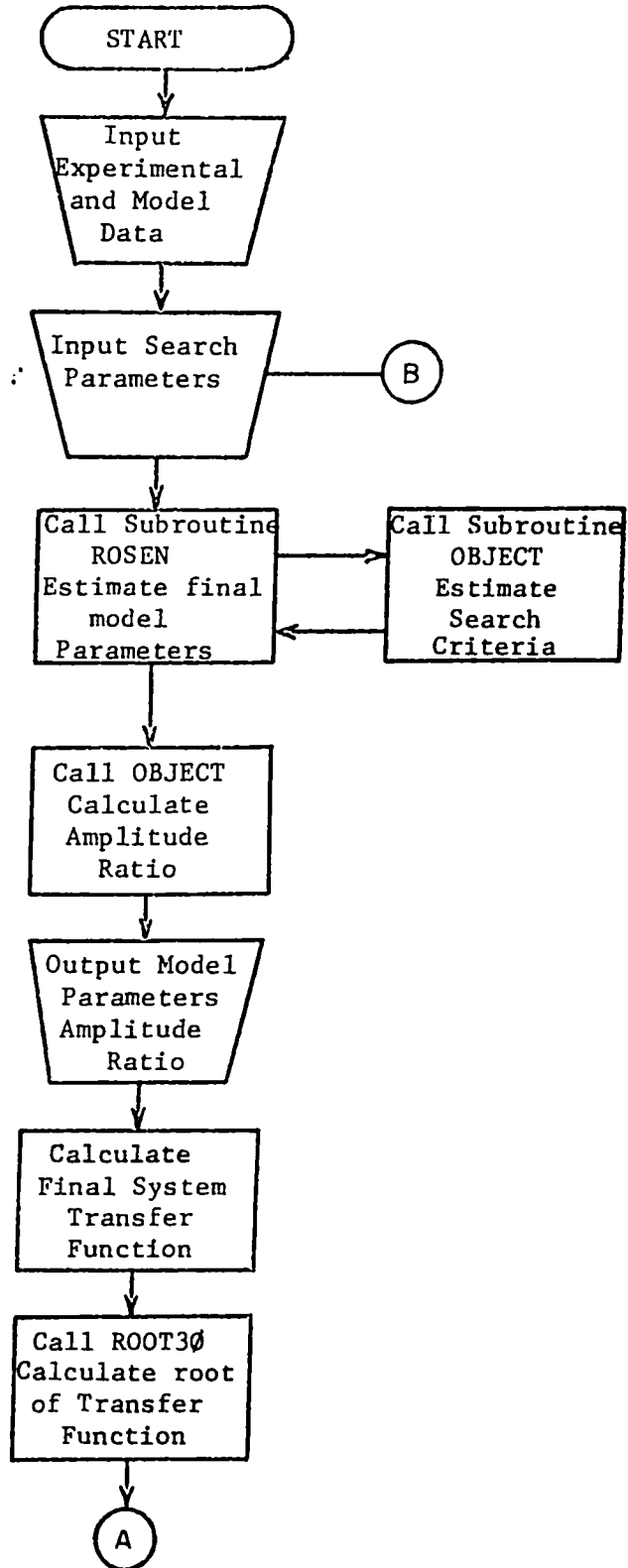
$$\frac{[\tau_2\tau_3(\tau-2\tau_1-\tau_2-\tau_4)(1.0/(\tau_2-2\tau_3))]s^2+(2\tau_1+\tau_2+\tau_3+\tau_4-\tau)s+1}{(\tau_1 s + 1) (\prod_{i=1}^4 (\tau_i s + 1))}$$

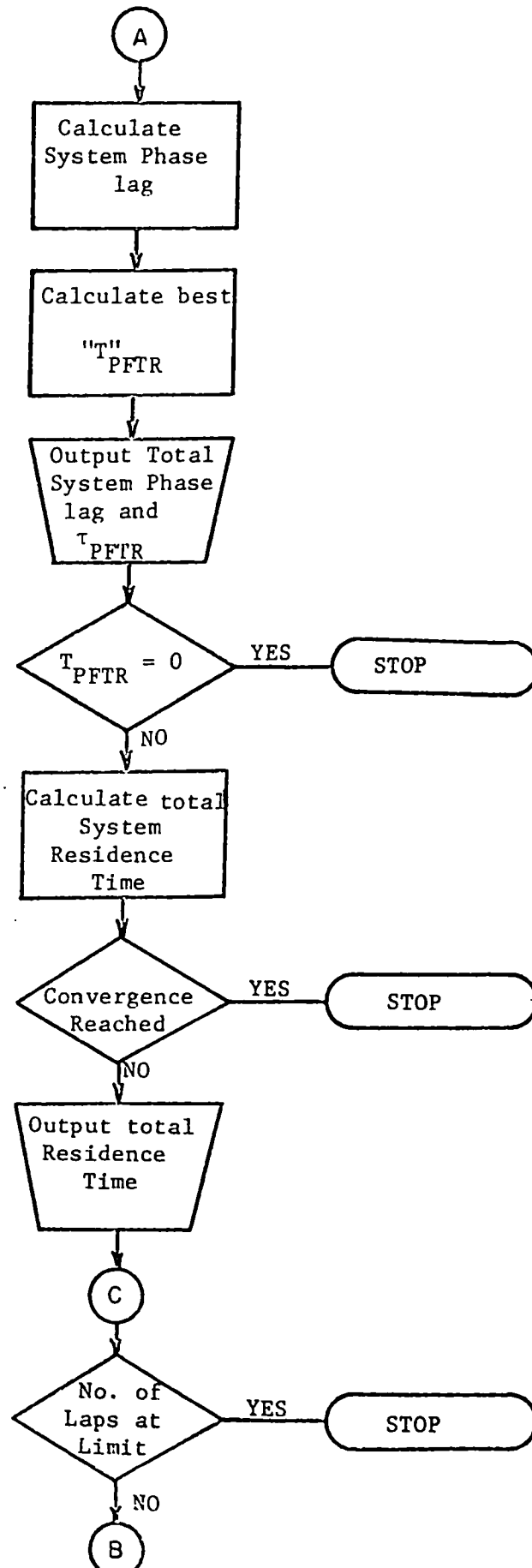
12

$$\frac{(\tau_3+\tau_2-\tau_b)(\tau_1+\tau_2-\tau_a) s^2 + (\tau_1+2\tau_3+\tau_3-\tau) s + 1}{(\tau_2 s + 1) (\prod_{i=1}^4 \tau_i s + 1)}$$

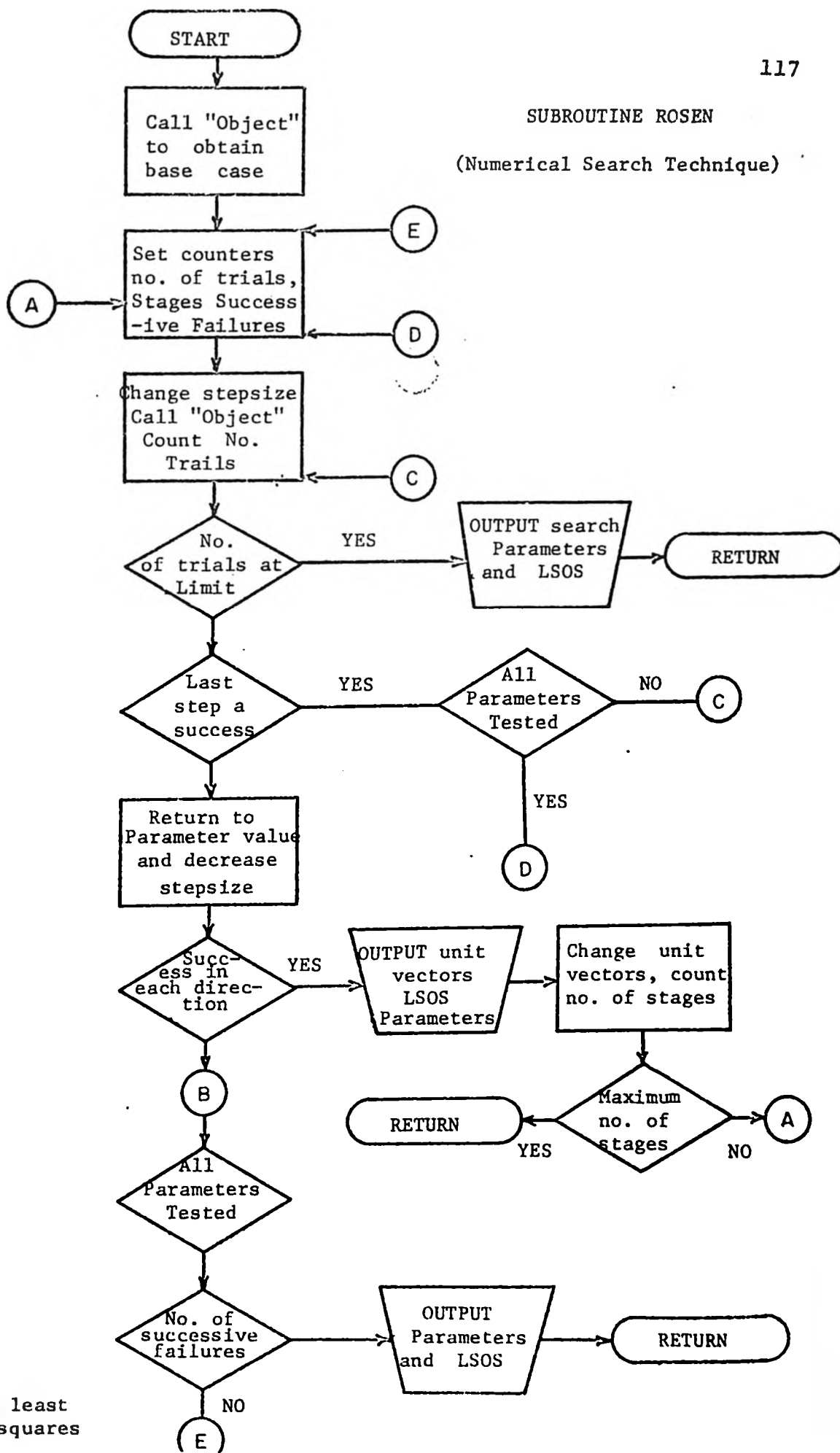
Where $\tau_a = K(\tau-\tau_4)$ and $\tau_b = (1-K)(\tau-\tau_a)$ and $\frac{K}{1-K}$ is the ratio of the volume of components 1 and 2 over components 3 and 4.

MAIN PROGRAM

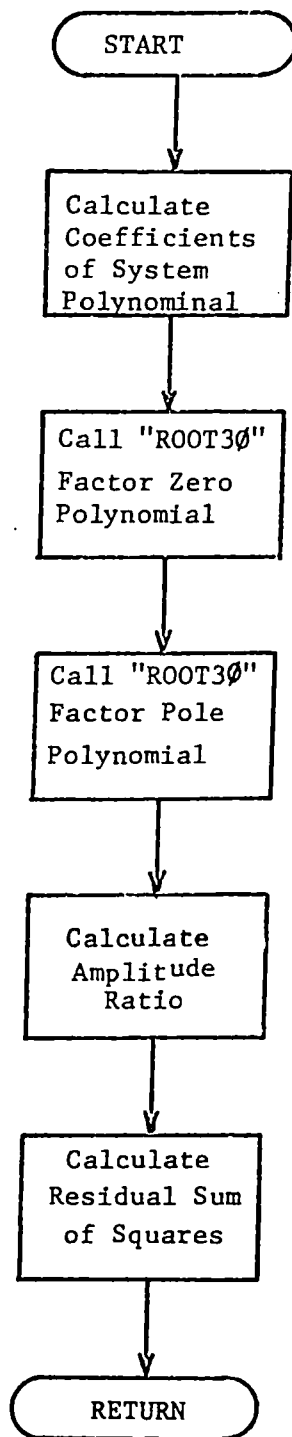




SUBROUTINE ROSEN
(Numerical Search Technique)



LSOS - least sum of squares



Con't.

TABLE III-2

	TRT			TPFTR	
	8.27			0.0	
NUM					
5					
	KM	MCYC	MAXK	MKAT	NSTEP
	5	40	40	999	1
EPS					
0.25	0.05		0.25	0.08	0.05
AKE					
6.0	0.3		6.0	0.5	0.25
	ALPHA			BETA	
	1.5			0.5	
V					
(1,0,0,0,0)	(0,1,0,0,0)	(0,0,1,0,0)	(0,0,0,1,0)	(0,0,0,0,1)	
	KZ	LP	KI	LI	
	2	5	2	5	

Con't.

Con't.

TABLE III-2

	<u>First Iteration</u>	<u>Second Iteration</u>
No. of Stages	26	2
No. of Times "Object" called	999	242
No. of Successive Failures	1	40
Parameter Estimates:		
#1	1.23	1.93
#2	0.23	.44
#3	7.78	6.45
#4	.30	.33
#5	.32	.14
In-Series Component	.581	.556
Residual Sum of Squares:		
(Amplitude Ratio Curve)	8.33	15.2
(Phase Lag Curve)	2,890	3,219
New Total Residence Time Estimate	7.689	7.714

TABLE III-2

Listing of Input Data and Output Results

(Experimental Data from Configuration B)
(Proposed Model Number 5A)

INPUT DATA

NN	AR	PM
I		
F		
0.281	-6.598	-77.2
0.412	-8.633	-87.0
2.55	-25.722	-252.0
3.93	-32.275	-335.0
1.73	-19.484	-205.0
3.55	-29.218	-298.0
0.556	-10.777	-93.0
0.732	-11.4054	-107.0
3.11	-28.536	-310.0
5.11	-39.042	-363.0
6.0	-43.33057	-448.0
0.061	-0.669	-20.5
0.996	-14.420	-126.0
0.163	-4.039	-46.9
0.201	-4.704	-75.0
2.04	-22.285	-213.0
3.55	-29.032	-332.0

Con't.

```

C - COMPUTER PROGRAM TO ESTIMATE THE MODEL PARAMETERS FROM FREQUENCY
C   RESPONSE DATA
      DIMENSION PR(25),DIFF(25),ADIFF(25),A(10),B(10),XX(10),YY(10),
      IZIMAG(10),ZREAL(10),PIMAG(10),PREAL(10),X1(15),X2(15),TPMARZ(25),
      ZTPMARZ(25),FPMAR(25)
      COMMON KM,MCYC,MAXK,MKAT,NSTEP,EPS(20),AKE(10),V(20,20),ALPHA,
      IBETA,SUMN,AFK(10),IRT,TPFTR,KZ,LP,F(25),AR(25),FMAG(25)
      COMMON NN,KAT
C - WRITTEN BY P. B. MELNYK
C - CHEM. ENG. DEPT. MCMASTER UNIVERSITY
C - READ IN OF EXPERIMENTAL DATA
C - AR(I) - AMPLITUDE RATIO (DECIBELS)
C - PM(I) - PHASE MARGIN (DEGREES)
C - TPFTR RESIDENCE TIME OF THE PLUG FLOW SECTIONS
C - F(I) - ASSOCIATED FREQUENCY
C - NN - NUMBER OF DATA POINTS
C - NUM - CONFIGURATION NUMBER
      READ(5,99) NN
      DO 1 I = 1,NN
1      READ(5,100) F(I),AR(I),PM(I)
      DO 2 J = 1,NN
2      PM(J) = -PM(J)
      READ(5,101) TRT,TPFTR
      READ(5,102) NUM
C - INPUT OF PARAMETERS FOR THE ROSENBROCK SEARCH
C   AKE = VARIABLES
C   EPS =STEP SIZE
C   E = TEMPORARY STORAGE FOR STEP SIZE
C   BETA =SCALE FACTOR FOR STEP SIZE WHEN STEP IS UNSUCCESSFUL
C   ALPHA =SCALE FACTOR FOR STEP SIZE WHEN STEP IS SUCCESSFUL
C   V =ORTHOGONAL UNIT VECTORS
C   SUMO = STORAGE FOR MINIMUM SUMN
C   OBJECT = SUBROUTINE FOR OBJECTIVE FUNCTION SUMN
C   NSTEP =2, USE STEP SIZE OF KTH STAGE FOR (K+1)TH STAGE
C   NSTEP =1, USE INITIAL STEP SIZE FOR EVERY NEW STAGE
C   MCYC = NO OF SUCCESSIVE FAILURES ENCOUNTERED IN ALL DIRECTIONS
C   KM = NO OF VARIABLES
C   KK1 =NO OF STAGES
C   KAT = NO OF TIMES OBJECT BEING CALLED
C   V IS A UNIT MATRIX INITIALLY
C   THE PROGRAMME TERMINATES AFTER MAXK STAGES
C       OR AFTER OBJECT BEING CALLED MKAT TIMES
C       OR AFTER MCYC SUCCESSIVE FAILURES BEING ENCOUNTERED
C   BEFORE TERMINATION
C   MAX NUMBER OF VARIABLES =20 ( LIMITED BY DIMENSION)
C - K AND L ARE THE ORDERS OF THE ZERO AND POLE POLYNOMIALS RESPECTIVELY
      IT = 0
1000 WRITE(6,200) NUM
      READ(5,103) KM,MCYC,MAXK,MKAT,NSTEP
      READ(5,104) (EPS(I), I = 1,KM)
      READ(5,105) (AKE(I), I = 1,KM)
      READ(5,106) ALPHA,BETA
      READ(5,107) ((V(I,J),J = 1,KM),I = 1,KM)
      READ(5,108) KZ,LP,K1,L1
      CALL ROSER
C - MAP FROM THE OPTIMIZED VARIABLES
      WRITE(6,201)
      WRITE(6,202)
      DO 30 I = 1,KM

```

```

39  AKE(I) = AFK(I)
    CALL OBJECT
    DO 3 J = 1,NN
3   DIFF(J) = AR(J)-FMAG(J)
    DO 4 J = 1,NN
4   WRITE(6,203) F(J),AR(J),FMAG(J),DIFF(J)
C - INSERT THE FUNCTIONAL RELATIONSHIPS BETWEEN THE SYSTEM POLYNOMIAL
C - COEFFICIENTS AND THE MODEL PARAMETERS HERE
C - TO CALCULATE THE PHASE MARGIN
C
C
    NTST = 2
C - TO CALCULATE THE ROOTS OF THE ZERO POLYNOMIAL
C - IF THERE ARE NO IMAGINARY COEFFICIENTS B(I) = 0.0
    IF(X1(1).GE.999.0) GO TO 50
    WRITE(6,205)
    MN = K1 + 1
    DO 5 I = 1,MN
    A(I) = X1(I)
    WRITE(6,206) A(I)
5   F(I) = 0.0
    II = K1
    CALL ROOT30(A,B,XX,YY,II)
    WRITE(6,207)
    DO 6 I = 1,II
    WRITE(6,208) XX(I),YY(I)
    ZIMAG(I) = -YY(I)
6   ZREAL(I) = -XX(I)
C - TO CALCULATE THE ROOTS OF THE POLE POLYNOMIAL
C - IF THERE ARE NO IMAGINARY COEFFICIENTS B(I) = 0.0
50  LL = L1 + 1
    WRITE(6,205)
    DO 7 I = 1,LL
    A(I) = X2(I)
    WRITE(6,206) A(I)
7   R(I) = 0.0
    II = L1
    CALL ROOT30(A,B,XX,YY,II)
    WRITE(6,209)
    DO 8 I = 1,II
    WRITE(6,208) XX(I),YY(I)
    PREAL(I) = -XX(I)
8   PIMAG(I) = -YY(I)
    PI = 3.1416
    IF(X1(1).GE.999.0) GO TO 9
    DO 10 J = 1,NN
    PMARZ = 0.0
    DO 10 I = 1,K1
    SIGN = 1.0
    IF(ZREAL(I).EQ.0.0) 11,12
11  PMARZ = 90.0 + PMARZ
    GO TO 13
12  THETA = (F(J) + ZIMAG(I))/ZREAL(I)
    IF(THETA.LT. 0.000) SIGN = 2.0
    ATHETA = ABS(THETA)
    IF(ATHETA .LT.0.002) GO TO 14
    IF(ATHETA.GT.600.0) GO TO 15
    PMARZ = (180.0/PI)*ATAN(THETA) + PMARZ

```

```

      GO TO 12
14  THETA = 0.0
      PMARZ = THETA + PMARZ
      GO TO 13
15  IF(SIGN.EQ.1.0) THETA = 90.0
      IF(SIGN.EQ.2.0) THETA = -90.0
      PMARZ = THETA + PMARZ
13  IF(I.EQ.K1) TPMARZ(J) = PMARZ
10  CONTINUE
      GO TO 16
9   DO 17 J = 1,NN
17  TPMARZ(J) = 0.0
16  DO 18 J = 1,NN
      PMARP = 0.0
      DO 18 I = 1,L1
      SIGN = 1.0
      IF(PREAL(I).EQ.0.0) 19,20
19  PMARP = 90.0 + PMARP
      GO TO 21
20  THETA = (F(J) + PIMAG(I))/PREAL(I)
      IF(THETA.LT.0.000) SIGN = 2.0
      ATHETA = ABS(THETA)
      IF(ATHETA.LT.0.002) GO TO 22
      IF(ATHETA.GT.600.0) GO TO 23
      PMARP = (180.0/PI)*ATAN(THETA) + PMARP
      GO TO 21
22  THETA = 0.0
      PMARP = THETA + PMARP
      GO TO 21
23  IF(SIGN.EQ.1.0) THETA = 90.0
      IF(SIGN.EQ.2.0) THETA = -90.0
      PMARP = THETA + PMARP
21  IF(I.EQ.L1) TPMARP(J) = PMARP
18  CONTINUE
      DO 24 J = 1,NN
24  FPMAR(J) = TPMARZ(J) - TPMARP(J)
C - INPUT OF PARAMETERS FOR ONE DIMENSIONAL SEARCH
C   LIM = TOTAL NUMBER OF TRIALS
      SUMO = 0.0
      KNT = 0
      LP = 1
      DELTA = 0.1
      LIM = 15
      TPFTR = 0.0
      DO 52 J = 1,NN
      ADIFF(J) = PM(J) - FPMAR(J)
52  SUMO = ADIFF(J)*ADIFF(J) + SUMO
      WRITE(6,211) SUMO,TPFTR
C   TO SEARCH ON IN SERIES COMPONENT SET NTST GREATER THAN 1.0
      RLUF = 0.0
      IF(NTST.EQ.1) GO TO 51
54  KNT = KNT + 1
      IF(KNT.GT.LIM) GO TO 55
      TPFTR = DELTA + TPFTR
      SUMN = 0.0
      DO 53 J = 1,NN
      ADIFF(J) = PM(J) - FPMAR(J) + (F(J)*TPFTR*180.0/PI)
53  SUMN = SUMN + ADIFF(J)*ADIFF(J)

```

```

WRITE(6,211) SUMN,TPFTR
IF(SUMO.LE.SUMN) GO TO 54
SUMO = SUMN
BLUE = TPFTR
GO TO 54
55 LP = LP + 1
IF(BLUE.EQ.0.0) GO TO 51
IF(LP.GT.3) GO TO 51
LIM = 10
KNT = 0
BLUE = BLUE-DELTA/2.0
DELTA = DELTA*0.1
TPFTR = BLUE
GO TO 54
51 WRITE(6,210) BLUE
DO 56 J = 1,NN
FPMAR(J) = FPMAR(J) - (F(J)*BLUE*180.0/PI)
56 ADIFF(J) = PM(J)-FPMAR(J)
WRITE(6,204)
DO 26 J = 1,NN
26 WRITE(6,203) F(J),PM(J),FPMAR(J),ADIFF(J)
C - ITERATION AND CONVERGENCE CONTROL
IT = IT + 1
IF(BLUE.LE.0.00) STOP
TRTI = 8.27
TRTN = TRTI-BLUE
DEV = ABS(TRT-TRTN)
IF(DEV.LE.0.0827) STOP
TRT = TRTN
WRITE(6,212) TRT
NI = 3
IF(IT.GT.NI) STOP
GO TO 1000
STOP
99 FORMAT(I2)
100 FORMAT(6F12.6)
101 FORMAT(2F10.5)
102 FORMAT(I3)
103 FORMAT(5I3)
104 FORMAT(6F12.6)
105 FORMAT(8F9.5)
106 FORMAT(2F10.5)
107 FORMAT(8F9.5)
108 FORMAT(4I2)
200 FORMAT(20X,51HOPTIMUM EVALUATION OF RESIDENCE TIMES FOR MODEL NO.,
1I3)
201 FORMAT(7/20X,52HTHE PLOT LISTING OF EXPERIMENTAL VS PREDICTED VALU
1ES)
202 FORMAT(10X,18HFREQUENCY (RAD/MIN),5X,28HEXPERIMENTAL AMPLITUDE RATIO
10,5X,36HPREDICTED AMPLITUDE RATIO - DECIBELS,5X,9HDEVIATION)
203 FORMAT(10X,F10.5,13X,F10.5,23X,F10.5,31X,F13.8)
204 FORMAT(7/10X,18HFREQUENCY (RAD/MIN),5X,24HEXPERIMENTAL PHASE SHIFT,
18X,31HPREDICTED PHASE SHIFT - DEGREES,10X,9HDEVIATION)
205 FORMAT(7/30X,35HTHE SYSTEM POLYNOMIAL COEFFICIENTS)
206 FORMAT(7/10X,E14.6)
207 FORMAT(7/16X,5HZEROS,7/10X,4HREAL,15X,9HIMAGINARY)
208 FORMAT(8X,2H( ,E14.6,5X,E14.6,2H )
209 FORMAT(8X,2H( ,E14.6,5X,E14.6,2H )
210 FORMAT(8X,2H( ,E14.6,5X,E14.6,2H )
211 FORMAT(8X,2H( ,E14.6,5X,E14.6,2H )
212 FORMAT(8X,2H( ,E14.6,5X,E14.6,2H )

```

```

210  FORMAT(/10X,48HTHE RESIDENCE TIME OF THE IN-SERIES COMPONENT IS,5X
      1,F10.5)
211  FORMAT(/10X,29HTHE RESIDUAL AND VARIABLE ARE,E14.6,3HAND,F10.5)
212  FORMAT(/10X,37HTHE ESTIMATE OF SYSTEM RESIDENCE TIME,2X,F10.5)
      END
      SUBROUTINE ROSER
C - WRITTEN BY H. PANG
C - CHEM. ENG. DEPT. MCMASTER UNIVERSITY
C   OPTIMIZATION BY ROSENBRUCK METHOD
      COMMON KM,MCYC,MAXK,MKAT,NSTEP,EPS(20),AKE(10),V(20,20),ALPHA,
      BETA,SUMN,AFK(10),TRT,TPFTR,KZ,LP,F(25),AR(25),FMAG(25)
      COMMON NN,KAT
      DIMENSION D(20),PLEN(20),BL(20,20),AJ(20),E(20),AL(20,20)
C   AJ= INDICATORS
C   AFK= OPTIMIZED VALUES FOR VARIABLES
C
      KAT =1
      CALL OBJECT
      SUMO = SUMN
      DO 812 K=1,KM
      AFK(K) =AKE(K)
812  CONTINUE
      KK1=1
      IF (NSTEP .EQ.1) GO TO 1000
      DO 350 I=1,KM
      E(I) =EPS(I)
350  CONTINUE
1000  DO 250 I=1,KM
      AJ(I) =2.0
      IF (NSTEP .NE.1) GO TO 250
      E(I) =EPS(I)
250  D(I) =0.0
      III=0
397  III=III+1
258  I=1
259  DO 251 J=1,KM
251  AKE(J) =AKE(J) +F(I) *V(I,J)
      CALL OBJECT
C *****
C   PRINT HERE IF DESIRED NO OF TIMES OBJECTIVE FUNCTION BEING CALLED
C   (KAT), OBJECTIVE FUNCTION(SUMN), VARIABLES(AKE(I))
C *****
      KAT =KAT +1
      IF (KAT .EQ. MKAT ) GO TO 1002
      IF(SUMN.LE.SUMO) GO TO 253
      DO 254 J=1,KM
254  AKE(J) =AKE(J) -F(I) *V(I,J)
      E(I) =-BETA*E(I)
      IF (AJ(I) .LT. 1.5) AJ(I) =0.0
      GO TO 255
253  D(I) =D(I) +5(I)
      E(I) =ALPHA *E(I)
      SUMO =SUMN
      DO 813 K=1,KM
813  AFK(K) = AKE(K)
      IF (AJ(I) .GT. 1.5) AJ(I) =1.0
255  DO 256 J=1,KM
      IF (AJ(J) .GT. 0.5) GO TO 299

```

```

256 CONTINUE
GO TO 257
299 IF (I.EQ. KM) GO TO 395
I=I+1
GO TO 259
399 DO 398 J=1,KM
IF (AJ(J) . LT.2. ) GO TO 258
398 CONTINUE
IF (III.LT. MCYC ) GO TO 397
GO TO 1001
257 CONTINUE
DO 290 I=1,KM
DO 290 J=1,KM
290 AL(I,J) =0.0
C
C   ORTHOGONALIZATION
C
WRITE (6,280 ) KK1
WRITE (6,281) SUMO,(AKE(I) ,I=1,KM)
IF(KM.EQ.1) GO TO 50
DO 260 I=1,KM
KL=I
DO 260 J=1,KM
DO 261 K=KL,KM
261 AL(I,J) =D(K) *V(K,J) +AL(I,J)
250 BL (1,J)= AL(1,J)
BLEN(1)=0.0
DO 351 K=1,KM
BLEN(1)= BLEN(1) +BL(1,K)*BL(1,K)
351 CONTINUE
PLEN(1) =SQRT(BLEN(1))
DO 352 J=1,KM
V(1,J) =BL(1,J) /PLEN(1)
352 CONTINUE
DO 263 I=2,KM
II=I-1
DO 263 J=1,KM
SUMAVV=0.0
DO 264 KK=1,II
SUMAV =0.0
DO 262 Y=1,KM
262 SUMAV=SUMAV + AL(I,K)*V(KK,K)
264 SUMAVV =SUMAV*V(KK,J) +SUMAVV
263 BL(1,J) =AL(I,J) -SUMAVV
DO 266 I=2, KM
PLEN(1) =0.0
DO 267 K=1,KM
267 BLEN(I) =BLEN(I) +BL(I,K) *BL(I,K)
BLEN(I) = SQRT(BLEN(I) )
DO 266 J=1, KM
266 V(1,J) =BL(1,J) / BLEN(I)
50 KK1 =KK1+1
IF (KK1.EQ.MAXK ) GO TO 1001
GO TO 1000
1002 WRITE (6,910 ) KAT
1001 WRITE (6, 1003) KK1, KAT ,III
WRITE (6, 1004) SUMO

```

```

WRITE (6, 294)
WRITE(6,815) (( V (I,J) ,J=1,KM),I=1,KM)
287 FORMAT(/73X, 12HNO OF STAGE=, 3X, I5/)
281 FORMAT (10X, 18HSUMC AND VARIABLES,3X, 6E12.4/)
294 FORMAT(/73X, 23HORTHOGONAL UNIT VECTORS/)
315 FORMAT (3X,9E12.4/)
710 FORMAT(/73X,25HPROGRAM HAS CALLED OBJECT,2X,I5, 2X,
1 25HTIMES WITHOUT CONVERGANCE/)
1003 FORMAT(/73X, 13HNO OF STAGES=,I5, 3X, 23HAND OBJECT BEING CALLED,
1 I5, 3X, 5HTIMES,3X,26HNO OF SUCCESSIVE FAILURES=,I5/)
1004 FORMAT(/73X, 7HOBJECT=, E15.5/)
1006 FORMAT(/73X, 16HTHE VAFIBLES ARE, 6E12.5/)
RETURN
END
SUBROUTINE OBJECT
C - WRITTEN BY P. B. MELNYK
C - CHEM. ENG. DEPT. MCMASTER UNIVERSITY JANUARY 1970
COMMON KM,MCYC,MAXK,MRAT,IRSTEP,EPS(20),AKE(10),V(20,20),ALPHA,
DELTA,SUMN,AFK(10),TRI,TPFTR,KZ,LP,F(25),AR(25),FMAG(25)
COMMON NN,KAT
DIMENSION X1(10),X2(10),XX(10),YY(10),ZIMAG(10),PIMAG(10),
IZREAL(10),PREAL(10),TZMAG(25),TPMAG(25),A(10),B(10)
C - TO CALCULATE POLYNOMIAL PARAMETERS
C - INSERT LIMITS ON PARAMETERS HERE
C - INSERT THE FUNCTIONAL RELATIONSHIPS BETWEEN THE SYSTEM POLYNOMIAL
C COEFFICIENTS AND THE MODEL PARAMETERS HERE
C
C
C - TO SOLVE THE ZERO POLYNOMIAL
IF(X1(1).GE.999.0) GO TO 1
C - IF THERE ARE NO IMAGINARY COEFFICIENTS B(I) = 0.0
MM = KZ+ 1
DO 2 I = 1,MM
A(I) = X1(I)
2 B(I) = 0.0
II = KZ
CALL ROOT30(A,B,XX,YY,II)
DO 3 I = 1,KZ
ZREAL(I) = -XX(I)
3 ZIMAG(I) = -YY(I)
C - TO SOLVE THE ROOTS OF THE POLE POLYNOMIAL
C IF THERE ARE NO IMAGINARY COEFFICIENTS B(I) = 0.0
1 LL = LP+ 1
DO 4 I = 1,LL
A(I) = X2(I)
4 B(I) = 0.0
II = LP
CALL ROOT30(A,B,XX,YY,II)
DO 5 I = 1,II
PREAL(I) = -XX(I)
5 PIMAG(I) = -YY(I)
C - TO CALCULATE THE AMPLITUDE RATIO
IF (X1(1).GE.999.0) GO TO 6
DO 7 J = 1,NN
ZMAG = 1.0
DO 7 I = 1,KZ
ZMAG = SQRT((F(J) + ZIMAG(I)**2 + (ZREAL(I)**2)*ZMAG
ZMAG = ZMAG**2 + ZREAL(I)**2)

```

```
7   CONTINUE
    GO TO 8
6   DO 9 J = 1,NN
9   TZMAG(J) = 1.0*X2(LL)
8   DO 10 J = 1,NN
    PMAG = 1.0
    DO 10 I = 1,LP
    PMAG = SQRT((F(** + PIMAG(I))**2 + (PREAL(I))**2)*PMAG
    IF(I.EQ.LP) TPMAG(J) = PMAG*FAC
10  CONTINUE
    TEMP = 0.0
    DO 11 J = 1,NN
    TEMP = TZMAG(J)/TPMAG(J)
11  FMAG(J) = 20.0*ALOG10(TEMP)
C - TO CALCULATE THE RESIDUAL
    SUMN = 0.0
    DO 12 J = 1,NN
    TVAR = (AR(J)-FMAG(J))**2
12  SUMN = SUMN + TVAR
    RETURN
    END
```

CD TOT 0428

APPENDIX IV

TABLE IV-1

Experimental Data

Configuration "A"

INPUT SIGNAL

Frequency (rad/min.)	Extremum Values			
	Current (milliamperes)	<u>TOP</u> Concentration (gm NaCl/l)	Current (milliamperes)	<u>BOTTOM</u> Concentration (gm NaCl/l)
0.515	8.81	1.454	3.72	.298
0.727	8.88	1.477	3.69	.293
0.727	8.98	1.510	3.77	.305
1.461	8.66	1.406	3.58	.276
0.323	8.82	1.458	3.64	.285
3.118	8.78	1.445	3.62	.282
0.992	9.09	1.547	3.77	.305
0.067	9.53	1.701	3.93	.330
0.204	9.37	1.644	3.88	.332
1.337	9.10	1.551	3.80	.310
1.971	8.99	1.514	3.78	.307
0.127	9.04	1.531	3.70	.295
0.539	8.93	1.494	3.70	.295
2.513	9.17	1.575	3.88	.322
1.244	9.16	1.571	3.82	.313
0.068	8.28	1.288	3.40	.250
4.66	8.12	1.240	3.53	.269
1.174	8.35	1.310	3.46	.259
1.137	8.85	1.467	3.41	.251
0.818	8.75	1.435	3.36	.244

Con't.

Con't.

TABLE VI-1
OUTPUT SIGNAL

Frequency (rad/min.)	Extremum Values			
	Current (milliamperes)	<u>TOP</u> Concentration (gm NaCl/l)	Current (milliamperes)	<u>BOTTOM</u> Concentration (gm NaCl/l)
0.515	6.14	1.042	5.06	0.807
0.727	5.93	0.994	5.35	0.867
0.727	6.08	1.028	5.51	0.901
1.361	5.174	0.830	5.07	0.809
0.323	5.98	1.005	4.07	0.617
3.118	5.18	0.831	5.16	0.828
0.992	5.45	.888	5.19	0.834
0.067	7.62	1.423	3.03	0.438
0.204	7.02	1.260	3.81	0.570
1.337	5.55	0.910	5.40	0.876
1.971	5.49	0.898	5.44	0.886
0.127	7.21	1.310	3.25	0.474
0.539	5.90	0.987	4.97	0.789
2.513	5.71	0.946	5.68	0.939
1.244	5.70	0.942	5.55	0.910
0.68	6.92	1.234	2.75	0.393
4.661	5.18	0.831	5.18	0.830
1.745	5.33	0.864	5.27	0.850
1.137	5.65	0.931	5.45	0.889
.818	5.64	0.929	5.21	0.838

Con't.

Con't.

TABLE IV-1
TRANSFORMED DATA

Frequency	Amplitude Ratio (decibels)	Phase Lag (degrees)
0.515	-13.832	-176.7
0.727	-19.398	-199.4
0.727	-19.530	-197.3
1.461	-34.649	-284.7
0.323	-9.59	-124.0
3.118	-49.911	-370.7
0.992	-27.134	-233.0
.067	-2.871	-31.0
.204	-5.654	-88.8
1.337	-31.735	-260.4
1.971	-40.875	-310.0
0.127	-3.397	-57.5
1.539	-15.627	-.80.0
2.513	-45.549	-355.7
1.244	-31.691	-259.5
.068	-1.834	-34.8
4.661	-59.477	-497.0
1.745	-37.745	-272.5
1.137	-29.240	-246.6
0.818	-22.284	-211.6

Con't.

Con't.

TABLE IV-1
Configuration "B"
INPUT SIGNAL

Frequency (rad/min.)	Extremum Values			
	<u>TOP</u>		<u>BOTTOM</u>	
	Current (milliamperes)	Concentration (gm NaCl/l)	Current (milliamperes)	Concentration (gm NaCl/l)
0.281	3.60	1.440	1.48	0.359
0.412	3.56	1.417	1.49	0.364
2.55	3.54	1.405	1.49	1.364
3.93	3.22	1.226	1.37	0.311
1.73	3.50	1.383	1.46	0.351
3.55	3.51	1.388	1.48	0.359
0.556	3.62	1.451	1.50	0.368
0.732	2.43	1.343	1.44	0.342
3.11	3.42	1.336	1.45	0.346
5.11	3.48	1.371	1.47	0.355
6.00	3.51	1.386	1.50	0.368
.0616	3.50	1.383	1.45	0.344
0.996	3.50	1.383	1.47	0.354
0.163	3.56	1.418	1.46	0.351
0.201	34.9	1.376	1.44	0.342
2.04	34.5	1.351	1.44	0.342
3.55	34.5	1.351	1.43	0.337

Con't.

TABLE IV-1
OUTPUT SIGNAL

Frequency (rad/min.)	Extremum Values			
	<u>TOP</u>		<u>BOTTOM</u>	
	Current (milliamperes)	Concentration (gm NaCl/l)	Current (milliamperes)	Concentration (gm NaCl/l)
0.281	3.9	1.130	2.68	0.625
0.412	3.77	1.070	2.83	0.680
2.55	3.36	0.896	3.23	0.842
3.93	3.15	0.809	3.10	0.787
1.73	3.41	0.915	3.14	0.805
3.55	3.24	0.848	3.16	0.812
0.556	3.60	0.999	2.84	0.686
0.732	3.51	0.959	2.85	0.690
3.11	3.29	0.867	3.20	0.830
5.11	3.15	0.807	3.12	0.796
6.00	3.19	0.824	3.17	0.818
0.06	4.35	1.338	1.99	0.376
0.996	3.53	0.960	3.05	0.770
0.163	3.96	1.158	2.31	0.488
0.201	3.97	1.163	2.51	0.561
2.04	3.36	0.896	3.17	0.818
3.55	3.30	0.869	3.21	0.833

Con't.

Con't.

TABLE IV-1
TRANSFORMED DATA

Frequency (rad/min.)	Amplitude Ratio (decibels)	Phase Lag (degrees)
0.281	-6.597	
0.412	-8.633	-77.2
2.55	-25.722	-87.0
3.93	-32.275	-252.0
1.73	-19.483	-335.0
3.55	-29.218	-205.0
0.556	-10.777	-298.0
0.732	-11.405	-93.0
3.11	-28.536	-107.0
5.11	-39.042	-310.0
6.00	-43.331	-363.0
.062	-0.669	-448.0
0.996	-14.420	-20.5
0.163	-4.039	-126.0
0.201	-4.704	-46.9
2.04	-22.285	-75.0
		-213.0

APPENDIX VCONDUCTIVITY PAPER

The following unpublished paper was co-authored by P. B. Melnyk, J. D. Norman, and A. W. Wilson. The paper describes in detail the construction of the conductivity monitoring system that was used in these studies.

CONTINUOUS CONDUCTIVITY MONITORING SYSTEM

INTRODUCTION

The measurement of an electrolyte concentration by means of conductivity is a swift, accurate and non-destructive analysis. In addition, because the analysis can be performed "on stream" or "in situ" this measurement technique is quite valuable for monitoring the ionic concentration of industrial flow streams, performing tracer studies, and measuring the extent of conversion of ionic chemical reactants.

In this report, the design criteria that must be considered in the construction of a conductivity monitor will be outlined. It will then be shown how such a device can be easily and economically constructed from "off the shelf" electrical components.

For our specific application, it was necessary to distinguish between small concentration differences (0.01 gm/l N_2Cl) over a limited concentration range (0.1 to 2.0 gm/l N_2Cl). Hence, the response of the meter for incremental variations in electrolyte concentrations should be reasonably constant over the range of interest. In addition, the conductivity monitoring system had to be continuous. As opposed to using a commercially available conductivity meter, a monitoring system was designed and built to meet these specific requirements. The approach outlined here is readily adaptable for designing an instrument capable of measuring any other electrolyte concentration range.

THEORY

When two electrodes are immersed in an electrolyte and a potential difference is imposed across them, the electrolytic solution between the electrodes can be idealized as a simple resistor. This resistance is

measured by measuring a current through it and relating this current to the resistance by means of Ohm's law.

The conductance (reciprocal of resistance) between two electrodes is a function of:

- (I) electrode separation and area
- (II) particular electrolyte
- (III) electrolyte concentration

A non-linear relationship exists between current and the concentration of a specific electrolyte. However, over small concentration ranges, this relationship is approximately linear.

In the design of a conductivity monitor, questions arise concerning:

- (I) current mode (A.C. or D.C.)
- (II) potential difference applied to the electrodes
- (III) electrode size and construction
- (IV) secondary effects.

A alternating current must be used. If a D.C. voltage were applied to the plates, ions of opposite sign would align themselves to the plates increasing the apparent resistance of the electrolyte to the point where dependence upon concentration is masked. This phenomenon is defined here as polarization. To overcome this effect, the current and polarity must reverse itself in a shorter time span than is required for ions to align themselves. Therefore, a lower limit of frequency is specified. An upper limit is also determined by the electrical capacitance effects of the cell as seen from the relationship, $G = \omega C$. This capacitive conductance "G" can be thought of as acting in parallel with

the conductance of the cell; therefore, it must be less to avoid shunting of the solution or cell conductance.

A suitable operating range is 300 or 1000 Hz.

The potential difference applied to the electrodes must be greater than the decomposition voltage of the particular electrolyte. A design range of between 0.5 to 6 V. is suitable.

Experiments conducted by Metrom, A.G. (1) show conductivity measurements to be independent of applied voltage in the 0.5 to 5 volt range. One suitable voltage source is an audio frequency generator. Using the line voltage in conjunction with a step-down transformer is a poor choice due to the low frequency of 60 Hz which will result in polarization of the electrolyte.

The conductivity of the solution is directly proportional to the electrode area and indirectly proportional to the electrode separation. Ideal electrode dimensions are: 1 cm² area and 1 cm. separation, thus identical to the volume outlined in the definition of specific conductivity. However, these dimensions may be varied to obtain a conductance and current density compatible with the measuring equipment. The electrodes may be constructed from an inert material such as platinum. Sensitivity is increased if the electrodes are "blackened" or "platinumized". This process re-defines the platinum surface by electrolytic deposition. To platinumize an electrode, it is immersed along with a separate platinum sheet in a 20% HCl solution with a 4 volt D.C. potential connected to the plates, positive to the electrode, negative to the platinum. The plating process is allowed to

proceed for approximately two minutes.

The temperature dependence of conductivity is approximately + 2% per degree of increasing temperature. Thus, accurate measurements over a wide range of temperature fluctuations require thermal compensation. This can be done automatically by incorporating a temperature sensitive resistor in the measuring circuit. A typical circuit has been developed by A.M. Turiscin (2) which has an accuracy of better than 2% over a 50 D.C. temperature range.

EQUIPMENT

A block/schematic diagram of the 2-channel conductivity monitoring system as built is shown in Figure I. A 19 Volt D.C. power supply (4) drives a 650 cps R-C oscillator (5) for each channel. The oscillating signal is amplified and fed to the conductivity cell and through a diode bridge where the alternating current signal is rectified and passed through a 10 ohm resistor. The voltage drop across this resistor is proportional to the current flowing through the conductivity cell, and hence, to the electrical conductivity of the fluid in the cell. The voltage drop is measured on a recorder.

Schematic diagrams illustrating the power supply and one oscillator circuit are shown in Figure II-a and II-b respectively. In the oscillator circuit, it was found that using a 10K variable resistor, rather than a constant 10K resistor for the load resistance R_L as suggested in the original reference (5) gave better performance. This resistance was adjusted to achieve maximum amplitude of the output signal. The oscillator

has an output voltage of approximately 5 volts r.m.s. and a very low power rating requiring a high impedance load. Consequently, the output signal cannot be fed directly to the conductivity cell; instead, it is boosted by an inexpensive 10 watt audio amplifier. The amplifier specifications are listed on Table I. A voltage divider (Figure II-c) is used to match the output and input impedances of the oscillator and amplifier. The 3K potentiometer is used to control the amplitude of the oscillations fed to the amplifier. A 16 ohm 10 watt load resistor (R_1 and R_3 in Figure I) is connected across the output terminals of the amplifier. The conductivity cell and diode bridge are connected in parallel with the load resistor. Because the impedance of the conductivity cell/diode bridge branch is much greater than the impedance of the 16 ohm load resistor in parallel with it, the r.m.s. output voltage of the amplifier is essentially constant. The vacuum tube voltmeter (Heathkit Model IM-28) connected to switch S_1 is used to check for drift in the amplifier output voltage. This voltage is maintained at the arbitrary value of 2.50 volts r.m.s. by adjusting either the amplifier gain control or the oscillator output amplitude control. The voltage drops across the 10 ohm diode bridge resistors R_2 and R_4 are measured and recorded by a two-channel, two-pen Honeywell Electronik 194 Lab/Test Recorder. This particular recorder has 19 full scale spans varying from 0.1 mv. to 100 volts. Input Impedance is 25K per m.v. of span up to 1 megohm maximum for the millivolt spans, and 4 megohms for all voltage spans.

If desired, a more economical arrangement of the components can

be made by dispensing with the diode bridge and using the rectifier circuit inside the V.T.V.M. itself, thereby allowing purchase of a less sensitive, and hence less expensive, recorder. For a single channel conductivity monitoring system, this modification is shown in Figure III. In the case, the V.T.V.M. is used not only to check the stability of the amplifier output voltage as discussed earlier, but also to measure the voltage drop across resistor R_2 . This voltage drop is proportional to the current flowing through the measuring cell, and hence, gives a direct indication of the conductivity of the fluid in the cell. A meter such as the Hewland Packard Model 400 which has recorder output terminals would be suitable for this purpose. Lacking this, a less expensive meter such as the Heathkit Model I.M.-28 mentioned earlier could be used and the recorder connected to the output of the 6AL5 tube half-wave double circuit.

Figure IV-a shows a typical flow-through conductivity cell used in this study. The cell is made of Teflon, 0.635 mm diam. platinum wire, and 0.254 mm thick platinum sheet. A teflon bonding epoxy cement was used to bond the platinum electrodes to the teflon support. The cell either could be used in a "dip" fashion, or could be inserted into the teflon block shown in Figure IV-b and installed in a flow-through pipe. Conductivity measurements were found to be independent of the mean flow-through velocities over the velocity range investigated (0 to 15 cm/sec.).

Table II Indicates the approximate cost (in Canadian Dollars), exclusive of the recorder cost, of the components used in a single channel continuous conductivity monitoring system.

Figure V illustrates typical calibration curves obtained with the conductivity meter as built in Figure I. The meter response is reported in milli-Amperes rather than conductance (ohm^{-1}). As was specified as a design requirement in the introduction, it can be seen that the system response approaches linearity.

In adapting this design approach to a different concentration range, it may be necessary to choose the cell resistance by altering the dimensions of the platinum electrodes. This must be done in such a fashion as to satisfy the following criterion:

$$\frac{[\text{cell resistance}]}{[\text{diode measuring bridge resistance}]} \geq \frac{.10}{1}$$

It was found that the response time of the system was essentially instantaneous. In our specific application, the response time of the recorder was the controlling factor.

Notation

where G - conductance
 ω - frequency
 C - capacitor constant

TABLE IAMPLIFIER SPECIFICATIONS

Power output	-	10 watts per channel music; 6 watts continuous at less than 2% harmonic distortion
Frequency Response	-	30 to 20,000 Hz 1/db
Input Sensitivity	-	100 mv
Signal/noise ratio	-	55 db at 6 watt output
Channel separation	-	40 db tone controls at flat setting
Tone Control	-	14 db at 10 Kc
Output impedance connections	-	4,8,16 ohms each channel
Power requirements	-	117 Volts, 60 cycle, 27 watts

TABLE II

APPROXIMATE MATERIAL COST OF SINGLE CHANNEL
CONTINUOUS CONDUCTIVITY MONITORING SYSTEM

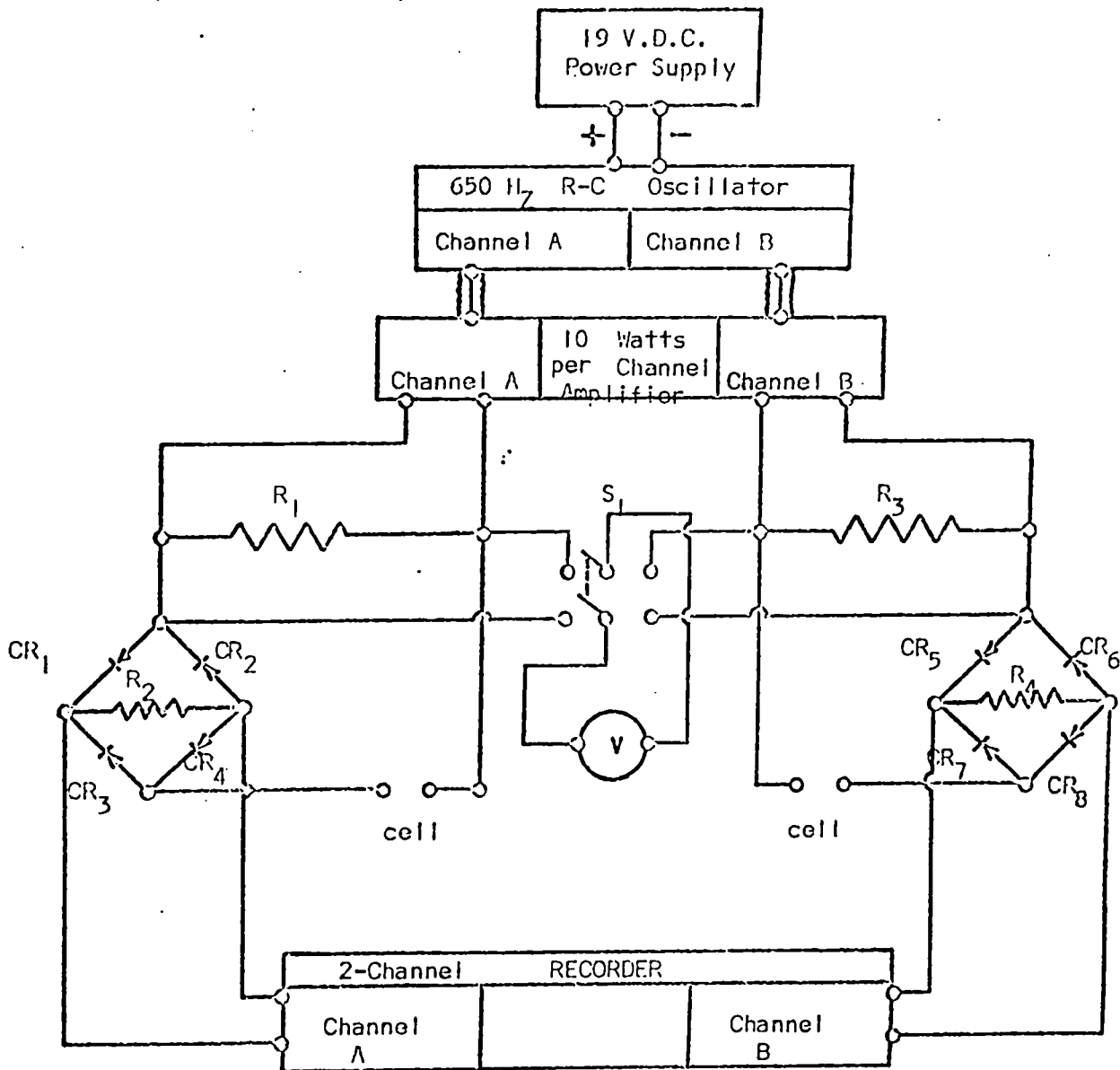
Teflon and Platinum for cells	-	\$30
D.C. Power Supply	-	\$15
Oscillator	-	\$ 5
Amplifier	-	\$35
V.T.V.M.	-	\$65
Miscellaneous *	-	\$20

Total	-	\$170

* Includes chassis boxes, switches, wires, terminals strips, etc.

REFERENCES

1. Metrohm, A.G., Bulletin 1, 28
2. Turiscsin, A.M., "Electric Measuring of Non-electric Quantities"
Muszaki Konyvkiado, Budapest
3. Dobos, D., Electronic Electrochemical Measuring Instruments, Terra,
Budapest 1966
4. R.C.A. Solid-State Hobby Circuits Manual, R.C.A. Victor Co. Ltd.
5. Handbook of Semiconductor Circuits, Tab Books, originally published by
U.S. Government, Printing Office as Military Standardization Handbook,
Selected Semiconductor Circuits, MIL-HDBK-215



R_1, R_3 = 16 Ohm 10 watt resistors

R_2, R_4 = 10 Ohm 1/2 watt resistors

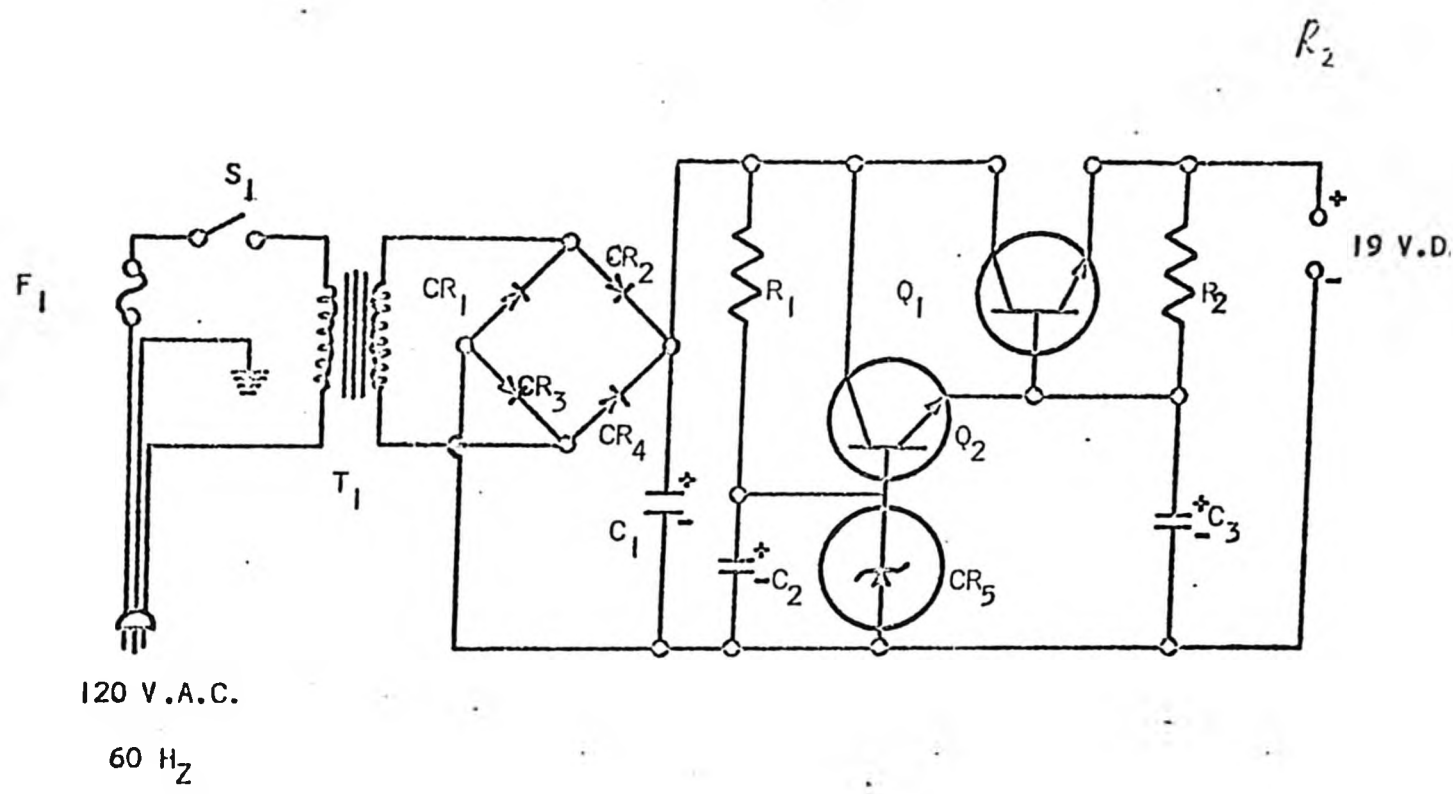
$CR_1, CR_2, CR_3, CR_4, CR_5, CR_6, CR_7, CR_8$ = 100 ma, 25 volt diodes

S_1 = Double Pole, Double Throw Switch

V = Heathkit Model III-28 Vacuum Tube Voltmeter

Figure 1

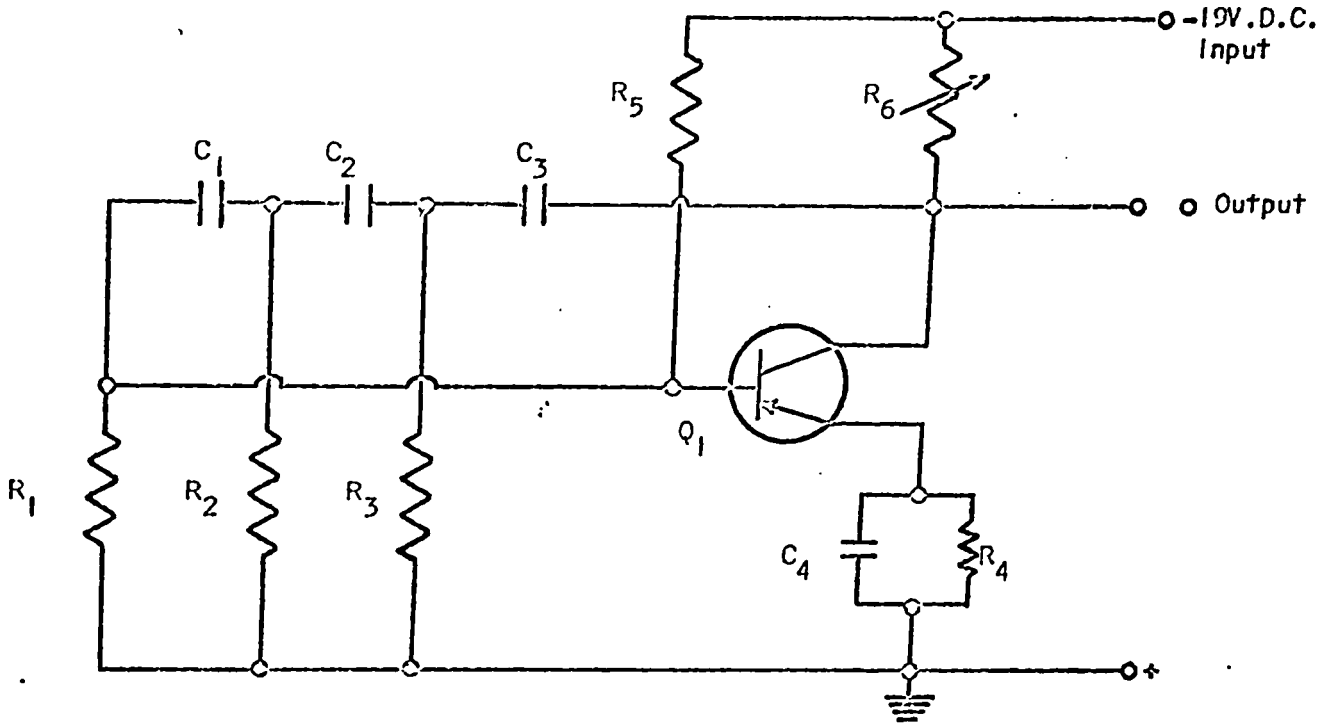
Block Schematic Diagram of Original Two Channel Conductivity Monitoring System



120 V.A.C.
60 Hz

- | | |
|--|--|
| <p>F_1 = Fuse, 1 ampere</p> <p>S_1 = Single-Pole, Single Throw
125 Volt Switch</p> <p>T_1 = Transformer, Primary = 120 Volts,
Secondary = 24 Volts, 1 ampere</p> <p>C_1 = Electrolytic Capacitor, 2500 μfd,
50 Volts</p> <p>C_2 = Electrolytic Capacitor, 100 μfd,
25 Volts</p> <p>C_3 = Capacitor, 0.1 μfd, 50 volts</p> | <p>R_1 = 470 ohms, 1/2 watt, 10%</p> <p>R_2 = 220 ohms, 1/2 watt, 10%</p> <p>Q_1 = Transistor, RCA SK 3027 or equiv.</p> <p>Q_2 = Transistor, RCA SK 3020 or equiv.</p> <p>$CR_1, CR_2, CR_3, CR_4,$ = Diodes, 50 volts,
1 ampere</p> <p>CR_5 = Two 1 watt, 10 volt, Zener
diodes in series.</p> |
|--|--|

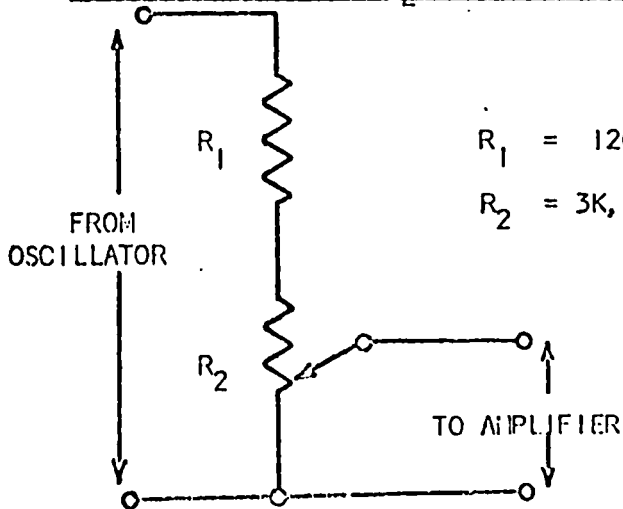
FIGURE 11-(a) POWER SUPPLY SCHEMATIC



$R_1, R_2, R_3 = 10K, 1/2 \text{ watt}, 10\%$
 $R_4 = 4.7K, 1/2 \text{ watt}, 10\%$
 $R_5 = 22K, 1/2 \text{ watt}, 10\%$
 $R_6 = 10K, 1/2 \text{ watt potentiometer}$

$C_1, C_2, C_3 = 0.01 \mu\text{fd}, 50 \text{ volts capacitor}$
 $C_4 = 25 \mu\text{fd.}, 10 \text{ volt electrolytic capacitor}$
 $Q_1 = \text{Transistor } 2N526$

FIGURE 11-(b) 650 H_z OSCILLATOR SCHEMATIC



$R_1 = 120K, 1/2 \text{ watt}, 10\%$
 $R_2 = 3K, 1/2 \text{ watt potentiometer}$

FIGURE 11-(c) VOLTAGE DIVIDER

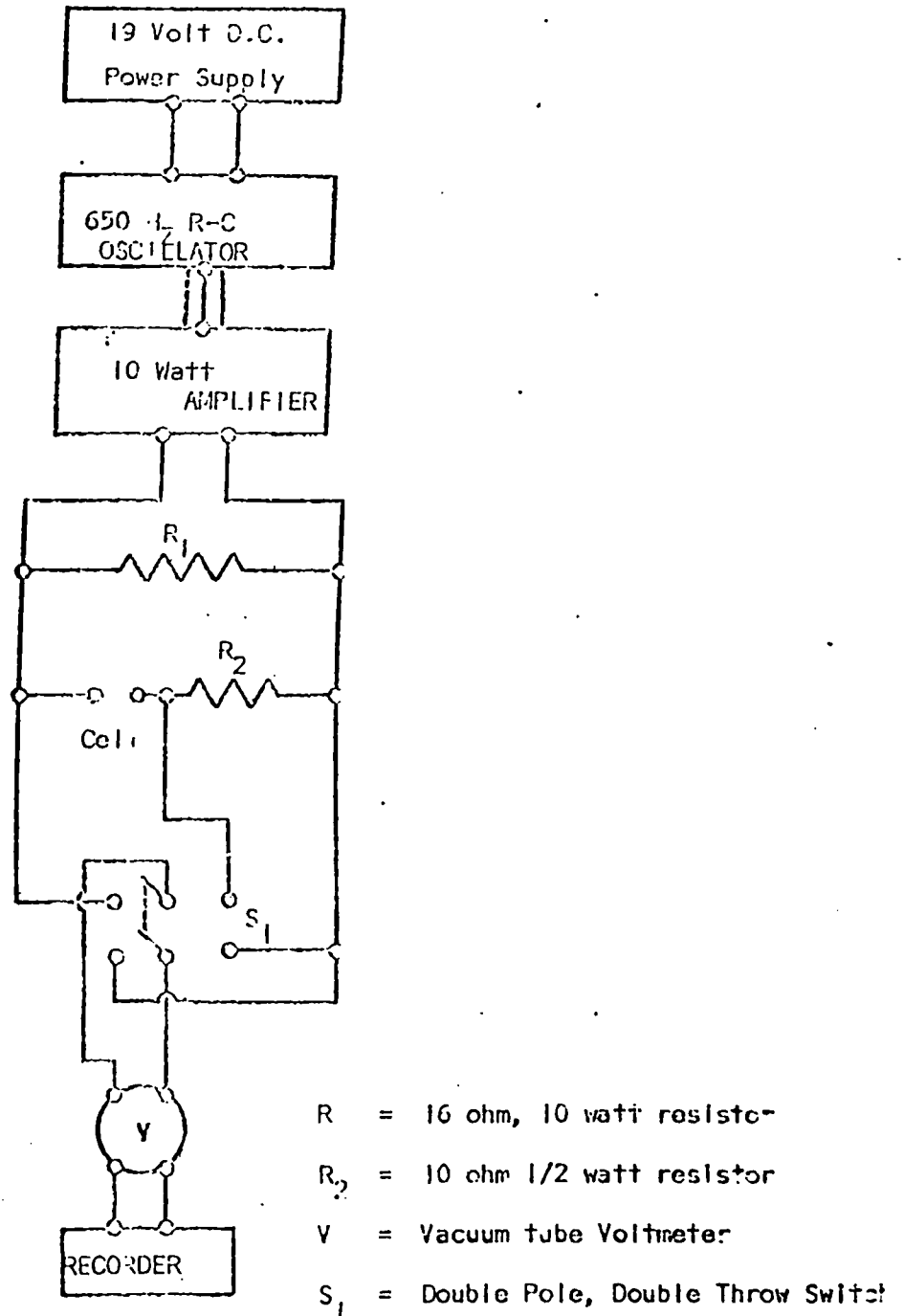


FIGURE III

MODIFICATION OF THE CONDUCTIVITY MONITORING SYSTEM

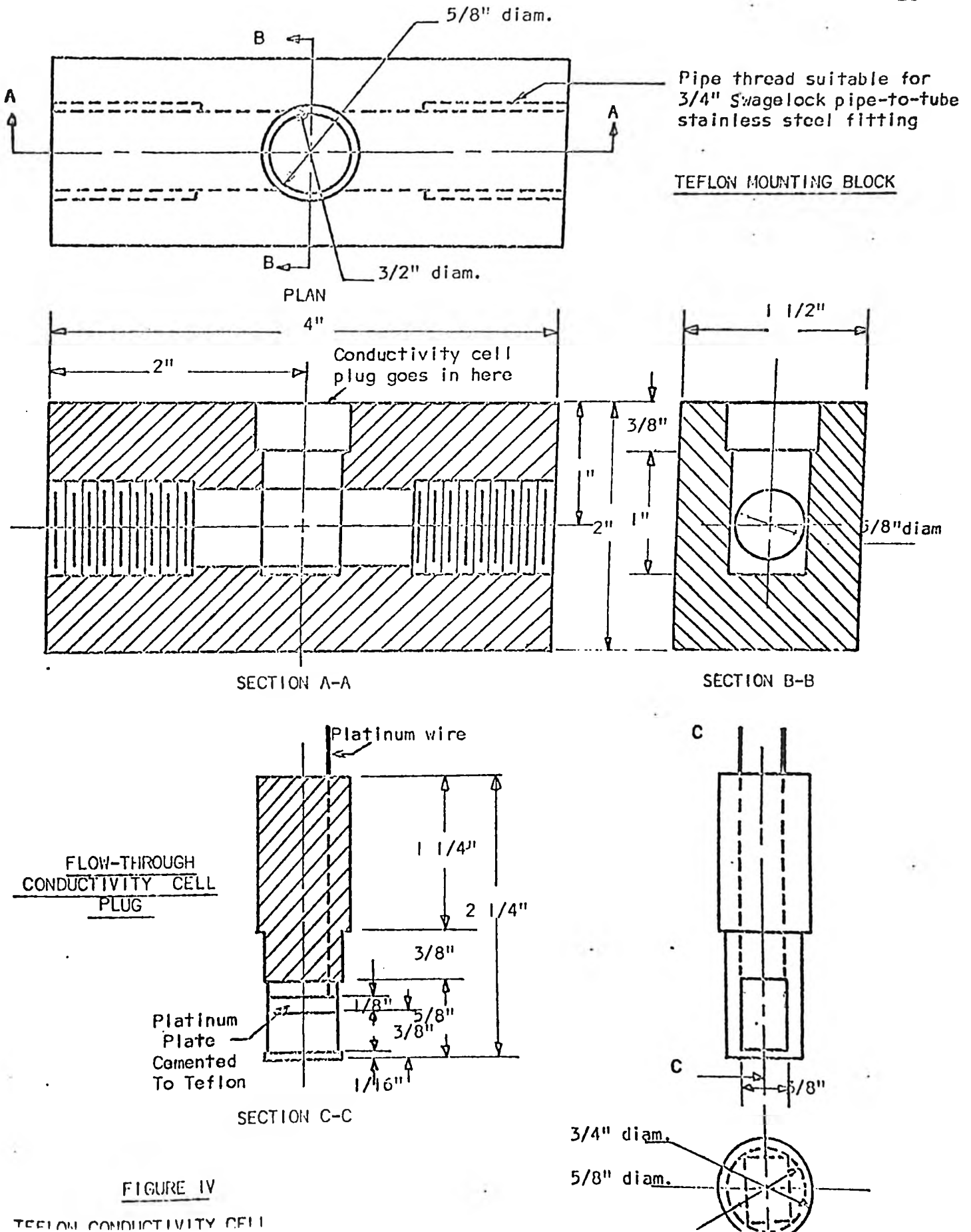


FIGURE IV

TEFLON CONDUCTIVITY CELL

SODIUM CHLORIDE CONCENTRATION (grams/liter)

